

POLITECNICO DI TORINO
Master of Science of Civil Engineering



A THESIS OF MASTER OF SCIENCE

**THERMAL CONDUCTIVITY OF
BACKFILLING MATERIALS FOR ROAD
PAVEMENTS IN TUNNELS.**

Supervisors:

Prof. Ing. Ezio Santagata

Ing. Pier Paolo Riviera

Ing. Davide Dalmazzo

Ing. Eldho Choorackal Avirachan

Student:

Ricardo Andrés Albrieu

DECEMBER, 2017

“Perseverance will sooner or later overcome intelligence.”

Jokoi Kenji.

INDEX

CHAPTER 1	1
INTRODUCTION	1
1.1 Background	1
1.2 Objectives and Scope of the Study.....	2
1.3 Outline of the Thesis	3
CHAPTER 2	4
THE CASE STUDY OF FREJUS TUNNEL	4
2.1 The Frejus tunnel	5
2.2 Second Tunnel.....	6
2.3. Characteristics of the Tunnel	8
CHAPTER 3	10
LITERATURE REVIEW	10
3.1 Soil	10
3.1.1 Structure of porous media	10
3.1.2 Soil Classification	11
3.1.3 Applications	14
3.2 Thermal Conductivity of Soils.....	15
3.2.1 Thermal Transport Mechanisms	15
3.3 Controlled Low-Strength Material (CLSM)	18
3.3.1. Applications	19
3.3.2. Materials.....	19
3.3.3 Properties	21
3.4 Thermal Conductivity of Cement Based Materials.....	23
3.5 Effect of Back-fill Thermal Conductivity on the Performance of Transmission Lines	24
3.6 Thermal Conductivity Measurement.....	26
3.6.1 Principle of Measurement	27
3.6.2 Factors Influencing Measurements	28

3.7 Models for the Prediction of Thermal Conductivity.	29
3.7.1 Kersten Model (1949)	29
3.7.2 Johansen Model (1975).....	30
3.7.3 Farouki Model (1981,1982)	31
3.7.4 Cote and Konrad Model (2005)	31
3.7.5 Thermal conductivity model in Concrete.....	31
CHAPTER 4	33
SOILS AND CLSM MIXTURES.....	33
4.1 Soil as Back-Fill Materials.....	33
4.1.1 Characterization of Soils	34
4.2 CLSM as Back-Fill Materials	37
4.2.1 Characterization of CLSM Aggregates	38
4.2.2 Cement	40
4.2.3 Aggregate	42
4.2.4 Water.....	43
4.2.5. Recycled Aggregates.....	44
4.2.6 Admixture	48
4.2.7 Formulation of Mixes.....	50
CHAPTER 5	53
EXPERIMENTAL INVESTIGATION	53
5.1 Research Project.....	53
5.2 Instrumentation and Laboratory Equipment	54
5.2.1 Precision Balance	54
5.2.2 Equipment for Granulometric Analysis of Aggregates.....	54
5.2.3 Pycnometer.....	55
5.2.4 Cylindrical Mould for Compaction Test	56
5.2.5 Automatic Compaction Machine - Matest	56
5.2.6 The CLSM Mixer.....	57
5.2.7 Slump Flow Test Equipment.....	58
5.2.8 Thermal Conductivity Device	58

5.3 Characterization of Soil.....	59
5.3.1 Particle Size Distribution	59
5.3.2 Specific Density	61
5.4 Proctor Compaction Test.....	63
5.5 Thermal Conductivity Measurement in Soils	66
5.5.1 Calibration of the KD2 pro	68
5.6. Aggregate Sludge CLSM and Stone Sawmilling Sludge Mixes.....	69
5.7 Thermal Conductivity Measurement in CLSM's.....	71
CHAPTER 6	73
RESULTS AND DISCUSSIONS	73
6.1 Proctor Compaction Test.....	73
6.2 Thermal Conductivity in Soil.....	75
6.2.1 Relation between Bulk Density and Thermal Conductivity.....	76
6.2.2 Relation between Water Content and Thermal Conductivity	77
6.2.3 Degree of Saturation and Thermal Conductivity	78
6.2.4 Volume of Soil Grains and Thermal Conductivity	79
6.3 Interpretation of Results.....	81
6.4 Thermal Conductivity Models of Soil.....	81
6.4.1 Kersten Model (1949)	82
6.4.2 Johansen Model (1975).....	83
6.4.3 Farouki Model (1981,1982)	84
6.4.4 Cote and Konrad Model (2005)	85
6.4.5 Evaluation of de Models. [28].....	86
6.5 Thermal Conductivity of CLSM's	87
6.5.1. Influence of Cement Content on Thermal Conductivity	87
6.5.2 Influence of Rap Content on Thermal Conductivity	88
6.5.3 Influence of Water Content on Thermal Conductivity.....	89
6.5.4 Influence of Age on Thermal Conductivity	90
6.6 Thermal conductivity model for CLSM.....	92
6.6.1 Relationship as a function of Cement Content.....	93

6.6.2 Relationship as a Function of RAP Content.....	94
6.6.3 Relationship as a function of W/P ratio.	94
6.6.4 Model Equation of Thermal Conductivity	95
6.7 Thermal Stability.....	97
6.8 Stone Sawmilling Sludge CLSM	99
CHAPTER 7	102
CONCLUSIONS.....	102
APPENDIX.....	105
APPENDIX 1: HVDC INTERCONNECTION IMPUTS AND PARAMETERS	106
APPENDIX 2: CHARACTERIZATION OF SOILS	109
REFERENCES.....	II

LIST OF FIGURES

FIG. 1 TUNNEL BACK-FILL SECTION.[1]	4
FIG. 2 SECTIONS OF THE TUNNEL.....	6
FIG. 3 THE SECOND TUNNEL	7
FIG. 4. TUNNEL CONSTRUCTION.....	8
FIG. 5. COATING RING	9
FIG. 6 DUCTS OF UNDERGROUND HIGH-TENSION NETWORK.....	9
FIG. 7 RANGE OF LIQUID LIMIT AND PLASTICITY INDEX FOR SOILS IN GROUPS [3].....	14
FIG. 8 CONCEPTUAL HEAT TRANSFER IN WET (LEFT) AND DRY (RIGHT) CONDITION IN SOIL [12]	17
FIG. 9 THERMAL PROPERTIES CHARACTERISTICS OF SOIL. [10]	17
FIG. 10 AMPACITY AS A FUNCTION OF NATIVE SOIL RESISTIVITY AND PRESENCE OF CONTROLLED BACKFILL [15].....	25
FIG. 11. THERMAL STABILITY OF THE TYPICAL BACKFILL MATERIALS [15].....	26
FIG. 12 GENERAL SCHEMATIC DIAGRAM FOR THE THERMAL CONDUCTIVITY PROBE [10].....	26
FIG. 13 PARTICLE SIZE DISTRIBUTION FOR A _{1-A}	35
FIG. 14 PARTICLE SIZE DISTRIBUTION FOR A ₇₋₆	36
FIG. 15 PARTICLE SIZE DISTRIBUTION OF AGGREGATE SLUDGE CLSM	39
FIG. 16. PARTICLE SIZE DISTRIBUTION OF STONE SAWMILLING SLUDGE CLSM	39
FIG. 17 AGGREGATE USED IN AGGREGATE SLUDGE CLSM.....	43
FIG. 18 STONE SAWMILLING SLUDGE CLSM “A ON THE RIGHT AND B ON THE LEFT”	43
FIG. 19. RAP MATERIAL USED IN LABORATORY TESTS	46
FIG. 20 HOT IN PLACE RECYCLING	47
FIG. 21 COLD IN PLACE MIXING.....	47
FIG. 22. SELECTION OF RAP.....	48
FIG. 23 ADVA® FLOW 455 SUPERPLASTICIZER.....	49
FIG. 24 PRECISION BALANCE	54
FIG. 25 SET OF SIEVES	55
FIG. 26 PYCNOMETERS	55
FIG. 27 PROCTOR MOULD [34].....	56
FIG. 28 AUTOMATIC COMPACTION MACHINE[33].....	57
FIG. 29 THE CLSM MIXER.....	57
FIG. 30 CYLINDER AND PLATE USED FOR THE SLUMP FLOW TEST.....	58
FIG. 31 KD2 PRO DEVISE WITH DIFFERENT PROBES AND CALIBRATION CYLINDERS.....	58
FIG. 32 SIEVING SCHEME [28]	59
FIG. 33 COLUMN OF SIEVE	60
FIG. 34 PYCNOMETER FULL OF A _{1-A} AND A ₇₋₆ SOIL.....	62
FIG. 35. MODIFIED PROCTOR TEST.....	64

FIG. 36 MATEST COMPACTION SEQUENCE [37]	65
FIG. 37 FLUSH AND WEIGHING – MODIFIED PROCTOR TEST	65
FIG. 38 THERMAL CONDUCTIVITY MEASUREMENT OF SOIL A1-A	67
FIG. 39. THERMAL CONDUCTIVITY MEASUREMENT OF SOIL A7-6	68
FIG. 40. VERIFYING SENSOR PERFORMANCE	68
FIG. 41 MOULDS FOR CASTING CLSM.....	69
FIG. 42 CAST CLSM SAMPLES IN THE MOLDS.....	70
FIG. 43 SEGREGATION PHENOMENA IN STONE SAW MILLING SLUDGE MIXES.....	71
FIG. 44 THERMAL CONDUCTIVITY MEASUREMENT ON CLSM’S SPECIMENS	72
FIG. 45 PROCTOR COMPACTION CURVE FOR SOIL A1-A	74
FIG. 46 PROCTOR COMPACTION CURVE FOR SOIL A7-6.....	74
FIG. 47 RELATIONSHIP BETWEEN DENSITY AND THERMAL CONDUCTIVITY – A1-A.....	76
FIG. 48 RELATIONSHIP BETWEEN DENSITY AND THERMAL CONDUCTIVITY – A7-6	77
FIG. 49 RELATIONSHIP BETWEEN WATER CONTENT AND THERMAL CONDUCTIVITY – A1-A.....	77
FIG. 50 RELATIONSHIP WATER CONTENT AND THERMAL CONDUCTIVITY – A7-6	78
FIG. 51 RELATIONSHIP BETWEEN DEGREE OF SATURATION AND THERMAL CONDUCTIVITY – A1-A ..	79
FIG. 52 RELATIONSHIP BETWEEN DEGREE OF SATURATION AND THERMAL CONDUCTIVITY – A7-6	79
FIG. 53 RELATIONSHIP BETWEEN VOLUME OF SOIL GRAINS AND THERMAL CONDUCTIVITY – A1-A .	80
FIG. 54 RELATIONSHIP BETWEEN VOLUME OF SOIL GRAINS AND THERMAL CONDUCTIVITY – A7-6..	80
FIG. 55 COMPARISON OF THERMAL CONDUCTIVITY CHARACTERISTICS OF SOIL	81
FIG. 56. COMPARISON BETWEEN PREDICTED THERMAL CONDUCTIVITIES A MEASURED VALUES - KERSTEN	83
FIG. 57. COMPARISON BETWEEN PREDICTED THERMAL CONDUCTIVITIES A MEASURED VALUES - JOHANSEN.....	84
FIG. 58 COMPARISON BETWEEN PREDICTED THERMAL CONDUCTIVITIES A MEASURED VALUES - FAROUKI.....	85
FIG. 59 COMPARISON BETWEEN PREDICTED THERMAL CONDUCTIVITIES A MEASURED VALUES – COTÉ AND KONRAD.....	86
FIG. 60 EVALUATION OF MODELS BETWEEN PREDICTED THERMAL CONDUCTIVITIES A MEASURED VALUES FOR A1-A SOIL.....	86
FIG. 61 EVALUATION OF MODELS BETWEEN PREDICTED THERMAL CONDUCTIVITIES A MEASURED VALUES FOR A7-6 SOIL	87
FIG. 62 THERMAL CONDUCTIVITY VARIATION WITH DIFFERENT CEMENT CONTENTS.....	88
FIG. 63 THERMAL CONDUCTIVITY VARIATION WITH DIFFERENT RAP CONTENT FOR C100_0.80.....	89
FIG. 64 THERMAL CONDUCTIVITY VARIATION WITH DIFFERENT WATER TO POWDER RATIO CONTENT FOR C100_0.80.....	90
FIG. 65 INFLUENCE OF AGE ON THERMAL CONDUCTIVITY WITH DIVERSE CEMENT CONTENTS	91

FIG. 66 INFLUENCE OF AGE ON THERMAL CONDUCTIVITY WITH DIVERSE %RAP CONTENT	91
FIG. 67 INFLUENCE OF AGE ON THERMAL CONDUCTIVITY WITH DIVERSE W/P RATIO FOR C100_20 ..	92
FIG. 68. NORMALIZATION CURVE OF CEMENT CONTENT	93
FIG. 69 NORMALIZATION CURVE OF RAP CONTENT.....	94
FIG. 70 NORMALIZATION CURVE OF W/P RATIO	95
FIG. 71. COMPARISON OF THE MEASURED AND CALCULATED VALUES FOR 7 DAYS.....	96
FIG. 72 COMPARISON OF THE MEASURED AND CALCULATED VALUES FOR 14 DAYS.....	96
FIG. 73 COMPARISON OF THE MEASURED AND CALCULATED VALUES FOR 28 DAYS.....	97
FIG. 74 COMPARISON OF THE MEASURED AND CALCULATED VALUE FOR MODEL ADOPTED.....	97
FIG. 75. THERMAL STABILITY CURVE FOR BACKFILL MATERIALS	99
FIG. 76 INFLUENCE OF AGE ON THERMAL CONDUCTIVITY WITH 0.7% W/P RATIO FOR SLUDGES CLSM	101

LIST OF TABLES

TAB. 1 GEOTECHNICAL PARAMETERS OF SOIL [2].....	11
TAB. 2 CLASSIFICATION OF HIGHWAY SUBGRADE MATERIALS [3].....	12
TAB. 3 THERMAL RESISTIVITY OF DIFFERENT SOIL MATERIALS [10].....	16
TAB. 4 PARTICLE SIZE DISTRIBUTION FOR A _{1-A}	35
TAB. 5. PARTICLE SIZE DISTRIBUTION FOR A ₇₋₆	36
TAB. 6 SPECIFIC DENSITIES OF A _{1-A} AND A ₇₋₆ SOILS	36
TAB. 7. VARIATION OF THE MOISTURE CONTENT IN BOTH SOIL	37
TAB. 8 PARTICLE SIZE DISTRIBUTION OF AGGREGATE SLUDGE CLSM.....	38
TAB. 9 PARTICLE SIZE DISTRIBUTION OF STONE SAWMILLING SLUDGE CLSM	39
TAB. 10 COMPRESSIVE STRENGTH REQUIREMENTS	41
TAB. 11 RESULTS OF CURVES OPTIMIZATION FOR AS_ CLSM (Q=0.21).....	51
TAB. 12 RESULTS OF CURVES OPTIMIZATION FOR STONE SAWMILLING SLUDGE CLSM (Q=0.21).....	51
TAB. 13 MIX PROPORTIONS.....	51
TAB. 14 TEST PARAMETERS FOR AGGREGATE SLUDGE_ CLSM.....	52
TAB. 15 TEST PARAMETERS FOR FRAME WIRE SAW SLUDGE_ CLSM AND DIAMOND WIRE CUT SULUDGE_ CLSM	52
TAB. 16 WEIGHT OF THE SIEVES.....	60
TAB. 17 MASS OF THE TEST PORTION AS FUNCTION OF MAXIMUM SIZE OF AGGREGATES	61
TAB. 18 TECHNICAL FEATURES	63
TAB. 19 OPTIMAL MOISTURE FOR MAXIMUM DENSITIES	75
TAB. 20 GEOTECHNICAL AND THERMAL PROPERTIES OF A _{1-A}	75
TAB. 21 GEOTECHNICAL AND THERMAL PROPERTIES OF A ₇₋₆	75
TAB. 22 SUMMARY OF K _{CALCULATED} AND K _{MEASURED} FOR A _{1-A} (KERSTEN).....	82
TAB. 23 SUMMARY OF K _{CALCULATED} AND K _{MEASURED} FOR A ₇₋₆ (KERSTEN).....	82
TAB. 24 SUMMARY OF K _{CALCULATED} AND K _{MEASURED} FOR A _{1-A} -JOHANSEN.....	83
TAB. 25 SUMMARY OF K _{CALCULATED} AND K _{MEASURED} FOR A ₇₋₆ - JOHANSEN	83
TAB. 26 SUMMARY OF K _{CALCULATED} AND K _{MEASURED} FOR A _{1-A} -FAROUKI.....	84
TAB. 27 SUMMARY OF K _{CALCULATED} AND K _{MEASURED} FOR A ₇₋₆ FAROUKI	84
TAB. 28 SUMMARY OF K _{CALCULATED} AND K _{MEASURED} FOR A _{1-A} -COTE AND KONRAD.....	85
TAB. 29 SUMMARY OF K _{CALCULATED} AND K _{MEASURED} FOR A ₇₋₆ - COTE AND KONRAD.....	85
TAB. 30 THERMAL CONDUCTIVITY MEASUREMENTS AS A FUNCTION OF CEMENT CONTENT.	87
TAB. 31 THERMAL CONDUCTIVITY MEASUREMENTS AS A FUNCTION OF RAP CONTENT	88
TAB. 32 THERMAL CONDUCTIVITY MEASUREMENTS AS A FUNCTION OF W/P RATIO	89
TAB. 33 CONDUCTIVITY RATIO WITH DIFFERENT CEMENT CONTENTS	93
TAB. 34 CONDUCTIVITY RATIO WITH DIFFERENT RAP CONTENT	94
TAB. 35 CONDUCTIVITY RATIO WITH DIFFERENT W/P RATIO	94

TAB. 36 COMPARISON MEASUREMENT AND CALCULATION VALUES WITH MODEL	96
TAB. 37 THERMAL CONDUCTIVITY AND RESISTIVITY MEASURED FOR SOILS SAMPLES	98
TAB. 38 RESULTS OF THERMAL CONDUCTIVITY AND RESISTIVITY IN WET AND DRY CONDITIONS FOR AS_CLSM SAMPLES.....	98
TAB. 39 THERMAL CONDUCTIVITY MEASUREMENTS ON STONES SAWMILLING SLUDGES CLSM'S.	100
TAB. 40 SUMMARY OF THERMAL CONDUCTIVITY MEASUREMENTS ON DWCS AND FWSS CLSM'S AND AS_CLSM	100

CHAPTER 1

INTRODUCTION

1.1 Background

Pavements in tunnels are different from conventional pavements due to several reasons. Various utility lines such as high voltage cables are present beneath the pavements in tunnels. Hence thermal conductivity of back-filling materials used for the construction of such pavements deserves major attention. Thermal property of the backfill materials influences the efficiency of power transmission through such cables. Compacted soil or muck excavated during the tunneling operation is commonly used for the back-filling application in tunnels, but their thermal conductivity is very low. This lower thermal conductivity of backfill material increases the temperature in the core of the cables and damages it in the long term. Therefore, these must meet various thermal filling requirements such as; High thermal conductivity to avoid transmission losses of buried cables, sufficient mechanical properties to resist any damage to the cables and support the transport of the vehicle through the tunnels, easy to place inside the tunnels and thermal stability during its useful life to avoid any change in thermal properties during power transmission.

Backfilling materials considered for the study includes two kinds of soils and two kinds of Controlled Low Strength Materials (CLSMs). Two soils considered for the study have distinct physical properties and mineralogical composition. The have Large quantity of recycled materials were used for the manufacture of CLSMs used in this study. Aggregate sludge, Recycled Asphalt Pavement aggregates (RAP) and stone saw sludge were reused for the production CLSMs. The objective of the study was to develop a sustainable backfilling material by reusing the waste materials of construction industry and to compare their performance with conventional soils for the application in pavements in tunnels. Reuse of such waste materials avoid the problem of land filling and related waste management problems.

1.2 Objectives and Scope of the Study

The thermal properties of the conductors and the backfill materials around buried high-power cables have a significant role in ensuring smooth transmission of power. They control the temperature of the transmission cable and helps in designing the power transmission parameters. At low temperature and stationary conditions, heat transport is controlled mainly by the thermal conductivity k [$Watt / m. ^\circ K$] of the back-fill and the surrounding soil.

In the lower part of the new section of the Frejus tunnel, different underground utilities will be located. One of them is a high voltage cables that run the entire length of the tunnel and perform the function of carrying power from one country to another. It is planned to install 4 cables of the high voltage electricity transmission network each one with 320kV. The transmission of electrical energy and especially in high voltage lines, produce an increase in temperatures inside them, generated by the resistance of the conductor to the passage of electrical current. This phenomenon can increase in situations when these cables are located underground and surrounded by backfilling materials of high thermal resistivity.

The company that provides the electric power service must guarantee 320 kV (DC voltage,) all times, but increases in temperature in the cables and poor dissipation of this in surrounding areas can lead both to the deterioration of the cable as well as reduction of the voltage carrying capacity (ampacity). If the temperature exceeds than $70^\circ C$, the voltage carrying capacity of the cables is considerably affected.

Sometimes the naturally available backfill materials such as soils do not meet the necessary requirements. Many a times they have low thermal conductivities as well as poor structural, mechanical, physical properties. Therefore also, it may be necessary to find a material or formulate a mix that has better heat transfer characteristics than native soil. The objective of the study is to identify a material that meets the all the requirements listed above, thus obtaining a back-fill material that guarantees the best operating conditions for the cable and deliver required power supply even in the long term. Backfilling materials considered for the study includes two kinds of soils and two kinds of Controlled Low Strength Materials (CLSMs) containing large quantity of recycled materials. Two soils considered in the study have distinct properties. The CLSMs were studied for their potential application as backfilling materials by changing their composition. CLSMs were formulated at different cement contents, RAP content and water to powder ratios, to study their thermal properties. CLSMs were considered for this study to maximize the reuse of waste materials and avoid its land filling to develop sustainable pavement solutions. Several factors affecting the thermal conductivity of backfilling materials are explained in this study and thermal stability of the back-fill materials are also discussed.

It should be noted that all analyses, sample preparation and measurements were made in the laboratory. This analysis should be accompanied by field measurements, since these provide true parameters for a certain time and location. However, through accurate laboratory analysis, samples can

be recreated that accurately sum up actual in-situ conditions. Any kind of in-situ tests were not conducted due to lack of time and not included in this thesis.

1.3 Outline of the Thesis

The second chapter of the thesis discusses about the Frejus tunnel where a cement based CLSM is planning to use as a backfilling material for the construction of a pavement. Third chapter summarizes the available literature on the area of thermal conductivity of construction materials such as soils and cement based materials. Different models available for the prediction of thermal conductivity of such materials are explained along with the factors affecting their thermal properties. Fourth and Fifth chapters explains the material and methods used to conduct this study. The factors affecting the thermal conductivity of considered backfilling materials and model for their prediction are explained in chapter six *Results and Discussions*. Thermal stability of the different backfill materials are also discussed in last chapter. Finally, the conclusions drawn from this study are presented.

CHAPTER 2

THE CASE STUDY OF FREJUS TUNNEL

Circular cross-sections are commonly adopted during the design of road or railway tunnels around the world. This is due to the various design considerations such as the type of terrain, size and length of the tunnel, availability of space etc. Frejus tunnel is one such tunnel with a circular cross-section (*Figure 1*). The excavation methodology adopted for this tunnel is full face mechanized method. The lower part of the tunnel section needs to be backfilled for the construction of the pavements. Normally, the backfilling is performed in different layers using a suitable backfilling material and it provides necessary bearing capacity for the pavements.

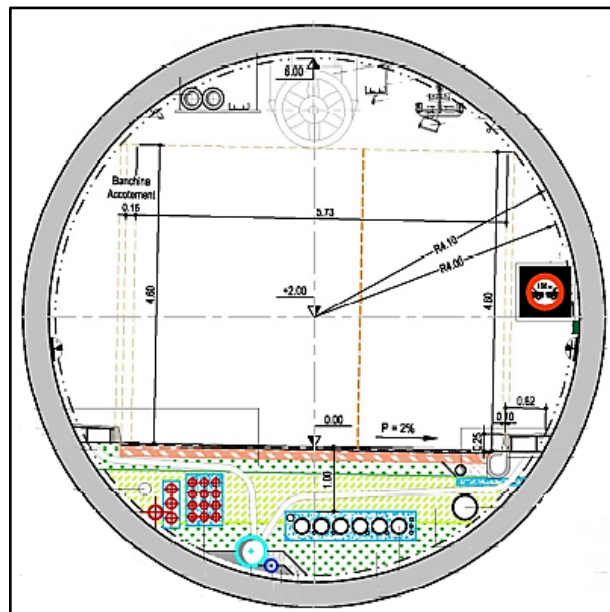


Fig. 1 Tunnel Back-Fill Section.[1]

The design of the asphalt pavement –layers- and their thicknesses on tunnels depend on several issues such as:

- Type of tunnel (immersed /precast or drilled/bored tunnel –where the bearing capacity of the subgrade may need to be considered);
- Design life of the pavement;
- Expected amount of traffic expressed on equivalent standard axle loads;
- Materials available locally;
- The temperature in the tunnel, and environmental conditions in general.

These requirements can be translated into functional requirements, in relation to the following issues:

- skid resistance (safety);
- safe in use and during accidents (safety);
- visibility / color / light reflection (safety / energy);
- longitudinal and transverse evenness (comfort);
- noise reduction aptitude (comfort);
- road construction - maintenance (efficient cost);
- durability (sustainability)

The requirements for roads in tunnels are comparable with the requirements for a traditional road surface in general. The surface layer should be safe and comfortable for drivers, sustainable and cost efficient.

The present study focuses on the backfilling of lower space, which is often used for the housing of various utility lines such as pipes and pumps for the collection of drainage water or for the passage of high-voltage lines that carry electricity to different localities or countries, such as France- Italy in the case of Frejus tunnel. The presence of high voltage cables brings more complexity to the selection backfilling materials. In such cases backfilling materials must have high thermal conductivity in order to ensure smooth power transmission for a long term. The filling material must comply with adequate specifications to dissipate the heat generated by the high voltage lines quickly without causing any problems to the transmission lines or deteriorate the cables.

2.1 The Frejus tunnel

The first Frejus road tunnel connects France and Italy through the Northern Alps. It is located between the town of Modane in France and Bardonecchia in Italy and runs parallel to the Frejus railway tunnel. The Frejus tunnel is the sixth longest road tunnel in the world (12.87m) and it was opened in 1980. It costed approximately two billions of francs at that time. SFTRF manages the French section of the tunnel, while the Italian section is managed by SITAF.

The tunnel construction started in 1973 and finished in 1979. The bore was driven by blasting through the Alpines using explosives. The French end of the tunnel has one vertical shaft, whereas the Italian end consists of two shafts for ventilation.

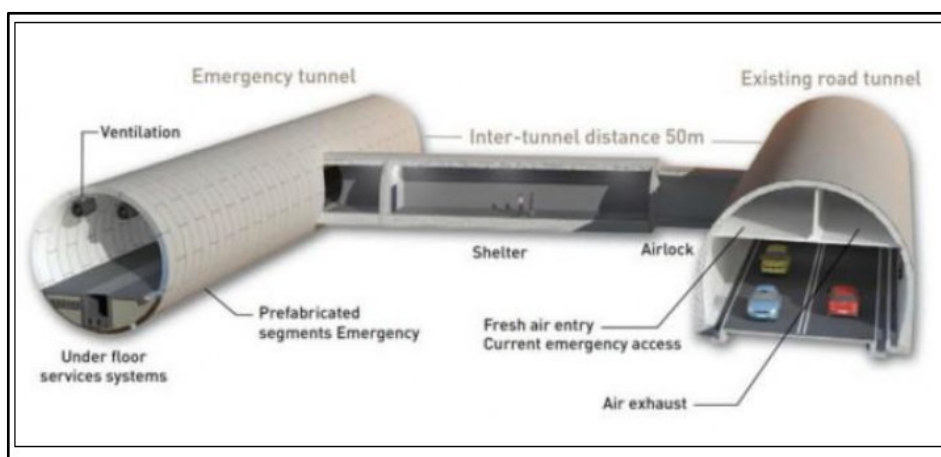


Fig. 2 Sections of The Tunnel

The Frejus tunnel sections (*Figure 2*) consist of two traffic lanes. The tunnel site is monitored continuously by 220 cameras. A parallel rescue tunnel is used in case of emergencies. In July 2011, started the excavation of the second tube to comply with EU directives for tunnels included in the Ten-T network. This second safety tunnel is also due to be built alongside the main tunnel at 50m. The safety systems at the site are also due to be improved, to meet new European Union standards that were enforced in 2014.

2.2 Second Tunnel

On July of 2011 began, in the French side, the excavation of the second tube to comply with EU directives of the galleries, included in the network Ten-T (English acronym for Trans-European Transport Networks, i.e. transport networks trans-European). The TBM "Anna" took 580 days to dig the French side and 504 days to complete the Italian front (non-stopping at the border, but continuing to dig into Italy), resulting in the breakthrough of the 17 November 2014.



Fig. 3 The Second Tunnel

The second tube (*Figure 3*), long 12.848m (6.495m in France, 6.353m in the Italian side) runs parallel to the one already in operation and will be joined to it by a series of connecting branches when installations and emergency shelters are located. It shall come into operation in 2019, thus making the Frejus tunnel the longest double-barreled European gallery, removing the title to the Gran Sasso tunnel. Doubling the Frejus comes from the need of more security; the initial project, in fact, predicted a profit of 5.50 m diameter, used only for the passage of emergency vehicles; work needed to comply with the standards required in the Community and to allow a second escape route in case of fire, avoid the recurrence of tragedies such as the Mont Blanc in March 1999.

The transit tunnel, instead, is configured to all effects as a second barrel of a twin-tube tunnel, with evident improvements on safety of users, related to the fact that the circulation within each barrel is in a unidirectional manner. The safety tunnel, in fact, increases the current safety standards only with respect to the speed and efficiency of assistance interventions, while the flow separation is an active safety system, which drastically reduces the chance of an accident and it eliminates the possibility that there may be a front crash. The separation of the streams also allows better management of ventilation (the smoke would go in the direction of travel) in normal operation, but especially in case of fire.

As for the skills about the realization of the work, there are two operating companies: the Italian SITAF and SFTRF French. In particular, the Italian Society for the Frejus Tunnel Motorway stock (SITAF S.p.A.), established the concession from 1973 until 2050 of the A32 Autostrada Torino - Bardonecchia and the Frejus Tunnel (T4). In turn, SITAF has been divided into four subsidiaries: Ok-Goals LTD, Tecnositaf S.p.A., Engineering S.p.A., Sitalfa S.p.A.; the latter (born for the realization and the direct execution of ordinary and extraordinary maintenance of the highway and civil installations and of the SITAF works) includes the production plant of Salbertrand, which provides directly the materials for the realization tunnel and, in our case under study, it will produce concrete for the foundation of the gallery.

2.3. Characteristics of the Tunnel

The Safety Gallery, in the new transit tunnel configuration, runs parallel to the existing tunnel of Frejus (T4), according to an average distance of 50 m between the two arches. The characteristics of the new tunnel are the following []

- Length 12.878 m at an average distance of 50 m from the service tunnel;
- Internal diameter of 8.00 m;
- Average slope 0.54% (France - Italy);
- 34 shelters (16 of Italian jurisdiction) with an average distance of 367 m and the surface for users of 110 m²;
- 10 Stations techniques with medium wheelbase of 1.430 m;
- longitudinal ventilation with accelerators to time and two additional plants.

The work has an excavation diameter of 9.46 m (diameter of the cutter head) or 9 m (top surface of the concrete segments) and an inner diameter (top surface of the precast segments) equal to 8 m. (*Figure.4*)



Fig. 4. Tunnel construction

The manufacture of the blocks of reinforced concrete (*Figure 5*) (concrete class Rck 45/55), forming the coating ring, took place at the plant in Salbertrand; the tunnel lining ring has been built simultaneously with the progress of the excavation of the drill (specifically mounted behind the TBM). Each ring consists of 7 different elements for which were built 5 identical metal moulds for each element.

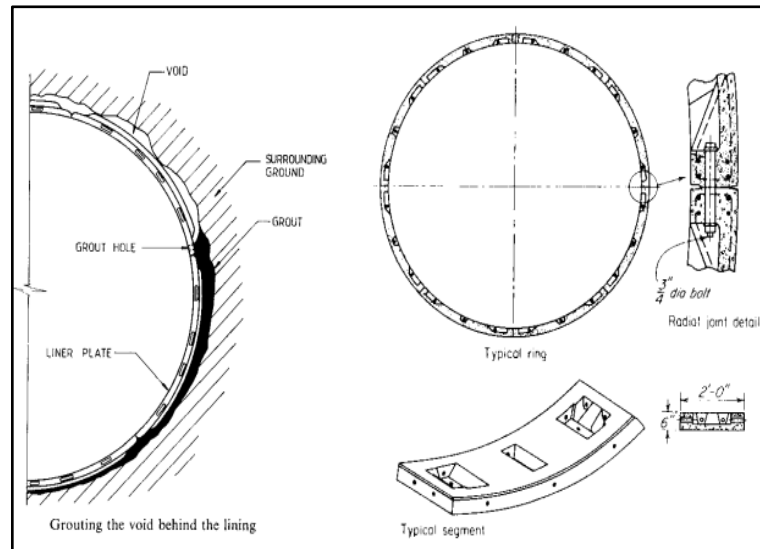


Fig. 5. Coating Ring

In the lower part of the section will be allocated underground utilities, which will be incorporated in the said cement filling material, the object of study. Such concrete is therefore created as a road foundation, adapting the characteristics of a concrete to the work requirements.

In the lower part of the section will be allocated underground utilities. One of them, is the location of high voltage cables (*Figure 6*) that run the entire length of the tunnel and perform the function of carrying power from one country to another. This is the object of study.

All of details of inputs and parameter are include in Appendix 1

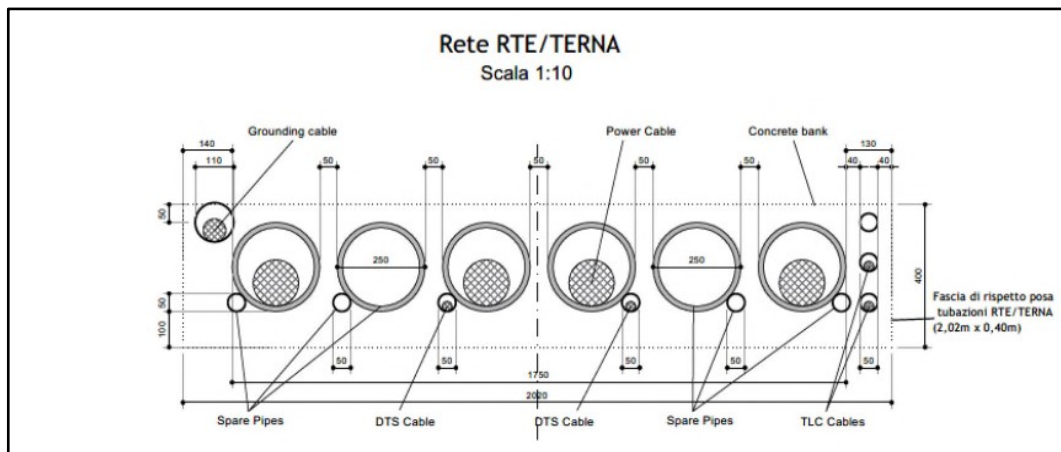


Fig. 6 Ducts of underground high-tension network

CHAPTER 3

LITERATURE REVIEW

It was necessary to conduct a literature search on the several types of backfilling materials to identify a material that possess all the required properties. This chapter explains the literature search on thermal conductivity of soils and cement based materials. Also, the influence of thermal properties of the backfill materials on the carrying capacity of high voltage in buried cables are discussed. The working principle of thermal conductivity measurement instrument used in the laboratory and its operation is also explained.

Definitions

-Thermal conductivity, k ($W/(m \cdot K)$): the ability for a material to transport thermal energy [2]

-Thermal resistivity, ρ ($cm \cdot ^\circ C/W$): a material's resistance to transport thermal energy. The thermal resistivity is the inverse of the thermal conductivity $\rho=1/k$ [2]

3.1 Soil

3.1.1 Structure of porous media

The principal structure of soils consists of solid soil particles (V_s), pore volume (V_p) and related masses (m). The pore volume is partly filled with water and air in nature, depending on its location with respect to the water table. if it is below, these will be completely filled with water. A well compacted soil has a lower pore volume (higher density). The relationship between the pore volume and the total volume is the porosity (V_p/V). The degree of water saturation (S_r) is a measure that represents how full are the pores with water ($S_r=V_w/V_p$). The density can be defined with mass-

volume ratios, γ . The dry density is the ratio between the dry solid mass (M_s) and the total volume (V). The water content is related to the mass of water (M_w) and the total mass (M) but in the geotechnical papers it is common to relate to the dry mass (M_s). Some definitions are clarified below:

Tab. 1 Geotechnical Parameters of Soil [2].

Density of solid particles, ρ_s (kg/m ³)	$\rho_s = m_s/V_s$
Bulk density, ρ (kg/m ³)	$\rho = m/V = \rho_d \cdot (1+w)$
Dry density, ρ_d (kg/m ³)	$\rho_d = m_s/V = \rho \cdot (1/(1+w))$
Water content, w_h (%)	$w_h = m_w/m$
Water ratio, w (%) (or water content)	$w = m_w/m_s$
Volumetric water content, Θ (%)	$\Theta = V_w/V = (\rho_d/\rho_w) \cdot w = n \cdot S_r$
Porosity, n (%)	$n = V_p/V = 1 - \rho_d/\rho_s$
Degree of water saturation, S_r (%)	$S_r = V_w/V_p$

3.1.2 Soil Classification

Different classification systems are adopted for the soil based on different criteria. Classification systems provide a way to express concisely the typical characteristics of soils. Two classification systems are commonly used. Both systems take into account the particle size distribution and Atterberg limits. These are the classification systems of the **American Association of State Highway and Transportation Officials** (AASHTO) and the unified system of soil classification.

In AASHTO classification the soils are classified into seven groups from A1 to A7 (*Table 2*), according to their granulometry and plasticity. More specifically, depending on the percentage of soil grains that passes through the screens No. 200, 40 and 10, and the Atterberg Limits of the fraction passing through the sieve No. 40. These seven groups correspond to two large categories of soil, granular soils (with no more than 35% passing through sieve No. 200) and silt-clayey soils (more than 35% passing through sieve No. 200).

Tab. 2 Classification of Highway Subgrade Materials [3]

General classification	Granular materials (35% or less of total sample passing No. 200)						
	A-1		A-3	A-2			
Group classification	A-1-a	A-1-b			A-2-4	A-2-5	A-2-6
Sieve analysis (percent passing)							
No. 10	50 max.		51 min.				
No. 40	30 max.	50 max.	10 max.	35 max.	35 max.	35 max.	35 max.
No. 200	15 max.	25 max.					
Characteristics of fraction passing No. 40							
Liquid limit			NP	40 max. 10 max.	41 min. 10 max.	40 max. 11 min.	41 min. 11 min.
Plasticity index	6 max.						
Usual types of significant constituent materials	Stone fragments, gravel, and sand		Fine sand	Silty or clayey gravel and sand			
General subgrade rating	Excellent to good						
General classification	Silt-clay materials (more than 35% of total sample passing No. 200)						
Group classification			A-4	A-5	A-6		A-7 A-7-5* A-7-6†
Sieve analysis (percent passing)							
No. 10							
No. 40			36 min.	36 min.	36 min.		36 min.
No. 200							
Characteristics of fraction passing No. 40							
Liquid limit			40 max.	41 min.	40 max.		41 min.
Plasticity index			10 max.	10 max.	11 min.		11 min.
Usual types of significant constituent materials			Silty soils		Clayey soils		
General subgrade rating	Fair to poor						
For A-7-5, $PI \leq LL - 30$							
For A-7-6, $PI > LL - 30$							

The category of granular soils; stones fragment, sand and gravel; it is composed of groups A-1, A-2 and A-3, and its behaviour is, in general, good to excellent, except subgroups A-2-6 and A-2-7, which behave like clay soils due to the high plasticity of the fines it contains, provided that the percentage of these exceeds 15%. The groups included by the granular soils are the following:

- A-1: Corresponds to a well-graded mixture of gravel, sand (coarse and fine) and fine non-plastic or very plastic. Also included in this group are well-graded mixtures of gravel and sand without fines.
- A-1-a: Includes soils with a predominance of gravel, with or without well-graduated fine material.
- A-1-b: Includes soils consisting mainly of coarse sands, with or without fine material well graduated.
- A-3: It corresponds, typically, to soils constituted by fine sand of beach or dune, of wind origin, without fine silty or clayey or with a small amount of non-plastic silt. This group also includes fluvial deposits of poorly graded fine sand with small amounts of coarse sand or gravel.
- A-2: This group includes all soils that contain 35% or less of material passing through sieve No. 200 and that cannot be classified in groups A-1 and A-3, because the percentage of fine or plasticity of these (or both) are above the limits set for these groups. For all this, this group contains a great

variety of granular soils that will be between those corresponding to groups A-1 and A-3 and groups A-4, A-5, A-6 and A-7.

- A-2-4 and A-2-5: These subgroups include soils that contain 35% or less of material that passes through the sieve No. 200 and whose fraction that passes through the sieve No. 40 has the characteristics of the Groups A-4 and A-5, of silty soils. These subgroups include soils composed of gravel and coarse sand with silt contents or plasticity indexes above the limitations of group A-1, and soils composed of fine sand with a proportion of non-plastic silt that exceeds the limitation of group A-3.
- A-2-6 and A-2-7: These subgroups include soils as those described for subgroups A-2-4 and A-2-5, except that the fines contain plastic clay with the characteristics of Groups A-6 and A-7. [3]

The category of silt-clayey soils is composed of groups A-4, A-5, A-6 and A-7. In this category, the soils are classified in the different groups based solely on their liquid limit and their plasticity index, according to the zones of the following plasticity graph. In this way, the soils of group A-2 are also classified in the different subgroups.

The groups included in the granular soils are the following:

- A-4: The typical soil of this group is a non-plastic or moderately plastic silty soil, which normally has 75% or more of material that passes through the No. 200 sieve. Also included in this group are the soils constituted by mixtures of fine silty soil and up to 64% gravel and sand.
- A-5: The typical soil of this group is similar to the one described in group A-4, except that it usually has diatomaceous or micaceous character, and can be very compressible, as indicated by its high liquid limit.
- A-6: The typical soil of this group is a clay clayey soil, which normally has 75% or more of material passing through the No. 200 sieve. Also included in this group are mixtures of fine clay soil and up to 64 % of gravels and sands. These soils generally experience large volume changes between dry and wet states.
 - A-7: The typical soil of this group is similar to that described in group A-6, except that it has the characteristics of high liquid limit of group A-5, and can be elastic and subject to large volume changes.
 - A-7-5: This subgroup includes soils with a moderate plasticity index in relation to the liquid limit and which can be highly compressible, in addition to being subject to significant changes in volume.
 - A-7-6: Soils with a high plasticity index in relation to the liquid limit and which are subject to very important changes in volume are included in this subgroup.

All this description can be summarized in the following *Figure 7* in function of the limits of Atterberg:

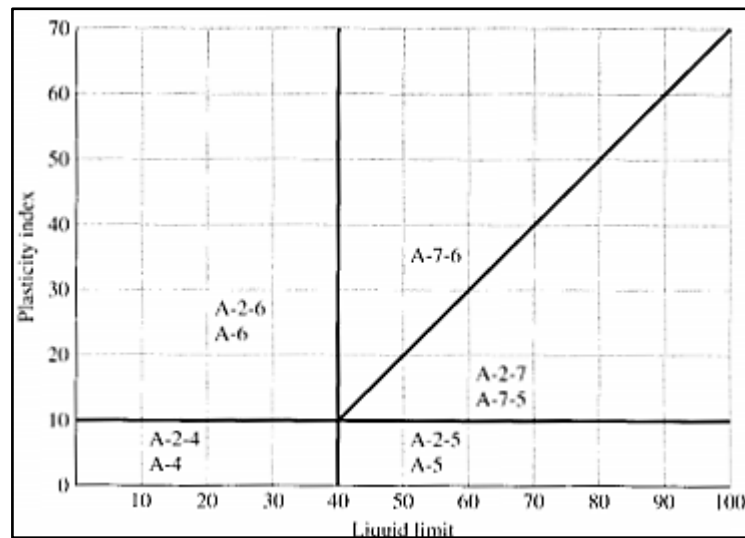


Fig. 7 Range of liquid limit and plasticity index for soils in groups [3]

3.1.3 Applications

Group A₁: In the drafting of the ground movement plan, the sub-group A1-a soil, especially if well-assorted granulometry, are typically reserved for earthworks requiring higher mechanical properties and / or underlying layers [4]

Group A₃: Usually the use without special arrangements is limited to the realization of reclamation of the laying plans of the detectors and of anti-capillary layers; lands of this group may be used to form the body of the detector if it has a uniformity coefficient (D_{60} / D_{10}) of not less than 7.

For sags with uniform granulometry, however, either a cement treatment, or a granulometric correction, or both, must be foreseen. [4]

Group A₂₋₄ and A₂₋₅: They generally have low permeability and low capillary rise: therefore, they do not require special measures to protect the underlay (or underfloor) layer from the frost and the above pavement. [4]

Group A₂₋₆ e A₂₋₇: When the fine fraction does not exceed 12% and if there are no large pieces of material ($D > 71$ mm), these lands have no particular constraints on constipation.

The gravel and the clayey sands of these subgroups are normally conveniently used for the formation of the data, especially when they have a $IG = 0$ group index. [4]

Put in situ, they have a low permeability medium and capillary rise height, which results in high risk of formation of ice lenses by frost action. For this reason, in the presence of superficial surface and prolonged duration of low temperature climatic conditions, their use should be avoided in the formation of substrate layers and limited to layers below 2.00 m from the floor of the pavement road, at the lower floor of an anti-capillary layer of not less than 30 cm thick.

Group A₄, A₅, A₆ e A₇: Surveys made with these soils should therefore be protected from inland and exterior waters, by anti-capillary layers, drainage screens, timely lateral hinges with inertia; - the presence of pebbles and larger pieces of material may prevent the action of the mixing means and thus make it impossible to stabilize the lime. [4]

The difficulties of compacting the clay of groups A₆ and A₇, the generally low mechanical properties of the layers as well as the protection measures from the waters to be put into effect limit the use of these lands to be found to be of little importance.

If there are no large-sized items, the lands of the A₆ and A₇ groups are well suited for lime stabilization. [4]

3.2 Thermal Conductivity of Soils

3.2.1 Thermal Transport Mechanisms

The thermal energy can be transported in the different materials by conduction, radiation, convection and by diffusion of steam and water. Thermal conduction is the most dominant transport mechanism in soils. High water content, density and quartz content are the most important factors that contributes to high thermal conductivity in soils.[2]

Radiation can have an influence in coarse materials and convection could have an influence in case of saturated soils.[2]

Thermal conductivity of soils is influenced by different parameters such as their mineralogy, moisture content and density. Thermal conductivity of soils increases with increase in bulk density and moisture content. Increase in the percentage of organic matter decreased thermal conductivity. Sandy soils have higher thermal conductivity than clayey soils due to their difference in mineralogical composition [5]. Thermal conductivity of soils could be also affected by the particle size, shape and gradation. Heat conduction takes place through the contact points since air is very weak in conduction.

Relationship between thermal properties of soils and volume fractions of soil, water, solids and air is an important point to analysed, because this variable have the more influence in the thermal ability to take away the heat.

Most importantly moisture state influences the thermal conductivity; it significantly increases when the soil is saturated. This is due to presence of the water on the void spaces which is otherwise filled with air . Comparing thermal conductivity of clay and sandy soils, an Increase in thermal conductivity with increase in bulk density was observed in both soils but rate of increase was higher in sandy soil compared to clay [6].

There are different models to predict the thermal conductivity of soils. Review of different models for the prediction of thermal conductivity of soils are presented by different researchers [7] [8] [9].

Based on the model analysis it was proposed that the quartz content and moisture content have the maximum influence on the thermal conductivity of the soils [7]. It was established that the ordered sequence of typical thermal conductivity values are;

$$k_{\text{air}} < k_{\text{dry_soil}} < k_{\text{water}} < k_{\text{saturated_soil}} < k_{\text{mineral}}$$

Heat transfer is predominantly taking place through conduction in soils [8].

Tab. 3 Thermal resistivity of different soil materials [10]

Soil Material	(ρ)(°C—cm/W)
Quartz Grains	11
Granite Grains	26
Limestone Grains	45
Sandstone Grains	58
Mica Grains	170
Water	165
Organic	400 Wet — 700 Dry
Air	4000

Soils shows a critical moisture content with respect to their thermal conductivity, Critical moisture content is the moisture content at which the continuous bridge mechanism of the water film inside soil microstructure breaks, hence further reduction in moisture content creates disproportionate increase in the thermal resistivity [11].

Low moisture content could show high values of thermal resistivity (inverse of conductivity) because when the soil is in a dry state, the spaces between the soil particles are completely occupied by air and as mentioned above, the air has more aptitude to resist the transfer of heat than water. ($K_{\text{aire}} \sim 45 \text{ } ^\circ\text{C.m/W}$ – $K_{\text{water}} \sim 1.65 \text{ } ^\circ\text{C.m/W}$). Through convection and radiation heat loss in free air are often more efficient than thermal conduction, in the confined, interstitial spaces between soil particles. this increase the thermal resistive. The *Figure 8.* show this.

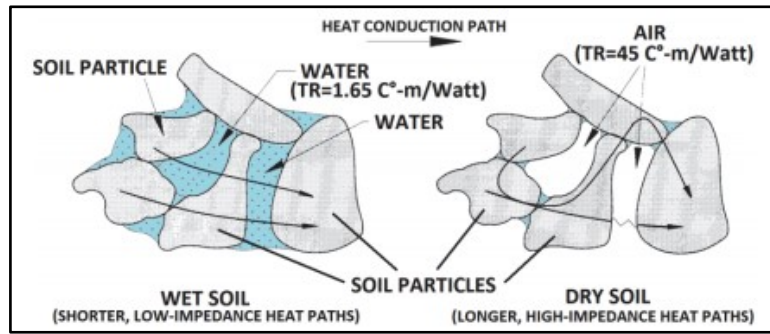


Fig. 8 Conceptual heat transfer in wet (left) and dry (right) condition in soil [12]

In the Figure 9, thermal behaviour of different types of soil with their the moisture content is shown. The presence of a critical moisture content can be identified, the resistivity sharply increases once the moisture content is lower than the critical moisture content. This phenomenon also depends on the type of soil. Some characteristic thermal resistivity versus moisture content curves for soils including sands, clays and silts are shown below.

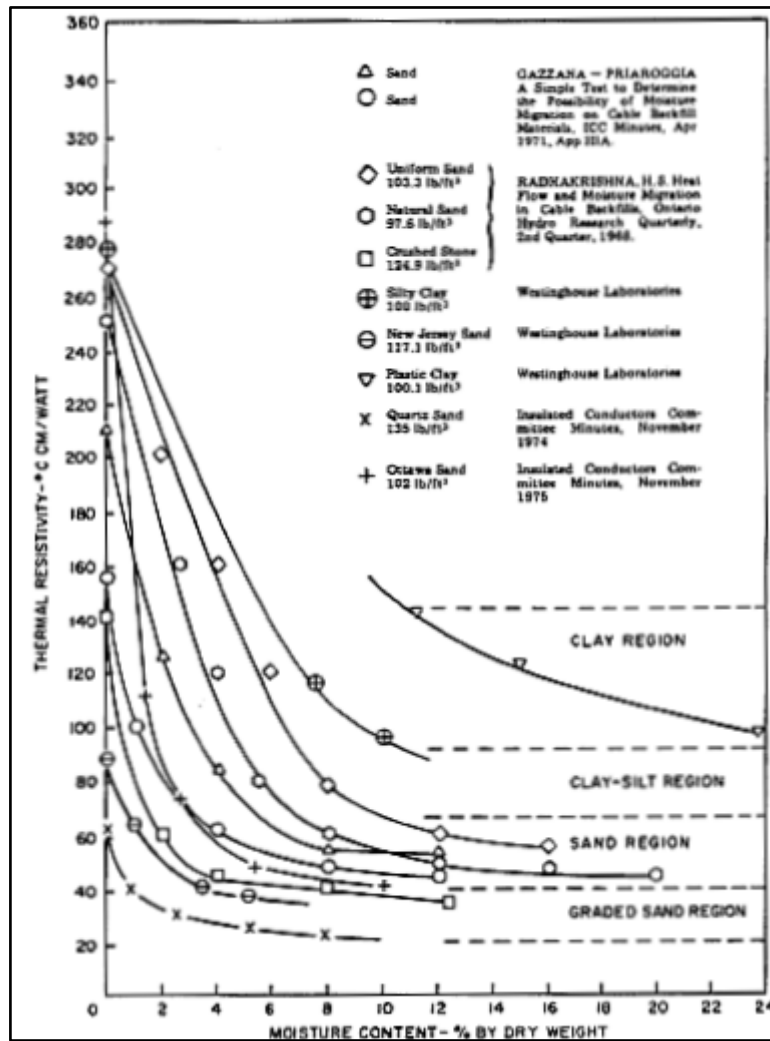


Fig. 9 Thermal Properties Characteristics of soil. [10]

3.3 Controlled Low-Strength Material (CLSM)

CLSM, as defined by American Concrete Institute (ACI) Committee 229, is a self-compacted, cementitious material used primarily as a backfill instead of compacted soil fill. Several terms are currently used to describe this material, including flowable fill, unshrinkable fill, controlled density fill, flowable mortar, plastic soil-cement, soil-cement slurry, K-Krete and other various names. Controlled Low-Strength Materials are defined by “Cement and Concrete Terminology (ACI 116R)” as materials that result in a compressive strength of 8.3 MPa or less. However, most current CLSM applications require unconfined compressive strength of 2.1 MPa or less. Some researchers consider the range of 0.3 to 1.1 MPa as a good index of sufficient strength and easy future excavation. For applications where future excavations are expected, the excavatability of CLSM is critical and this may determine the success of CLSM in practices such as utility bedding.

CLSM is typically specified and used in lieu of compacted fill in various applications, especially for backfill, utility bedding, void fill, and bridge approaches. Backfill includes applications such as backfilling walls (e.g., retaining walls) or trenches. Utility bedding applications involve the use of CLSM as a bedding material for pipe, electrical, and other types of utilities and conduits. Void-filling applications include the filling of sewers, tunnel shafts, basements, or other underground structures.

CLSM is also used in bridge approaches, either as a subbase for the bridge approach slab or as backfill against wingwalls or other elements. There are various inherent advantages of using CLSM instead of compacted fill in these applications. These benefits include reduced labor and equipment costs (due to self-leveling properties and no need for compaction), faster construction, and the ability to place material in confined spaces. The relatively low strength of CLSM is advantageous because it allows for future excavation, if required. Another advantage of CLSM is that it often contains by-product materials, such as fly ash and foundry sand, thereby reducing the demand on landfills, where these materials may otherwise be deposited.

The CLSMs provide corrosion protection under the pipes: in fact, since the mid-1970s, some Iowa agencies have started to build underground pipes for electrical wiring in the CLSM foundations, which can prevent crack water from entering the tubes and the base, thus eroding the support. In addition, by adding a colorant to CLSM blends that does not affect the characteristics of the material, you can protect the pipes from accidental damage caused by probable future excavations.

From laboratory tests it turned out that CLSMs resist erosion better than many other materials; of the comparison with sand and clay, and it is evident that the loss of material and the presence of suspended particles after having been subjected to a water jet at speeds of 1.7 feet / second are amply contained. Precisely because of this corrosion-proof property, often the small lacerations present on the banks of rivers, basins or under the drainage channels of the dams are filled with CLSM, replacing the fillings made with crushed rock; In addition to this, such mortars are also used to fill existing

voids under pavements, sidewalks, bridges and other structures where natural soil or non-cohesive granular fillings have been eroded or eliminated by atmospheric agents.

3.3.1. Applications

As stated earlier, the primary application of CLSM is as a structural fill or backfill in lieu of compacted soil. Because CLSM needs no compaction and can be designed to be fluid, it is ideal for use in tight or restricted-access areas where placing and compacting fill is difficult. If future excavation is anticipated, the maximum long-term compressive strength should generally not exceed 2.1 MPa. The following applications are intended to present a range of uses for CLSM

- **Blackfills**

CLSM can be readily placed into a trench, hole or other cavity. Compaction is not required; hence, the trench width or size of excavation can be reduced. Granular or site-excavated backfill, even if compacted properly in the required layer thickness, cannot achieve the uniformity and density of CLSM.

- **Structural fills**

Depending upon the strength requirements, CLSM can be used for foundation support. Compressive strengths can vary from 0.7 to 8.3 MPa (100 to 1200 psi) depending upon application. In the case of weak soils, it can distribute the structure's load over a greater area. For uneven or nonuniform subgrades under foundation footings and slabs, CLSM can provide a uniform and level surface. Compressive strengths will vary depending upon project requirements. Because of its strength, CLSM may reduce the required thickness or strength requirements of the slab.

- **Pavement bases**

CLSM mixtures can be used for pavement bases, subbases, and subgrades. The mixture would be placed directly from the mixer onto the subgrade between existing curbs. For base course design under flexible pavements, structural coefficients differ depending upon the strength of the CLSM. Based on structural coefficient values for cement-treated bases derived from data obtained in several states, the structural coefficient of a CLSM layer can be estimated to range from 0.16 to 0.28 for compressive strengths from 2.8 to 8.3 MPa.

Another important application of these blends is the filling of tunnels, galleries, abandoned drainage systems; thanks to the above-mentioned high workability of the material, the discharge of the concrete mixer takes place in a very easy way.

3.3.2. Materials

Conventional CLSM mixtures usually consist of water, Portland cement, fly ash or other similar products, and fine or coarse aggregates or both. Some mixtures consist of water, portland cement, and fly ash only. Although materials used in CLSM mixtures meet ASTM or other standard requirements, the use of standardized materials is not always necessary. Selection of materials should

be based on availability, cost, specific application, and the necessary characteristics of the mixture, including flowability, strength, excavability, and density.

Cement: provides the cohesion and strength for CLSM mixtures. For most applications, Type I or Type II portland cement conforming to ASTM C 150 is normally used. Other types of cement, including blended cements conforming to ASTM C 595, can be used if prior testing indicates acceptable results;

Fly ash Coal-combustion: is sometimes used to improve flowability. Its use can also increase strength and reduce bleeding, shrinkage, and permeability. High fly ash-content mixtures result in lower-density CLSM when compared with mixtures with high aggregate contents. Fly ashes used in CLSM mixtures do not need to conform to either Class F or C as described in ASTM C 618. Trial mixtures should be prepared to determine whether the mixture will meet the specified requirements;

Admixtures: Based on organic compounds, plasticizers manage to optimize concrete designs, decreasing the needs of water and cement to achieve the properties required by construction.

The direct effect of a plasticizer on the cement paste is to decrease the viscosity of the same. A plasticizer causes the cement paste to become more "liquid", to flow faster. It does this by coating the cement particles and causing a repulsion between them. When the particles repel each other, there is less resistance to the flow of the set (less friction), a micro-floccule elimination also takes place, which allows the release and better distribution of the water.

In this way the cement paste flows more and therefore the concrete also does. A greater fluidity of the concrete then allows the amount of water to be reduced, thus modifying the properties of the paste (or glue), which with less water will increase its strength in a hardened state.

Water: that is acceptable for concrete mixtures is acceptable for CLSM mixtures;

Aggregates: are often the major constituent of a CLSM mixture. The type, grading, and shape of aggregates can affect the physical properties, such as flowability and compressive strength.

Aggregates complying with ASTM C 33 are generally used because concrete producers have these materials in stock. Granular excavation materials with somewhat lower-quality properties than concrete aggregate is a potential source of CLSM materials, and should be considered. Variations of the physical properties of the mixture components, however, will have a significant effect on the mixture's performance. Silty sands with up to 20% fines passing through a 75 μm (No. 200) sieve have proven satisfactory. Also, soils with wide variations in grading have shown to be effective. Soils with clay fines, however, have exhibited problems with incomplete mixing, stickiness of the mixtures, excess water demand, shrinkage, and variable strength. These types of soils are not usually considered for CLSM applications;

3.3.3 Properties

The properties of CLSM cross the boundaries between soils and concrete. CLSM is manufactured from materials similar to those used to produce concrete, and is placed from equipment in a fashion similar to that of concrete.

In-service CLSM, however, exhibits characteristic properties of soils. The properties of CLSM are affected by the constituents of the mixture and the proportions of the ingredients in the mixture. Because of the many factors that can affect CLSM, a wide range of values may exist for the various properties

Workability

Fluidity is what makes the CLSM unique as filling material because it allows self-leveling, flowing and filling all the voids and cavities that have been created during excavation, self-compacting without the aid of suitable equipment. This parameter is determined by spreading on plate, according to the requirements of ASTM D 6103.

Hardening

The hardening time is represented by the time required for cement mortar to pass from a fluid state to a solid, achieving sufficient strength to support a person's weight. Hardening is strongly related to the amount of water and cement used.

Pumping

The distribution of CLSMs may be by using the usual pumping equipment used for ordinary concrete; the excavations must be filled with mixtures with sufficient cohesiveness since they must be subjected to a significant pumping pressure to ensure a constant flow of material.

Segregation

Avoid the segregation phenomena that may cause separation of the constituents of the mixture, especially for mixtures packed with high water / cement ratios. Proper proportionality between the constituents allows the achievement of high degree of machinability, avoiding the emergence of segregative phenomena, which irretrievably compromise the final mechanical requisites. To this end, it is recommended to use aerated additives, which allow to maintain high working standards, reducing the water content, thus reducing the risk of segregation.

Thermal insulation, conductivity, permeability;

CLSMs have good thermal insulation properties; to increase this feature, they must have a low density and high porosity. To reduce density, mixtures containing light aggregates, including flying ash, are used to obtain good thermal conductivity, however, high density and low porosity must be obtained. It is therefore necessary to take into account parameters such as mineralogical composition, shape and particle size, organic content and specific weight. As far as permeability is concerned, it is similar to that of granular fillings, whose values fluctuate between 10^{-4} and 10^{-5} cm / sec. The permeability increases with the decrease in cement materials and the increase in aggregate content.

Strength:

Unconfined compressive strength is a measure of the load-carrying ability of CLSM. A CLSM compressive strength of 0.3 to 0.7 MPa (50 to 100 psi) equates to an allowable bearing capacity of a well-compacted soil. Maintaining strengths at a low level is a major objective for projects where later excavation is required. Some mixtures that are acceptable at early ages continue to gain strength with time, making future excavation difficult.

Density

Wet density of normal CLSM in place is in the range of 1840 to 2320 kg/m³ which is greater than most compacted materials. A CLSM mixture with only fly ash, cement, and water should have a density between 1440 to 1600 kg/m³. Pondered ash or basin ash CLSM mixture densities are typically in the range of 1360 to 1760 kg/m³. Dry density of CLSM can be expected to be substantially less than that of the wet density due to water loss. Lower unit weights can be achieved by using lightweight aggregates, high entrained-air contents, and foamed mixtures.

Permeability

Is similar to compacted granular fills. Typical values are in the range of 10^{-4} to 10^{-5} cm/sec. Mixtures of CLSM with higher strength and higher fines-content can achieve permeability as low as 10^{-7} cm/sec. Permeability is increased as cementitious materials are reduced and aggregate contents are increased.⁴ However, materials normally used for reducing permeability, such as bentonite clay and diatomaceous soil, can affect other properties and should be tested prior to use.

Shrinkage (cracking)

Shrinkage and shrinkage cracks do not affect the performance of CLSM. Several reports have indicated that minute shrinkage occurs with CLSM. Ultimate linear shrinkage is in the range of 0.02 to 0.05%

Excavability

The ability to excavate CLSM is an important consideration on many projects. In general, CLSM with a compressive strength of 0.3 MPa or less can be excavated manually. Mechanical equipment, such as backhoes, are used for compressive strengths of 0.7 to 1.4 MPa. The limits for excavability are somewhat arbitrary, depending upon the CLSM mixture. Mixtures using high quantities of coarse aggregate can be difficult to remove by hand, even at low strengths. Mixtures using fine sand or only fly ash as the aggregate filler have been excavated with a backhoe up to strengths of 2.1 MPa. When the re-excavability of the CLSM is of concern, the type and quantity of cementitious materials is important. Acceptable long-term performance has been achieved with cement contents from 24 to 59 kg/m³ and Class F fly ash contents up to 208 kg/m³. Because CLSM will typically continue to gain strength beyond the conventional 28-day testing period, it is suggested, especially for high cementitious-content CLSM, that long term strength tests be conducted to estimate the potential for re-excavability. In addition to limiting the cementitious content, entrained air can be used to keep compressive strengths low.

General characteristics

The CLSM therefore allows filling in trenches perfectly, in addition to ensuring perfect sealing at piping joints, the excellent filling resulting therefrom avoids the usual fluid leakage that occurs with loose soil fillings. The use of these blends also allows the excavation areas to be reopened quickly: in fact, after only 24 hours from the jet, the conglomerate reaches a deformation resistance equal to that of a compacted soil and after 48 hours reaches the performance of a cemented mix. The filling of filling due to the repeated loads of traffic is avoided: in fact, due to the perfect adhesion between the mortar and the wall of the excavation, and the homogeneity of the rigidity of the material, there are no usual cuts (with breakage of the bitumen restoration road) which occur when the filling is carried out with molten stone material or with conventional cementitious conglomerates.

3.4 Thermal Conductivity of Cement Based Materials

Cement based materials shows high thermal stability. Conventional cement concrete has very high strength and it's not recommended to use as a backfill material. Low strength cement based materials such as CLSMs could be used as a backfill material. Thermal conductivity of cement based mixes depends on its composition. Aggregates have the maximum thermal conductivity in concrete. At low W/C (water/cement), high thermal conductivity is obtained in cement based materials because cement has a higher conductivity than water. Thermal conductivity of fine aggregate is higher than coarse aggregate and aggregates are uniformly distributed in the mix with the inclusion of fine aggregates.

Fluidized Thermal Backfills (FTB) are special backfilling materials with high thermal conductivity and thermal stability. Thermal conductivity of class F flyash was examined for their future application as a Fluidized Thermal Backfill. Resistivity of fly ash decreases as the density and moisture content increases [13]. Different researchers studied the thermal properties of cement-based materials. Application of coal ash in thermal beds was demonstrated, Coal ash mixed with black cotton soil could be used as an engineered FTB [14].

Importance of FTB is shown with a real field example [15] There also exists a US patent on FTB[16]. Thermal conductivity of concrete was studied in detail [17]. Controlled Low Strength Materials (CLSMs) could be engineered to achieve high thermal conductivity and the density, porosity and moisture content are the main parameters that affect the thermal properties of a CLSM [18].

Thermal conductivity of cement based materials such as cement paste, concrete and mortar were studied previously by Kim et al. Predictive equations for thermal conductivity were formulated based on the parameters water to cement ratio, age, temperature and aggregate volume. It was found that the age of the specimen doesn't have any significant effect on the thermal conductivity[19].

Factors affecting the thermal properties of concrete and predictive models based on the composition of the mixes are also being developed [20]

3.5 Effect of Back-fill Thermal Conductivity on the Performance of Transmission Lines

The DC (Direct Current) power cable generates heat due to the electrical resistance in the cable. The ampacity (capacity for transport of electric current) of a cable system is influenced by the ability of the installation to dissipate heat in the surrounding medium since, the electrical resistance increases with the elevated temperature.

The cable is designed for an ampacity that generates a certain maximum temperature, related to the thermal conductivity of the filling material. If the design temperature is exceeded, it may influence the life of the cable.

The temperature of a buried cable is controlled by:

- the initial soil temperature at the actual depth and its variation
- the power distribution by time in the cable and the effective total thermal resistance of the surrounding media.

Thermal conductivity of the back-fill material influences transmission loses in electric conductors. [21][22][23]. Soil back fills tends to undergo a drying out with time which increases the thermal resistivity of the backfill. Resistivity of natural soil is very high, and it is highly variable depends on different parameters. Engineered backfills with a stable thermal conductivity will ensure

that the transmission cable will perform as per the design throughout its life time. . The cable's temperature during their operation is affected by the following factors [2]:

- Thermal properties of natural soil
- Natural undisturbed temperature and temperature variation in the ground
- A cable's thermal properties at different temperatures
- Type of cable, wire size and number of cables
- Laying depth for cable
- Distance between cables
- Dimensioning Electric power and its duration

Fluidized thermal backfill (FTB) is a specialized type of CLSM used around underground electric transmission and distribution cables to conduct heat away from the cable [24]. Different researchers work on the development of FTB. A new material with a very high thermal conductivity even in completely dry state was developed by the collaboration of Heidelberg Cement, nkt cables Cologne and of the University Duisburg-Essen [23]. Thermal conductivity of class F fly ash was determined [13] to be used in the thermal back-fills. Suitability of coal ash in FTB was estimated based on the available empirical equations[14].

The influence of thermal conductivity of the backfill material on the ampacity (current carrying capacity) of the high voltage cables is studied by different researchers. The ampacity significantly improves as the thermal conductivity of the backfill material increases as shown in *Figure 10*.

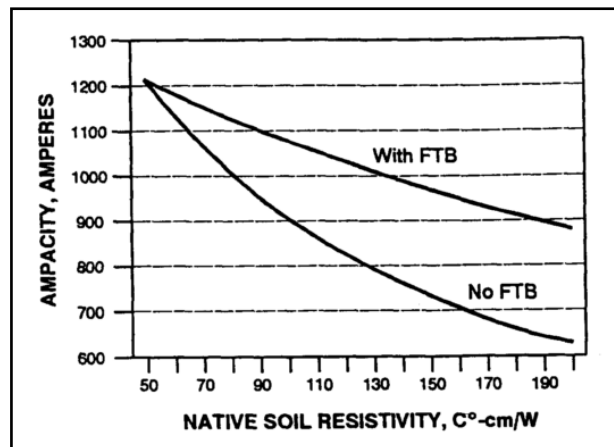


Fig. 10 Ampacity as a Function of Native Soil Resistivity and Presence of Controlled Backfill [15]

Thermal stability of the backfill material is an important property to ensure the same condition for the buried cable throughout its life time. Soils around the cables generally exhibit a dry out phenomena as the temperature around the cable increase. FTB shows better thermal stability and the influence of moisture on its thermal performance is very limited (*Figure 11*).

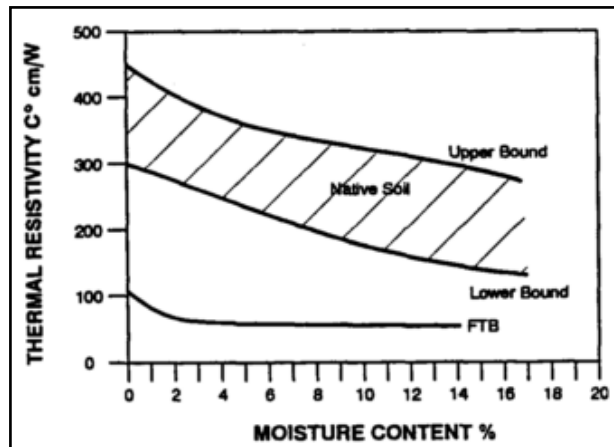


Fig. 11. Thermal stability of the typical backfill materials [15]

3.6 Thermal Conductivity Measurement

Thermal conductivity can be measured by using different techniques. There are direct and indirect methods for the determination of thermal conductivity. Laboratory techniques to measure the thermal conductivity include transient and steady state methods. In a transient technique, change in the thermal properties was monitored over a time after the application of a heat source where as in a steady state, the specimen was allowed to attain its steady state thermal condition before measurement and then it is disturbed with a heat source to measure the changes. In the present work, thermal conductivity was measured using a commercial needle probe. General Schematic Diagram for the thermal conductivity probe can be seen in the figures bellow

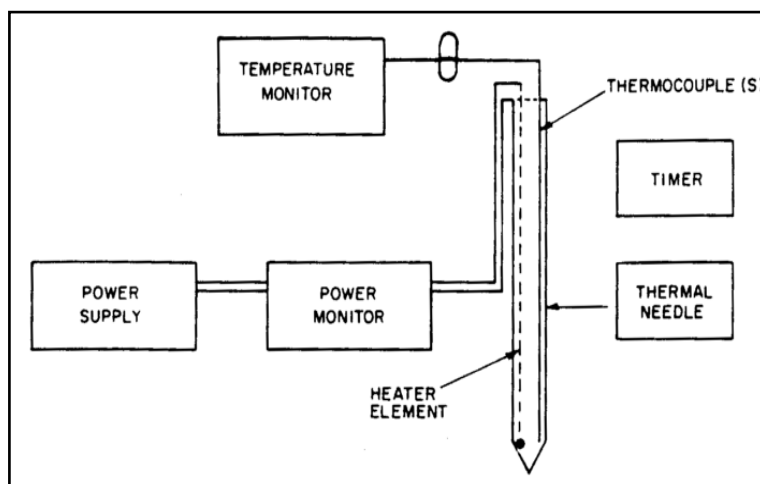


Fig. 12 General Schematic Diagram for the thermal conductivity probe [10]

There are various testing devices and their interpreting methods for measurement of thermal conductivity of concrete. These three distinct methods are generally used. First, the Two-Linear Parallel- Probe (TLPP) method, originally proposed by Carslaw, has been widely accepted to determine thermal conductivity. Two probes are inserted into two parallel holes drilled in the sample, where one probe is used as a heating source and the other as a temperature sensor. Also used are the plane-heat-source (PHS) method, and the hot-guarded plate (HGP) method to evaluate thermal conductivity. They are similar to the TLPP method in their basic principle but require additional efforts to cut the sample thin, and then firmly place the thermal probe on with epoxy.

3.6.1 Principle of Measurement

The applicability of cylindrical needles for the measurement of thermal conductivity was initially demonstrated by De Vries and Peck [25]. Needle probes for the measurement of thermal conductivity essentially consist of a heating wire, a current is passed through the heating wire and temperature of the probe is monitored over time. Analysis of the probe temperature is used to determine the thermal conductivity.

• Single Needle Algorithm

Heat is applied to a single needle for a time, t_h and temperature is monitored in that needle during heating and for an additional time equal to the after heating. Two needle sizes are used; One (the KR-1) is 6 cm long and 3.9 mm diameter. The other (the TR-1) is 2.4mm diameter and 10 cm long. The temperature during heating is computed from *equation 1*:

$$T = m_0 + m_2 \cdot t + m_3 \cdot \ln(t) \quad [eq. 1]$$

- m_0 is the ambient temperature during heating (which could include some offset for contact resistance and the heating element being adjacent to the temperature sensor inside the needle),
- m_2 is the rate of background temperature drift, and
- m_3 is the slope of a line relating temperature rise to logarithm of temperature.

During cooling the model is

$$T = m_1 + m_2 + m_3 \cdot \ln\left[\frac{t}{t < t_h}\right] \quad [eq. 2]$$

The thermal conductivity is computed from

$$k = \frac{q}{4\pi m_3} \quad [eq. 3]$$

Since these equations are long-time approximations to the exponential integral equations, we use only the final $\frac{2}{3}$ of the data collected (ignore early-time data) during heating and cooling. This approach has several advantages. One is that effects of contact resistance appear mainly in these early time data, so by analysing only the later time data the measurement better represents the thermal conductivity of the sample of interest. Another advantage is that can be solved by linear least squares, giving a solid and definite result. The same data, subjected to a non-linear least squares analysis can give a wide range of results depending on the starting point of the iteration because the single needle problem is susceptible to getting stuck in local minima. The linear least squares computation is also very fast.

3.6.2 Factors Influencing Measurements

The temperature rise of buried cables is directly dependent on the resistivity of the adjacent materials. The conductivity value that is used for temperature rise calculations is normally derived from materials thermal conductivity measurements.

During the measurement of soil thermal conductivity, there are factors that may adversely affect the accuracy of the test measurement:

- The migration of soil moisture
- The redistribution of moisture due to gravity
- Power supply stability

The migration of soil moisture away from the needle during the test may vary the results, thus giving a higher or lower conductivity. This may increase when the input power per unit area of the needle is high. The migration of moisture associated with the preliminary mass transfer can reduce the measurements of heat loss when the initial moisture content of the soil is less than 5% in some soils, particularly in the sands. Moisture migration can take place towards the end of the test, which results in a decrease in the apparent thermal conductivity of the soil.

The redistribution of moisture due to gravity. the results may vary in laboratory measurements of the soil. If this redistribution of moisture occurs during the measurement, the measurement of the conductivity normally increases. The error can be significant if the resistivity is sensitive to the change in moisture content at the density of the dry soil selected for the test.

Power supply stability must be maintained throughout the test. The power dissipated in the needle must be controlled so that variation in the magnitude of heat flux is kept within $\pm 1\%$.

3.7 Models for the Prediction of Thermal Conductivity.

In order to get closer to the most exact possible determination of the thermal conductivity in composite materials, it is necessary to resort to an important part of the literature on heat transfer and a large number of effective thermal conductivity models have been proposed to compare whether the thermal conductivities determined through these models are similar to those measured in the laboratory.

- *Thermal Conductivity Models on soils:* In the literature, you can find several types of models, which have been reviewed and categorized within the following groups: [8]

-*Mixing Models:* This type of model conceptualizes the multi-phase systems as a certain of combination of series and parallel soil, air and/or water blocks in the cubic cell or REV (representative elementary volume); and the effective thermal conductivity is calculate by mixing those block.

Empirical Models: this group is characterized by creating relationships between relative thermal conductivities and the degree of saturation or water contents, through an effective normalized value of thermal conductivity or also called Kersten number under the differences between saturation states thermal conductivities k_{sat} and dry states of thermal conductivity k_{dry} .

Mathematic Models: These models were adopted from predictive models of other physical properties, such as dielectric permittivity, magnetic permeability, electrical conductivity, and hydraulic conductivity; which are calculated by mathematical algorithms giving a thermal conductivity for each component in their volume fractions.

In this thesis, four types of empirical models will be used; Kersten (1949), Johansen (1975), Farouki (1981,1982) and Cote and Konrad (2005) models.

3.7.1 Kersten Model (1949)

It was created based on the relationships that were derived from the empirical data. Is based on the measurement of thermal conductivity in nineteen different types of soil between them; gravel, sands, clays, crushed stones and organic soils. The method used by Kersten was the single thermal probes method. Although the effects of the degree of saturation, minerology and texture of the soil were analyzed, the mathematical expressions of this model are based on moisture content and density. Kasten provides an equation for silts or clays and another for sandy soils. [7]

- Silts or Clay

$$k = [0.13 \log w - 0,0288] x 10^{0,0006243 \gamma d} \quad [eq. 4]$$

- Sandy Soil

$$k = [0,101 \log w + 0,0577] x 10^{0,0006243 \gamma d} \quad [eq. 5]$$

Where k is the thermal conductivity of soil, W/m.°K; w is the moisture content of soil, % ; γ_d is the dry unit weight of soil, kg/m³.

3.7.2 Johansen Model (1975)

He was the first to propose the concept of k_r (normalized thermal conductivity) which is also known as the Kersten number. he reported another relationship K_r - S_r . It can be used for soils both coarse and fine-grained in frozen or unfrozen state. [7]

The normalized thermal conductivity (k_r) is expressed by equation 6.

$$k_r = \frac{k - k_{dry}}{k_{sat} - k_{dry}} \quad [eq. 6]$$

where k_{sat} and k_{dry} are the soil thermal conductivities under fully saturation and dry condition respectively, [W/ m °K.]

In terms of thermal conductivity of saturated soils, equation 7 has been widely used as given below.

$$k_{sat} = k_w^n k_s^{1-n} \quad [eq. 7]$$

where k_w and k_s are the thermal conductivities of water and solid, [W/ m °K.], and n is the porosity

Johansen [26] also improved De Vries (1963) model, and then proposed an equation to predict thermal conductivity of dry soils

$$k_{dry} = 0.039n^{-2.2} \quad [eq. 8]$$

In addition proposed the following empirical relationships K_r - S_r for soils studied by Kersten (1949): [7]

- For median and fine Sand

$$k_r = 0.7 \log(S_r) + 1 \quad [eq. 9]$$

- For fine soil

$$k_r = \log(S_r) + 1 \quad [eq. 10]$$

According to Eqs (6,7,8,9/10), the thermal conductivity model proposed by Johansen is shown in the equation 11

$$k = (k_{sat} - k_{dry})k_r + k_{sat} \quad [eq. 11]$$

3.7.3 Farouki Model (1981,1982)

Farouki evaluated many theoretical and empirical models for the computation of thermal conductivity of soils. In general, the model proposed by Johansen (1975) gave the best results in the widest range of soils and degrees of saturation. [27]

Using the thermal conductivities in the saturated state derived from *equation 7* and in the dry state as *equation 12*. A modified form of the geometric mean method was thus developed as expressed by *equation 12* (in W/m°C), where fitting parameters α and β were set to 0.59 and 0.73 to fit experimental data:

$$k_{sat} = k_s^{(1-n)\alpha} k_a^{n\beta} \quad [eq. 12]$$

Simple mathematical equations are proposed to express the normalized thermal conductivity

$$k_r = \frac{4.7S_r}{1+3.75S_r} \quad [eq. 13]$$

Finally, the thermal conductivity is calculated from *equation 11*

3.7.4 Cote and Konrad Model (2005)

This model propose a k_r - S_r relationship incorporating a parameter κ that considers the type of soil. This has created a new generalization of thermal conductivity models for soil and construction materials.

$$k_r = \frac{\kappa S_r}{1+(\kappa-1)S_r} \quad [eq. 14]$$

Where κ is the parameter related to the soil type effect on k_r - S_r relationship, the suggested values are 4.5 for gravel, coarse sand; 3.55 for median and fine sand; and 1.69 for silts and clay.

Cote and Konrad model, proposed an equation to predict thermal conductivity of dry soils

$$k_{dry} = \chi 10^{-n\eta} \quad [eq. 15]$$

Where $\chi=1.7$ and $\eta=1.8$ for rocks and gravels, while $\chi=0.75$ and $\eta= 1.20$ for natural mineral soils.

After that the thermal conductivity is calculated from *equation 11*

3.7.5 Thermal conductivity model in Concrete.

There are not many models for the prediction of thermal conductivity of concrete as in the case of soils. It was understood that the age of the specimens doesn't have an effect on the thermal conductivity of the concrete, Therefore, thermal conductivity of concrete can be predicted by the relationship as functions of aggregate volume fraction, fine aggregate fraction, W/C ratio, temperature, and moisture condition in concrete as follows:[19]

$$k_c = k_{ref} \cdot [0.293 + 1.01AG] \cdot \left[0.8 \left(1.62 - 1.54 \left(\frac{W}{C} \right) \right) + 0.2R_h \right] [1.050.0025T] [0.86 + 0.0036 \left(\frac{S}{A} \right)] \quad [eq. 16]$$

where k_c denotes thermal conductivity of concrete, k_{ref} is a referenced thermal conductivity measured from specimens at a condition of $AG = 0.70$, $W/C = 0.4$, $S/A = 0.4$, $T = 20 \text{ } ^\circ\text{C}$, and $R_h = 1.0$, AG is an aggregate volume fraction in concrete., T is a temperature, S/A as fine aggregate volume fraction, Reveals a close relationship between thermal conductivity of concrete predicted from equation and its measured values can be plot and determinate the values of the sample correlation coefficient R .

For the determination of the equation described above, was taken into account the dependence of each test parameter on the thermal conductivity assumes a linear relationship to simplify the prediction equations. the measured thermal conductivity of the base sample was selected as reference and was called k_{ref} .

The relationships were:

- Relationship as a function of aggregate volume fraction.
- Relationship as a function of temperature.
- Relationship as a function of moisture condition.
- Relationship as a function of fine aggregate fraction

CHAPTER 4

SOILS AND CLSM MIXTURES

This chapter explains about the materials used to conduct this study. The properties of soils such as particle size distribution, Atterberg limits and specific gravity are discussed. In case of CLSMs, properties of different material used for the formulation of CLSM mixtures are described.

4.1 Soil as Back-Fill Materials

After carrying out the respective analyses of each of the assembled sets of soils, the decision was made to work with two of them. One refers to a granular soil (with no more than 35% passing through the No. 200 sieve) from Massa Carrara and other silty-clayey soils (more than 35% passes through the No. 200 sieve) coming from the Naples airport.

This decision was taken to observe how the granulometric distribution, water retention capacity in the pores, mineralogy, grain density, etc., of two completely different soils can influence the conduction of heat.

In the following table, the soils that will be analyzed are shown.

MASSA CARRARA			
ID	Weight [Kg]	Tests	Classification
Survey n°1	30	*- Particle size distribution - Water content	A _{1-a}
Survey n°2	5	- Atterberg Limit	A _{1-a}
Survey n°10	30	- Classification UNI EN - Specific Density	A _{1-a}

NAPLES			
ID	Weight [Kg]	Tests	Classification
Survey n° 4	50KG	*- Particle size distribution - Water content - Atterberg Limit - Classification UNI EN - Specific Density	A ₇₋₆

4.1.1 Characterization of Soils

The first step of the experimentation focuses on the analysis of the soils. The following section shows all the results of the analysed aggregates. The material has been characterized from the point of view of grain size. The particle size distribution has been possible thanks to an analysis carried out by previous studies. *Figures 13 and 14* shows the particle size distribution curves obtained from the granulometric analysis, both for the three soil samples A_{1-a} and for soil A₇₋₆. As mentioned above, the following study was based on previous research, where materials prepared for work must have the same characteristics.

The calculation Atterberg limit are given in *Appendix 2*.

- Particle Size Distribution

It can be seen in *Figure 13,14* the granulometric distribution of soils. These data have been provided by previous analyses, where it has been verified that the soils that we will use are: A_{1-a} and A₇₋₆. In the *Appendix 2* and you can find all the calculations and data about Atterberg Limit and classification UNI EN for each of the soils.

Soils A_{1-a} show a same behaviour and continuous distribution, where a uniform distribution of grains can be observed, that is, that it contains equitable fractions of each size.

For the soil extracted from the Naples airport (A₇₋₆) its distribution is a not distribution with more than 35% intern in the 0.063 sieve.

Tab. 4 Particle size distribution for A_{1-a}

D [mm]	Passing [%]		
	Sond 1	Sond. 2	Sond 10
31,5	73,1	74,0	62,2
22	65,3	61,1	56,2
16	59,9	53,0	52,2
8	47,8	42,9	45,5
6,3	44,3	40,0	43,4
4	39,2	35,1	39,8
2	33,6	30,2	35,0
1	28,8	26,0	30,4
0,5	24,8	22,4	26,4
0,4	23,6	21,4	25,5
0,125	13,3	11,8	14,7
0,063	8,9	8,2	9,8
Filler	-	-	-

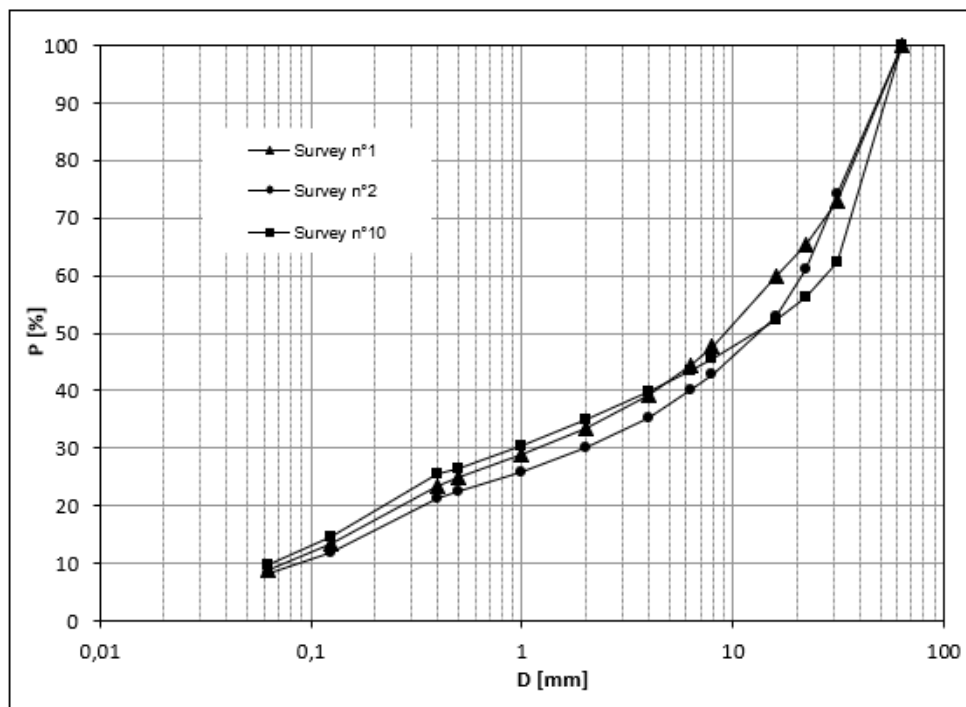


Fig. 13 Particle size distribution for A_{1-a}

Tab. 5. Particle size distribution for A₇₋₆

D [mm]	Passing [%] RIF 4
31,5	100,0
22	100,0
16	99,8
8	99,7
6,3	99,5
4	99,0
2	97,8
1	94,5
0,5	88,0
0,4	85,4
0,075	57,6
Filler	-

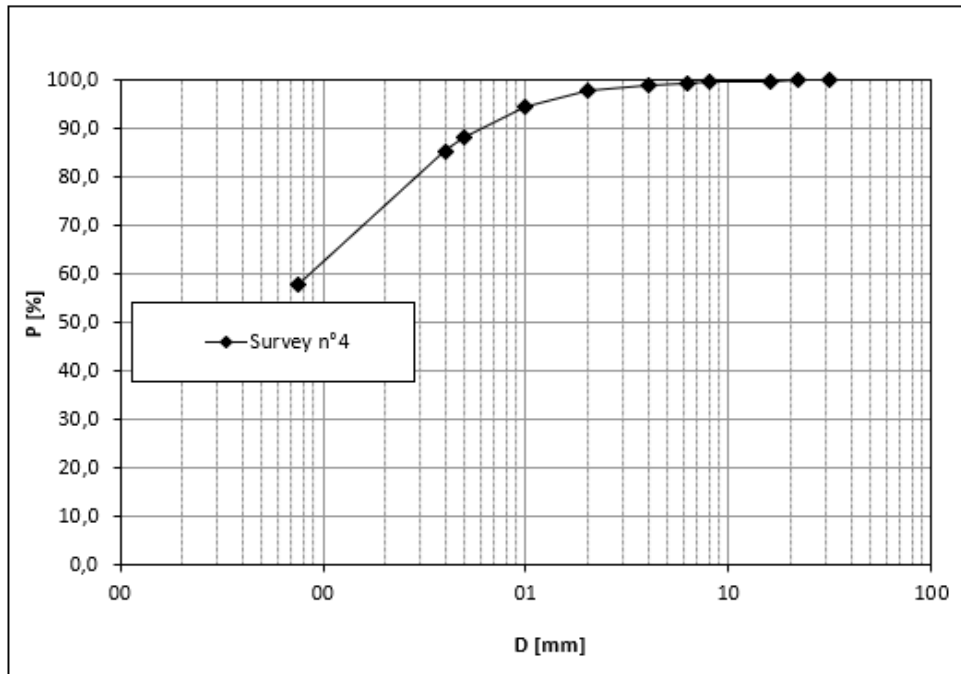


Fig. 14 Particle size distribution for A₇₋₆

- **Specific Density**

The results of respective analyses of Specific Density are expressed in the *Table 6*. The table of calculation can be seen in the *Appendix 2*

Tab. 6 specific densities of A_{1-a} and A₇₋₆ soils

Soil	P _{calc} [g/cm ³]
A _{1-a}	2,714
A ₇₋₆	2,667

One of the objectives of this thesis is the search of which of these two soils is the most appropriate as back-filling material in high voltage cables in terms of their ability to remove the heat generated by these. For this reason, and as explained in *Chapter 2*, the variables that are most influential in thermal conductivity are; soil moisture, density, degree of saturation, solid volume, etc. so, to evaluate the influence of these variables, is started to vary the moisture content of soils and with modified Proctor tests obtain densities of dry soil (density vs moisture), then by means of the specific density analysis with pycnometers obtain the volumetric mass to determine; Volume of solid and degrees of saturation as a function of water and air content within pores of the soil structure. The description of each methodology and results will be exposed in later chapters

Tab. 7. variation of the moisture content in both soil

A_{1-a}	A_{7-6}
W_{nominate}	W_{nominate}
[%]	[%]
0,0	12,5
3,5	15,0
5,0	17,5
6,0	20,0
7,5	22,5
10,0	26,0

4.2 CLSM as Back-Fill Materials

Two kinds of CLSMs were studied one is called as *Aggregate Sludge CLSM (AS_CLSM)*, which is manufactured using recycled asphalt pavement aggregates (RAP) and aggregate sludge as the main components. Aggregate sludge is obtained after the crushing and washing of aggregates. The other *Stone Sawmilling Sludge CLSM* was prepared using recycled asphalt pavement aggregates (RAP) and two types of stone saw sludge. The *Stone Sawmilling Sludge* were obtained during the the cutting and polishing of ornamental stones. *Stone Sawmilling Sludge* were of two types, one is *Diamond Wire Cut Sludge (DWCS)* which is obtained when diamond wire was employed for the cutting operation. The other one is *Frame Wire Saw Sludge (FWSS)* which is produced when a frame wire saw is used for the cutting operation of ornamental stones. These two sludges could have different chemical composition due to the different methodology adopted for their cutting.

For the preparation of CLSMs, the same materials used in the traditional concrete (cement, water, aggregates) were used. Recycled aggregates (RAP and Sludge) were used to increase the sustainability

of production, A superplasticizer was included in the formulation in order to increase the flowability of the mix. .

Aggregate skeleton of the “*AS_CLSM*” consists of coarse sand, gravel, recycled asphalt pavement aggregates (RAP) and aggregate sludge. Cement of grade CEM II / A-L 42.5 R used in the mixes, specific gravity of the aggregates, and a polycarboxylate based superplasticizer (ADVAFLOW 455 of Grace Products) was used. Different Aggregate Sludge_*CLSM* compositions were prepared to study the following objectives

- I. Influence of cement content on thermal conductivity
- II. Influence of RAP content on thermal conductivity
- III. Influence of water to powder (w/p) ratio on thermal conductivity
- IV. Influence of age on thermal conductivity.

4.2.1 Characterization of *CLSM* Aggregates

The particle size distribution and specific gravity of all the aggregates were determined. This is required for performing the mix design of *CLSM*s.

- *Particle size distribution*

The particle size distributions of the aggregates used for Aggregate *Sludge CLSM* and *Stone Sawmilling Sludge CLSM* are shown in the *Table 8,9* and *Figure 15,16* .

Tab. 8 Particle size distribution of Aggregate Sludge *CLSM*

D [mm]	Passing [%]			
	Coarse sand 0-8	Gravel 8-18	RAP	Sludge
31,5	100,0	100,0	100,0	100,0
20	100,0	100,0	100,0	100,0
16	100,0	100,0	100,0	100,0
12,5	100,0	84,6	100,0	100,0
8	100,0	15,0	88,7	99,7
6,3	99,3	2,6	80,2	99,3
4	86,3	0,2	58,4	98,8
2	64,4	0,2	32,8	98,2
1	43,1	0,2	14,8	97,3
0,5	26,2	0,2	6,2	96,2
0,25	12,6	0,2	3,0	93,2
0,125	6,0	0,2	1,8	85,8
0,063	3,0	0,2	0,9	73,7

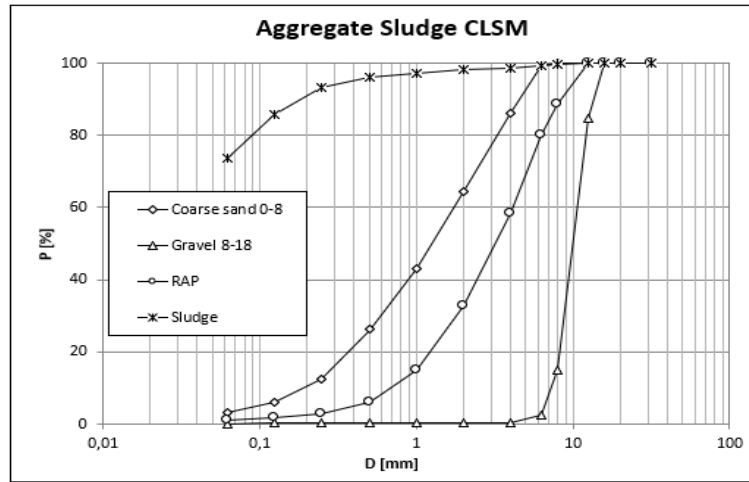


Fig. 15 Particle size distribution of Aggregate Sludge CLSM

For Stone Sawmilling Sludge CLSM

Tab. 9 Particle Size Distribution of Stone Sawmilling Sludge CLSM

D [mm]	Passing [%]				
	Coarse sand 0-8	Gravel 8-18	RAP	DIAMOND WIRE CUT SLUDGE (DWCS)	FRAME WIRE SAW SLUDGE (FWSS)
31,5	100,00	100,00	100,00	100,0	100,00
20	100,00	100,00	100,00	100,0	100,00
16	100,00	100,00	100,00	100,0	100,00
12,5	100,00	84,59	100,00	100,0	100,00
8	100,00	15,04	88,74	100,0	100,00
6,3	99,29	2,61	80,15	100,0	99,05
4	86,29	0,23	58,36	99,7	98,10
2	64,40	0,21	32,82	99,3	96,15
1	43,11	0,20	14,79	97,2	92,59
0,25	12,59	0,18	3,00	89,9	77,84
0,125	6,00	0,16	1,78	86,8	56,23
0,063	3,04	0,15	0,94	84,4	49,63
Filler	0,00	0,00	0,00	0,0	0,00

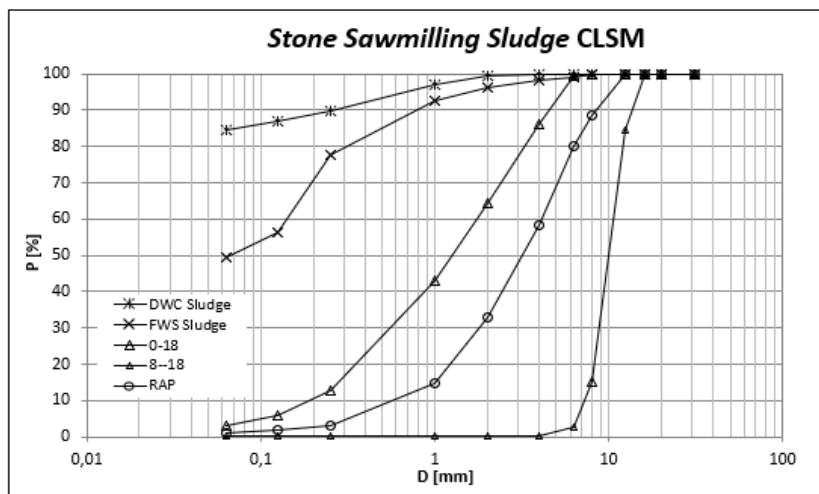


Fig. 16. Particle Size Distribution of Stone Sawmilling Sludge CLSM

4.2.2 Cement

Cement is a hydraulic binder, a finely ground inorganic material which, when mixed with water, forms a paste which sets and hardens by means of hydration reactions and processes and which, after hardening, retains its strength and stability even under water. Cement conforming to EN 197-1, termed CEM cement, shall, when appropriately batched and mixed with aggregate and water, be capable of producing concrete or mortar which retains its workability for a sufficient time and shall after defined periods attain specified strength levels and also possess long-term volume stability.

The most correct definition of the cement is given by the EN 197-1, which defines composition, specifications and compliance criteria of common cements. In it, the cement is defined as a hydraulic binder, a finely ground inorganic material which, when mixed with water, form a dough which coagulates and hardens, as a result of reactions and processes of hydration and that, once hardened, it maintains its resistance and its stability even under water. The cement conforming to European standard, is identified with the abbreviation CEM and suitably dosed and mixed with aggregate and water, must can produce a mortar or concrete capable of preserving the workability for a sufficient period of time to reach, after certain periods, levels of predetermined mechanical strength, as well as possess a long-term volume stability. Portland cement clinker is made by sintering a precisely specified mixture of raw materials (raw meal, paste or slurry) containing elements, usually expressed as oxides, CaO, SiO₂, Al₂O₃, Fe₂O₃ and small quantities of other materials. The raw meal, paste or slurry is finely divided, intimately mixed and therefore homogeneous. Portland cement clinker is a hydraulic material which shall consist of at least two-thirds by mass of calcium silicates (3CaO SiO₂ and 2CaO SiO₂), the remainder consisting of aluminium and iron containing clinker phases and other compounds. The ratio by mass (CaO)/(SiO₂) shall be not less than 2,0. The content of magnesium oxide (MgO) shall not exceed 5,0 % by mass. The hardening of the hydraulic cement CEM is mainly due to hydration of calcium silicates (tricalcium silicate 3CaO • SiO₂ and dicalcium silicate), but also other chemical compounds, for example calcium aluminates (the tricalcium aluminate 3CaO • Al₂O₃ and ferroalluminato tetracalcico) taking part in the hardening process. From a point of view of regulatory control, the sum of the percentages of calcium oxide content (CaO) and silicon oxide (SiO₂) in the reactive cement CEM, must be at least 50% by mass.

From the variability in the composition of the cements, the need arose for a rule which classifies them, both based on the amount of the constituents, both with respect to mechanical strength. The European standard EN 197 meets these requirements and the objective of allowing the distribution of cement in a unified manner across the European Union. In the table below shows the five main types of cement, divided according to their composition alongside the main ingredient (clinker); Portland cement (contains at least 95% of clinker) is indicated with the character I, while the same, with the addition of other mineral constituents, is inserted in the category II; for other cements, slag containing the working metal or composite, it has the name depending on the categories of membership:

Aggregate is one of the basic component of concrete. Its properties influence the behaviour of the cementitious mixture. It constitutes the skeleton of concrete whose cohesion is given by the cement paste. It does not take part to the curing process, but it has the main role in terms of concrete properties.

The European norm EN 197-1 defines five classes of common cement that comprise Portland cement as a main constituent.

- Type I: Portland cement
- Type II Portland-composite cement
- Type III Blastfurnace cement
- Type IV Pozzolanic cement
- Type V Composite cement

For each type of cement, it is then provided different classes of resistance that allow to categorize according to their mechanical requirements. The early strength of a cement is the compressive strength determined in accordance with EN 196-1 at either 2 days or 7 days and shall conform to the requirements in *Table 10*. Two classes of early strength are included for each class of standard strength, a class with ordinary early strength, indicated by N, and a class with high early strength, indicated by R. The resistance class is also an index of cement fineness, which increases with increasing class.

Tab. 10 Compressive strength requirements

Strength class	Compressive strength MPa				Initial setting time min	Soundness (expansion) mm
	Early strength		Standard strength			
	2 days	7 days	28 days			
32,5 N	-	≥ 16,0	≥ 32,5	≤ 52,5	≥ 75	≤ 10
32,5 R	≥ 10,0	-				
42,5 N	≥ 10,0	-	≥ 42,5	≤ 62,5	≥ 60	
42,5 R	≥ 20,0	-				
52,5 N	≥ 20,0	-	≥ 52,5	-	≥ 45	
52,5 R	≥ 30,0	-				

In this work the size of the aggregates comes to 18 mm.

The cement significantly influences the rheology of the concrete during the packaging phase and installation, as well as its mechanical characteristics, both in the short and long term. In the absence of a specific experiment, it was considered appropriate to use cement Type II / A-L 42.5 R, or cements, Portland composite, belonging to strength class 42, 5 R.

4.2.3 Aggregate

Aggregate is one of the basic component of concrete. Its properties influence the behaviour of the cementitious mixture. It constitutes the skeleton of CLSM's whose cohesion is given by the cement paste. It does not take part to the curing process, but it has the main role in terms of concrete properties.

Aggregate particles provide mechanical properties to the paste (strength and stiffness mainly), in term of stiffness, which is essential in any engineering use. In particular, the shape and the texture of fine aggregates affect the workability, while coarse aggregates affect the mechanical strength in concrete. A good concrete mix design is usually obtained varying the shape and dimensions of aggregates in order to limit high internal stress concentration and bond failure. Rough, textured surfaces will improve the mechanical component of the bond. Aggregate constitutes about the 60-70% of the final concrete mix and is the less expensive material used in the production. Their large amount in the mix allows to limit also the quantity of the binder providing a considerable reduction of costs. Its use is not only due to economical reason but also because concrete has no strength and rigidity without it.

Aggregates properties do not affect only the concrete mixture proportions but also the behaviour of both fresh and hardened mix. There are several classification systems of aggregates that are based on different parameters, such as weight, grading, applications etc. Currently the main classification among aggregates is based on geological origins: the natural aggregates and alternative aggregates.

Natural mineral aggregates, such as crushed stones, sand and gravel, are derived from different types of rock, that are themselves composed by several mineral and natural substances with a defined chemical composition and a specific crystalline structure. The natural sources from which aggregates can be extracted are:

- Igneous rocks, formed on cooled of magma (granite, basalt etc.) That give excellent aggregates;
- Sedimentary rocks, accumulated by wind and glacial actions (limestone, sandstone etc.) That can provide materials with various properties; and
- Metamorphic rocks, that changed the chemical structure or mineralogy composition due to physical and chemical conditions (marble, schist etc.); even in this case, it is possible to get aggregates ranging from very good to very poor material.

The aggregates used to produce Aggregate Sludge CLSM's samples are:

- Sand 0-8
- Gravel 8-18
- RAP (Recycled Asphalt Pavement)
- Sludge



Fig. 17 Aggregate Used in Aggregate Sludge CLSM

The *Stone Sawmilling Sludge CLSM*'s samples used:

- Sand 0-8
- Gravel 8-18
- Rap
- Stone Sawmilling Sludge CLSM “A and B”



Fig. 18 Stone Sawmilling Sludge CLSM “A on the right and B on the left”

4.2.4 Water

According to the D.M. 9/1/96, published on G.U. 5/2/96 Annex 1, point 3, water for the dough must be clear, free of Sali (and in particular sulphates and chlorides) and must not be aggressive.

Unfortunately, the role of water in the packaging of such mortars is often underestimated, with risks to the integrity of the material. Water is one of the fundamental components and its dosage and composition are crucial to provide the material with the required performance: in fact, water interacts with its chemical and physical properties in all phases of concrete life, hydrating the concrete, giving it

to the concrete a workability and plasticity that allows it to be easily installed and involved in the cohesion of the hardened material.

The amount of water required for the assembly of the conglomerate is much greater than that theoretically necessary for the hydration of the cement; it is necessary to take into account the water that remains in the micropore originated from hydrated silicate and alumina and the water needed to moisten the aggregates.

All drinking water and most of the natural (including seawater) waters are suitable for the packaging of such mortars, while the use of water from industrial waste or polluted ones requires extreme caution. It is important to pay attention to its composition: suspended substances, such as dissolved salts, intervene in the grip of mortar and in its rheology, creating problems of any efflorescence on hardened material.

Suspended substances (clay, vegetable residues, algae, microorganisms) should not exceed 2 g / l as they may interfere with the mortar hardening process and, above all, weaken the adhesion between the aggregate and the concrete paste, resulting in worsening of the mechanical resistances.

Dissolved substances deserve attention to carbonates and bicarbonates, sulphates, chlorides and organic substances. Carbonates and bicarbonates are tolerated in a dough water up to 2 g / l. their presence influences the take-up times and therefore when they are present in levels higher than grams per liter, it is convenient to perform mechanical grip and mechanical resistance tests. Sulphates are considered to be highly aggressive agents, using as seawater dough water (containing about 5 g / l of sulphates), the amount of sulphate content of the dough is considerably negligible so without any appreciable consequence for the features of mortar. Organic substances, generally found in limited quantities in drinking water and fluvial waters, slow down the mortar grip, resulting in less development of mechanical strengths at short maturing.

For CLSM it is considered appropriate and advisable to use potable water as it is almost free of impurities in suspension and containing a small amount of dissolved substances [28]

4.2.5. Recycled Aggregates

Nowadays, there are still some barriers in recycling that depends on different reasons. For instance, recycling is not always the most convenient solution from an economical point of view. The available material can be located in different zones, so costs are not negligible when long distances have to be covered for carrying it. Everything is connected with the problem of the lack of a suitable technology that allows the recycling process being on a commercial scale.

In comparison with other European countries, Italy is still reluctant in the use of recycled materials. This is due to several factors, such as:

- Attention to land and natural resources protection;
- The slowness of the administration in implementing technical innovations and changing outdated specifications, in which reference is made exclusively for the traditionally used materials;

- The strong cultural resistance to the use of recycled aggregates: these are usually considered poor materials when compared to ordinary natural materials it is clear therefore, the need to develop laboratory tests to understand deeply the behaviour of recycled material to support
- comparison in terms of mechanical performance with the ordinary quarry material;
- The delay and, sometimes, the inadequacy of regulations to promote the use of recycled materials and their use. However, a greater awareness of our public administration can be recently seen, also gained thanks to recycling and reusing policies promoted by European Union.

Even if the presence of these barriers is still a real problem, it is well known that the use of recycled aggregates for concrete production in the world is growing thanks to the environmental issues and sustainability policy that are developing in the last years. The need of recycled aggregates is important since they reduce the demand of new resources, cut down the cost and effort of transport and production, and lead to the use of waste which would otherwise be disposed in landfill.

Nowadays the category of recycled aggregates can be divided into three separate groups:

- From Construction and Demolition Wastes (CDW)
- From Industrial waste
- From returned concrete.

Aggregates from CDW

Two different groups that can be recycled:

- The concrete category that is made up by reinforced and not-reinforced concrete, industrial wastes and discarded material from prefabrication.
- The rubbles category, constituted by demolition waste material such as bricks, tiles, roads pavements etc.

Focusing the attention in the second group noticed previously result important talk about "reclaimed asphalt" as an aggregate in concrete

Recycled Asphalt Pavement Aggregates (RAP)

Existing asphalt pavement materials are commonly remove during resurfacing, rehabilitation, or reconstruction operations. Once removed and processed, the pavement material becomes RAP, which contains valuable asphalt binder and aggregate (*Figure 19*). In the early 1990s, FHWA and the U.S. Environmental Protection Agency estimated that more than 90 million tons of asphalt pavement were reclaimed (converted into material suited for use) every year, and over 80 percent of RAP was recycled, making asphalt the most frequently recycled material. RAP is most commonly used as an aggregate and virgin asphalt binder substitute in recycled asphalt paving, but it is also used as a granular base or subbase, stabilized base aggregate, and embankment or fill material. It can also be used in other construction applications. RAP is a valuable, high-quality material that can replace more expensive virgin aggregates and binders.[28]



Fig. 19. RAP material used in laboratory tests

Recycling processes

Typically, the asphalt pavement is either removed by milling of upper surfaces or full depth removal of the entire pavement section itself. A milling machine is used remove top 5 cm. of the surface with a single pass whereas a rhino horn on a bulldozer is used for full depth removal of the entire pavement in several broken pieces. These pieces are subjected to crushing, screening, conveying and stacking in stockpiles. Typically, this processing is performed at a central processing plant.

Another form of RAP material can be produced by in situ recycling of the old pavements by pulverizing them first and then incorporating them into base courses with or without additives. These processes are referred in the literature as cold in-place and hot in-place recycling methods, with hot process requires the heating of the upper asphalt surface layers of typically 5 cm. using a hot recycling machine shown in *Figure 20*. Cold in-place mixing can be carried out to different depths and a schematic showing this process of in-place mixing can be seen in *Figure 21*. It should be noted that the RAP materials produced from both central processing facility and in situ recycling methods can be used in the following applications:

- asphalt concrete aggregate;
- asphalt cement binder;
- granular base aggregate;
- stabilized base aggregate;
- embankment or fill material;

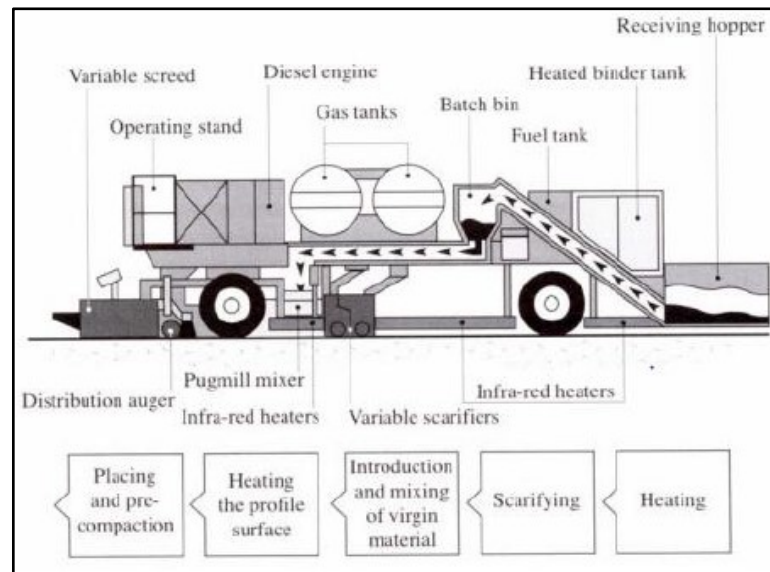


Fig. 20 Hot in place recycling

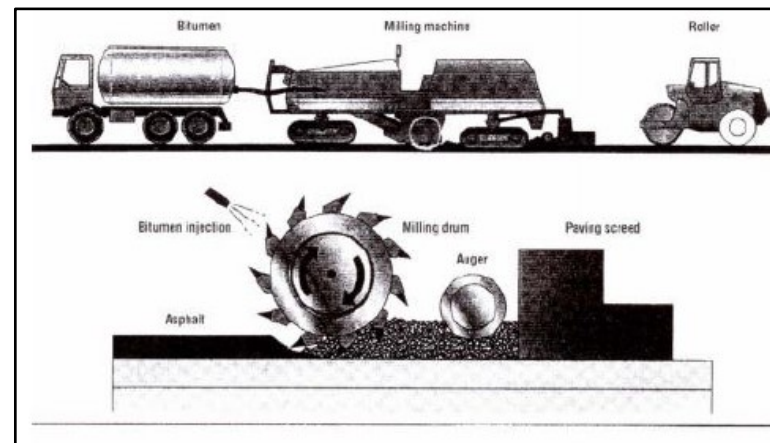


Fig. 21 Cold in place mixing

Utilizing in these applications result in several benefits, which are summarized in the following:

- lower costs;
- lower utilization of virgin materials which are becoming scarce;
- reduced land-filling;
- reduced energy consumptions by eliminating fuel consumptions required for land-filling trips;
- faster construction if in-place recycling methods are employed.

The use of the RAP material is regulated by UNI EN 13108, however, currently there is no provision for re-use of it into the concrete. In Italy, the production of RAP is bigger than the use and recycling, this cause by two main reasons: the first one because of environmental regulations, and second because,

with a few exceptions, the particular specifications do not provide recycling or introduce a very limited use. In the *Figure 22* show how is selected the rap, wanting to have a size from 16 mm down



Fig. 22. Selection of RAP

4.2.6 Admixture

Admixtures are added to concrete batch immediately before or during mixing concrete. Concrete admixtures can improve concrete quality, fluidity, acceleration or retardation of setting time among other properties that could be altered to get specific results. [29]

From a theoretical point of view, the amount of water to be added to obtain a concrete (assuming the saturated state / dry surface of aggregates) will coincide with that strictly necessary to hydrate Portland cement particles. In the aforementioned ideal, the mixing water would react with said particles transforming into a solid of almost zero porosity and, consequently, of high resistance.[29]

The actual situation differs significantly from the previous assumption and to better understand the operation of these additives it is necessary to remember the water-cement behavior in the concrete mixing and setting process. First the binder paste is formed as a result of the lubrication of the cement and aggregate particles after the adsorption of the water, and then this paste becomes a cementing product of the chemical reaction that takes place between both at the beginning of the setting.

In the first of these stages is when the mixture of the components and the first electrochemical reactions between water and cement occurs, appearing the characteristics of fresh concrete as workability, docility, consistency, etc. These characteristics are governed mainly by the reactions electrochemical produced between water molecules and cement grains, which have a large number of ions in solution on their surface. These ions tend to form, due to an electrostatic affinity, flocs or layers of solvation upon contact with water during the kneading operation.

The water retained is not usable to lubricate the concrete mass nor to contribute to the hydration of the cement grains, which implies the need to incorporate an additional substitute quantity. This added water, as it cannot react with the anhydrous cement grains, causes an increase in the porosity of the cement paste, which implies a certain loss of strength of the hardened concrete and an increase in its permeability.[30]

Given that the relationship w/c of a concrete has a transcendental importance in its characteristics, especially in its mechanical resistance, it is interesting that in concrete this ratio is as low as possible, but this entails certain difficulties such as a very efficient mixing system for to obtain a homogeneous mixture and to have very energetic means of compaction. With the use of these additives these drawbacks can be eliminated without the need to increase the amount of mixing water.

The harmful effects of the flocculation of the cement particles can be counteracted, at least partially, by the incorporation into the concrete mass of certain additives, such as water-reducing or fluidifying agents. These products added to mortars or concrete, at the time of kneading, increase the docility of the same, allowing placing on site concrete masses that otherwise would be very difficult or, reduce the water needed for the kneading for the benefit of the mechanical and durability resistances.

The Superfluidizing or reducers of water are chemical products of organic nature formed by macromolecules tensoactivas able to neutralize the electrical charges of the grains of cement and, consequently, his flocculation capacity.[30]

For our mix a commercial product has been used ADVA® Flow 455 (Figure23), a new generation low-dosage superplasticizer to deliver highly smooth, non-segregating properties to cement mixtures and produce self-compacting concrete (SCC) in industrial prefabrication. Is based on modified carboxylated polymers and is produced under strict conditions checked to offer the best guarantees of constancy of quality. Conforming to the following standards [31]:

EN 934-2

Prospectus T 3.1 / 3.2

ASTM C 494 - A, F

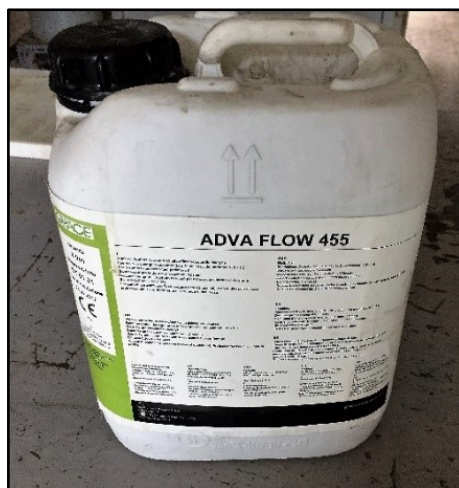


Fig. 23 ADVA® Flow 455 Superplasticizer

Is compatible with all the cements provided by UNI-ENV 197/1, and in particular with Portland Cements, composite Portland Cements, Pozzolanic and Blast Cements and Lime Cements; ADVA Flow 455 is also compatible with concretes containing ash and / or silica smoke.[31]

4.2.7 Formulation of Mixes

After characterizing the materials through sieve analysis and specific gravity tests the dosages will be determined according to the mix design. In the mix design process, the design curve *equation 18* has been optimized with respect to the reference curve through the least square method. This reference curve has been plotted according to the equation given by the modified Andreasen and Andersen model *Equation 19* based on the larger diameter of the aggregate particles, the smaller diameter of aggregate and a "q" adjustment coefficient, which from previous analyses determined that the best adjustment is made for a $q = 0.21$ [32]

Where the fraction of employment is:

$$\alpha_{0-8} + \alpha_{8-18} + \alpha_{RAP} + \alpha_{sludge} = 1 \quad [eq. 17]$$

$$P_{p(Di)} = \alpha_{0-8} \cdot P_{0-8} + \alpha_{8-18} \cdot P_{8-18} + \alpha_{RAP} \cdot P_{RAP} + \alpha_{sludge} \cdot P_{sludge} \quad [eq. 18]$$

$$P(D) = \frac{D^q - D_{min}^q}{D_{max}^q - D_{min}^q} \quad [eq. 19]$$

$$\sum [P_D - P_p]^2 = \min \quad [eq. 20]$$

Where:

- α_i = coefficient for each fraction of aggregate used
- P_i = fraction of Passing
- D (mm) = diameter of aggregate particle
- D_{min} = minimum diameter of aggregate in design curve
- D_{max} = maximum diameter of aggregate in design curve
- q = adjustment coefficient

The SOLVER tool provided by Excel was used to determine the coefficients for each fraction. Where the program automatically calculates the least square error for a given objective.

In the next *Tables* can be see the percentage in weight for each aggregate and mix *Aggregate Sludge CLSM (AS_CLSM)* and for *Stone Sawmilling Sludge CLSM*

Tab. 11 Results of curves optimization for AS CLSM (q=0.21)

Aggregate	PERCENTAGE IN WEIGHT [%]			
	Coarse sand 0-8	57	44	39
Gravel 8-18	22	18	17	14
RAP	0	15	20	30
Sludge	21	23	24	25

Tab. 12 Results of curves optimization for Stone Sawmilling Sludge CLSM (q=0.21)

Aggregate	PERCENTAGE IN WEIGHT [%]	
	Frame wire saw sludge	Diamond wire cut sludge
Coarse sand 0-8	26	40
Gravel 8-18	18	17
RAP	20	20
Sludge	36	23

More details of the optimization can be found in the *Appendix 2*. The entire mix formulation was performed to know the influence of various factors such as age, amount of cement [kg/m³], amount of RAP [%], water-powder ratio (w/p), moisture state of the sample and different types of silt sludge on the thermal conductivity. To analyse the sensitivity of each test parameter, a series of different variables were selected, as shown in *Table 11*, for CLSM's samples.

Tab. 13 Mix Proportions

Parameters	Variables for test	mixture type
Age (Days)	2,7,14,28	CLSM
Cement Content [Kg/m ³]	60,80,100	CLSM
RAP [%]	0,15,20,30	CLSM
w/p ratio	0.70,0.75,0.80	CLSM

In this study, has been proposed the combination of several variables in the dosages of the samples to observe how these can influence when analysing their thermal conductivity. It is thus, that 8 (eight) different combinations for *Aggregate Sludge CLSM* were made varying the content of cement, the percentage of RAP and the water/powder ratio. Powder are referring to cement + sludge, this influence when calculating the amount of water added to the mix, since it is not only the one demanded for the creation of CLSM, but it will have to add the one that the filler needs so that each particle can be hydrated, that is to say that, the water that the mix needs is the sum of the water demanded by the aggregates plus the water that the fines demand. Another two mixes were developed with the Stone Sawmilling Sludge. but in this case with only one cement content, RAP content and varying with two combination of w/p ratio. All dosages were calculated for a volumetric content of 1 m³. *Tables 14 and 15* summarizes mix proportions for all the batches considered in this study.

Tab. 14 Test Parameters for Aggregate Sludge CLSM

Parameters	Name of specimens	Cement Content [Kg/m ³]	RAP [%]	W/P [%]	Type of cementitious materials	Unit Content [Kg/m ³]					
						Water	0-8	_8-18	RAP	Sludge	Admixture
Cement Content	C60_20_0.80	60	20	0,80	Type II	366,30	646,92	281,99	331,75	398,11	0,30
	C80_20_0.80	80	20	0,80	Type II	374,56	631,32	275,19	323,75	388,50	0,40
	C100_20_0.80	100	20	0,80	Type II	382,82	615,71	268,39	315,75	378,90	0,50
RAP Content	C100_0_0.80	100	0	0,80	Type II	359,95	950,83	366,99	0,00	350,31	0,50
	C100_15_0.80	100	15	0,80	Type II	375,20	706,63	289,07	240,90	369,37	0,50
	C100_20_0.80	100	20	0,80	Type II	382,82	615,71	268,39	315,75	378,90	0,50
w/p ratio	C100_30_0.80	100	30	0,80	Type II	389,36	479,97	216,76	464,48	387,07	0,50
	C100_20_0.70	100	20	0,70	Type II	349,93	650,53	283,56	333,60	400,32	0,50
	C100_20_0.75	100	20	0,75	Type II	366,73	632,74	275,81	333,60	389,38	0,50
	C100_20_0.80	100	20	0,80	Type II	382,82	615,71	268,39	315,75	378,90	0,50

Tab. 15 Test Parameters for Frame Wire Saw Sludge_CLSM and Diamond Wire Cut Sludge_CLSM

Parameters	Name of specimens	Cement Content [Kg/m ³]	RAP [%]	W/P [%]	Type of cementitious materials	Unit Content [Kg/m ³]					
						Water	0-8	_8-18	RAP	Sludge	Admixture
Frame wire saw sludge	C100_20_0.70	100	20	0,70	Type II	472,67	354,77	245,61	272,90	491,21	0,50
Diamond wire cut sludge	C100_20_0.80	100	20	0,80	Type II	372,42	636,35	270,45	318,18	318,18	0,50

CHAPTER 5

EXPERIMENTAL INVESTIGATION

This chapter of the thesis explains the details of experimental investigation. Different procedures and instruments used for the characterization of both soils and the CLSMs are described in this chapter. To achieve this goal, different laboratory tests have been developed, following European standards. A general description of all the instruments used to carry out the experimental analysis will be described. The main technical aspects will be analysed, the use for characterization of the materials as well as the procedures for packing specimens and the execution of laboratory tests. All the equipment and equipment described are part of the equipment provided by the DIATI (Department of Environmental Engineering, Territory and Infrastructure) of the Polytechnic, where this experimental study was conducted.

5.1 Research Project

The goals of the present project have been defined at the beginning of the experimental research and were divided into two different analyses. the first referred to the soils and the second to CLSM.

The methodology is the follow:

- Characterization analysis of soil properties
 - Particle size distribution
 - Specific Density
 - Atterberg Limit
 - The ASHTO classification
- Proctor Compaction Test
- Thermal conductivity Measurement in soil

- Characterization of CLSM
 - Particle size distribution
 - Specific Density
- Dosage of *CLSM*'s for thermal conductivity tests
- Flowability Test
- Thermal conductivity Measurement in samples for 2,7,14,28 days

5.2 Instrumentation and Laboratory Equipment

5.2.1 Precision Balance

This is a very accurate balance, able to estimate the millimeter of grams. From a strictly technical point of view, it is equipped with a seven-segment digital LCD screen. It is essential for the accuracy of the weighing process that a priori proceed with the "bubble" of the balance using the appropriate knobs located at the bottom end of the balance.

It has been useful for numerous tests such as; weighing materials, granulometric analysis, specific density, Compaction Proctor Test, proportions amount for CLSM's samples, etc., where in most cases it has been used for weighing proportions, materials and instrumentation.

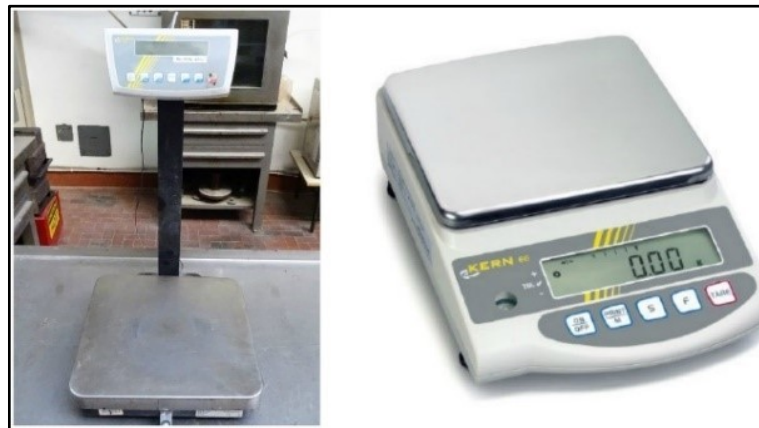


Fig. 24 Precision Balance

5.2.2 Equipment for Granulometric Analysis of Aggregates

To obtain the granulometric performance of the soils and aggregates used in the different studies, the TYLER mushroom set was used, opening the square meshes from 31.5 mm to 0.063 mm, and then inserting the sieve series in a mechanism that guarantees rototranslation (at least 15 minutes) and thus obtain the proportions of retained in each sieve.



Fig. 25 Set of Sieves

5.2.3 Pycnometer

Pycnometer or specific gravity bottle, is a glass vessel with volume between 500 ml and 5000 ml used to determine the densities of different substances. It is also known as a density bottle. It consists of a small glass bottle with a narrow neck, closed with a frosted, hollow plug and ending at the top in a capillary tube with graduations in such a way that a volume can be obtained with great precision. This allows to measure the density of a fluid, in reference to that of a fluid of density known as water or mercury.[28]



Fig. 26 Pycnometers

5.2.4 Cylindrical Mould for Compaction Test

Used for determining the relationship between the moisture content and density of compacted soil. The mould includes collar, mould body and base plate. The rammer construction includes a guide sleeve with vent holes.[33]

Different versions are available that conform to the various commonly used standards. They are all made of plated steel and are identical in shape, only differing slightly in diameter and capacity.

In this section moulds and rammers conforming to ASTM/AASHTO are shown. The dimensions of the mold are: $d = 152,4$ mm and $h = 116,4$ mm for AASHTO Modified – T 180

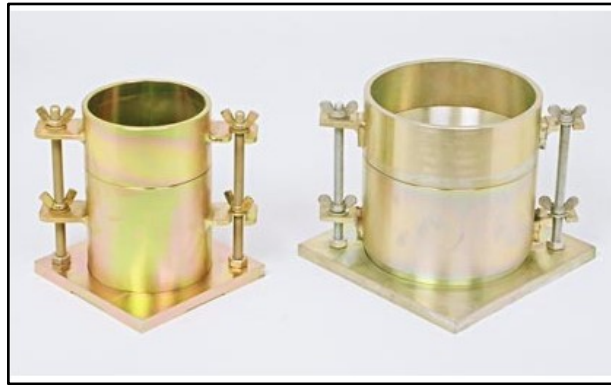


Fig. 27 Proctor Mould [34]

5.2.5 Automatic Compaction Machine - Matest

This apparatus automatically rams specimens in order to determine "dry density - water content curve", "maximum dry density", and "appropriate water content curve" of the soil that has been passed 37.5 mm sieve regulated in JIS A 1210. [33]

An originally designed mould receiver does not allow fails in ramming, and strong actions of two pulleys makes perfect even finishing.

The dropping mechanism working with the mould receiver realizes high speed ramming and makes the testing time shorter.



Fig. 28 Automatic Compaction machine[33]

5.2.6 The CLSM Mixer

The concrete mixer shown in the *Figure 29* has been used to produce the CLSM's samples, in order to be able to perform a sufficient number of specimens more quickly to determine the mechanical properties of the materials. The capacity is 11 liters and 38 kg in the Basque for the volume of the mass, the operating power reaches 0.375 kw and Volt 380. Its dimensions are 560mm in height and 570 in depth.



Fig. 29 The CLSM mixer

5.2.7 Slump Flow Test Equipment

The apparatus for performing the slump flow test consists of: a plastic cylinder of 7.5cm of diameter and 15cm of high, and a flat plate base *Figure 30*. The surface of the mould has to be totally clean of moisture and hard concrete before starting the test. The mould is placed on smooth horizontal rigid surface and then is filled by fresh material. The test was performed according to the ASTM D 6103 standard.



Fig. 30 Cylinder and plate used for the slump flow test.

5.2.8 Thermal Conductivity Device

Thermal conductivity of the soil and CLSM's samples were measured by KD2pro manufactured by Decagon devices. This is a handheld device used to measure thermal properties. The base KD-2 Pro package consists of a handheld controller and one sensor kit of your choice. There are several sensors available that operators can insert into almost any material. The single needle sensors measure thermal conductivity and resistivity; while the dual-needle sensor measures thermal conductivity, resistivity, volumetric specific heat capacity and diffusivity. In this thesis will be use the single needle sensor.[35]



Fig. 31 KD2 Pro Device with Different Probes and Calibration Cylinders

5.3 Characterization of Soil

The characterization of the material has been conducted by referring to European standards. The investigate characteristics are:

5.3.1 Particle Size Distribution

The granulometric analysis was carried out only for two types of aggregates (8-18 and silts with metallic content). since for others, they have been provided from previous studies. For silt, the washing technique should be used in order to completely separate the finer fraction (filler) from the grains and the complete disintegration of lumps of possibly present material.

The particle size distribution (PSD) represents the measurements technique of the particles' dimensions. It is performed through the sieving method, specified in the standard EN 933-1. Before starting the measurement, the material is dried by means of a ventilated oven, thermostatically controlled to maintain a temperature of 110 ± 5 °C. When the aggregate is cold, the material should be homogenized, then divided into quarters and taken around 1.2 or 1.5 Kg. The test portion is put inside the column of sieves, as shown in *Figure 32*. The test has the goal to divide the material in particles with a specific size. The sieve consists in a vessel in which the bottom part has a metallic screen to filter the particles greater than the mesh size.

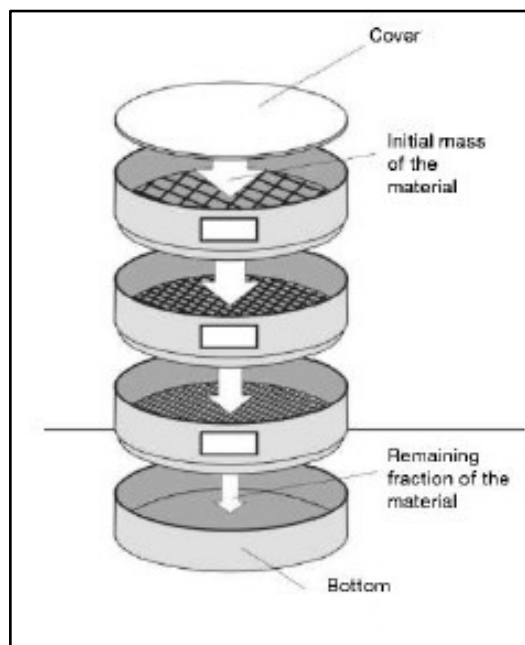


Fig. 32 Sieving scheme [28]

The numbers and the sieves opening are stabilized by the standard EN 933-2 and it is consistent with the ISO 3310-1 and ISO 3310-2 requirements. In *Table 16* reports the weights of the sieves used for the analysis, these are: 0.063 mm, 0.125 mm, 0.25mm, 1 mm, 2 mm, 4 mm, 6.3 mm, 8 mm, 12.5mm, 16 mm, 22 mm, 31.5mm

Tab. 16 Weight of the sieves

Sieve (ISO 3310-2) mm	31,5	20	16	12,5	8	6,3	4	2	1	0,25	0,125	0,063
PESO (g)	1291,7	1319,8	1304,7	1054,4	1073,8	1054,4	1110,1	976,3	866,9	726,8	425,1	767,8



Fig. 33 Column of Sieve

Once the shaking procedure is completed, the sieve with the material inside is weighed. This operation allows to obtain the value of retained material and by the knowledge of the tare (weight of the sieve), the value of the passing can be calculated.

The "wet" granulometric analysis is the technique where the material is weighed before (P) and after drying (P1), the material is subjected to a stream of water for the complete separation of the finest fraction (filler). All this is poured into a column made exclusively of sieves of mesh of 2 mm and 0.075 mm, helping to dispense the filling with jets of water. The material retained by the sieves will dry again at 105 ° C and, once cooled, it will be weighed again (P2) and sifted through a set of Tyler sieves arranged in a column and in descending order, starting from the sieve with opening of mesh of 31.5 mm and arriving to that with opening of 0.063 mm. The sieve passage of 0.063 mm is obtained as the difference between the initial total weight before washing and the final weight:

$$P_{0,075} = P_1 - P_2 \quad [eq. 21]$$

The analysis could also be carried out dry, but from a point of view of equity and reliability, moisture analysis is more reliable because it is more precise about the amount of filler present.

5.3.2 Specific Density

The test was developed following the norm EN 1097-6 [36]. To characterize the soil and the aggregate in terms of density and water absorption the sample should be divided in the fraction 0.063–4 mm and 4–31.5 mm. The testing procedure is basically the same for the two groups. The only difference is the mass of the specimen that is function of the maximum size of the aggregates. table 17 shows the values that the norm imposes to test a sample of significant mass.

Tab. 17 Mass of the Test Portion as Function of Maximum Size of Aggregates

Dimensione massima degli aggregati mm	Massa minima delle porzioni di prova kg
31,5	5
16	2
8	1
Nota Per dimensioni differenti, la massa minima della porzione di prova può essere ricavata per interpolazione dalle masse specificate nel prospetto 2.	

In additional analysis of the aggregates was carried out for the determination of the apparent volume mass (MVA), which was carried out in accordance with CNR A.D. d. 63. The "apparent bulk density of an aggregate" is the mass of a unit volume of solid material, including internal pores to unsaturated grains with water. For the determination of MVA, a representative sample of approximately 1200 grams of each of the soils was taken, dried at $100 \pm 5 \text{ } ^\circ \text{C}$ and allowed to cool to room temperature. The material thus obtained was weighed with an accuracy of 10 grams and it introduced in a pycnometer, previously calibrated. In the pycnometer, distilled water was poured to cover the water aggregate, and everything was left to rest for 3 to 4 hours.

After the time of rest of the material, through the suction pump, the content of the pycnometer was dehydrated by extracting the air contained in the water and between the granules. To this end, the pycnometer was subjected to a partial vacuum, corresponding to an air pressure not exceeding 13.33 KPa, for at least twenty minutes, periodically shaking, to release air between the aggregates. Once the deaerating was complete, the pycnometer was filled with distilled water and discharged until reaching the mark line of the pycnometer with the lower surface of the meniscus.



Fig. 34 Pycnometer full of A1-a and A7-6 soil.

At this point, the pycnometer was weighed, taking care to dry the exterior walls thereof of any water and the internal temperature was evaluated with an appropriate thermometer.

The apparent mass of the aggregate, expressed in grams per cubic centimetre, is given by:

$$\gamma_g = \frac{p}{p - p_2 + p_1} \cdot \gamma_w \quad [eq. 22]$$

where:

- p is the mass of the dry aggregate contained within the pycnometer;
- p_1 is the mass of the pycnometer filled with aggregate and distilled water at the test temperature t ;
- p_2 is the mass of the pycnometer filled with aggregate and distilled water at the test temperature t ;
- γ_w is the mass of water at the test temperature t .

In this thesis, this method was used to plot a zero air voids (ZAV) curve as a reference for each soil's two compaction curves. (A_{1-a} and A₇₋₆)

A small sample for each of the soils was taken to perform AASHTO T84 (ASTM C 128) procedures.

5.4 Proctor Compaction Test

The Proctor Compaction Test is a laboratory geotechnical test method used to determine the properties of soil compaction, specifically, to determine the optimum water content in which the soil can reach its maximum dry density. There are two ways to perform this test. The AASHTO Standard - T 99, which was later modified and called the Modified Proctor Test (AASHTO modified - T 180). The difference between the two tests lies mainly in energy compaction. In this thesis the Modified Proctor Test was used where the technical characteristics are described below according to UNI EN 13286-2 (2005). The technical characteristic of this test can be seen in *Table 18*.

Tab. 18 Technical Features

AASHTO Modified -T180	
Number of layer	5
Hammer weight	4,535 kg
Constant fall height	457 mm
Blow Rate	56
Mould Height	116,4mm
Mould Diameter	152,4mm
Energy for unit of volume [N/cm ²]	269

The Proctor compaction test consists of compacting soil samples at various water contents in a mold with fixed compaction energy. The soil to be compacted is dried at 110 ° C for 24 hours or until the difference between two weightings less than 1%. Then, the soil is divided into quarters and a fraction of each of these is taken until approximately 5.5 kg is collected for each test. The water content of each sample is adjusted by adding water (increments of 2.5% or less depending on the type of soil and each case), after this operation, they are mixed (water and soil) in a continuous manner until the entire sample is homogenized. The sequence can be seen in the *Figure 35*.



Fig. 35. Modified Proctor Test

Once this is done, the mould is weighed without a collar. Then, the soil is placed in the Proctor compaction mould in five different layers where each layer receives 56 blows from the hammer. Before placing each new layer, the surface of the previous layers is scratched to ensure a uniform distribution of the effects of compaction.

Automatic Compaction Machine - Matest is easy to use and ensures an extremely uniform degree of compaction, providing reliable and repeatable test results. This Machine is a software that allows to select and perform different compaction cycles in a fully automatic system, strictly complying with the aforementioned international standards.

The blows are distributed automatically as requested by the selected standard, this occurs by rotating the base at 55° and 6 strokes per turn plus a central hit. The original elevation system of the rammer can be selected at 12" or 18", or at 300 or 450 mm, which guarantees a correct and constant fall height. Tamping speed of the rammer: 1 stroke every 2 seconds. The compactor accepts moulds that have. 4" and 6", 100 and 150 mm, both Matest made as well as other producers, thanks to its universal mold fixing system. The sequence of the compaction can be seen in next *Figure 36*. [37]

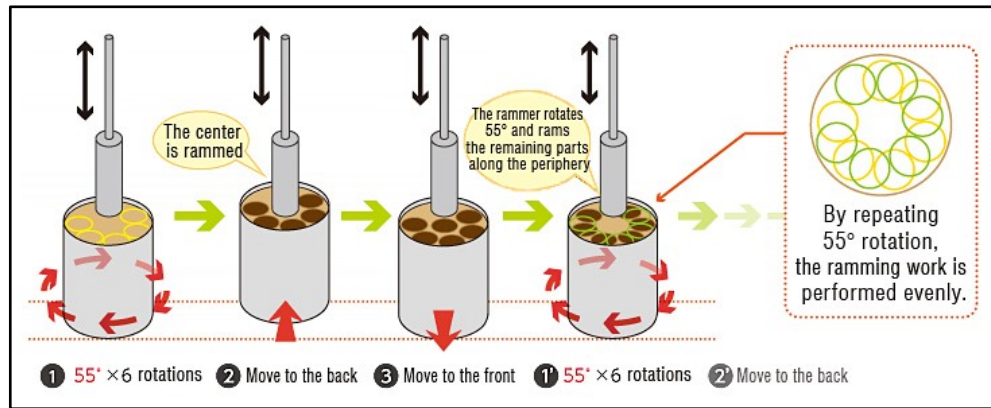


Fig. 36 Modified Proctor Sequence [37]

At the end of the process, the mold is extracted, it is carefully leveled for subsequent weighing of the mold + compacted soil. This will help determine the amount of soil inside the mold making the difference between them.



Fig. 37 Flush and Weighing – Modified Proctor Test

At the end of the test, approximately 500 g of soil is extracted from the core of the mould and the sample is dried at 110 ° C. Then, the dry density and the water content of the sample are determined for each Proctor Compaction Test. Based on the result set, a curve is drawn for the density of the dry unit as a function of the water content. From this curve, the optimum water content can be obtained to reach the maximum dry density.

The volume of the mould is obtained from a methodology knowing the density of standardized sand where its density is known. Take the weight of the mould and the weight of the mould plus sand, thus, you get the total sand used that divided by the density of the standard sand you get the geometric volume of the mould. In *Appendix 3* you can see what is mentioned

$$V_{mould} = \frac{W_{m+sand} - W_m}{\rho_{sand}} \quad [eq. 23]$$

Where:

- V_{mould} = Mould volume
- W_m = Mould Weight
- W_{m+s} = Mould+ standard sand Weight
- P = Density of standard sand.

For both the A1-a and the A7-6 soil, the same process was carried out with moisture contents mentioned in the previous chapter.

5.5 Thermal Conductivity Measurement in Soils

Thermal conductivity of the soil samples were measured at different water contents. The water content was varied around the optimum moisture content of that soil obtained from the modified proctor test. The thermal conductivity was determined using the device mentioned in the previous chapter (the probe KD2 pro). This was used by different researchers in the past [38].

The device has four types of sensors, each for different materials. In this thesis two types of them were chosen according to the materials to be analyzed.

Selection of sensor

TR-1: The large (100 mm long, 2.4 mm diameter) single needle TR-1 sensor measures thermal conductivity and thermal resistivity. It is designed primarily for soil, concrete, and other granular or solid materials where an appropriate sized hole can be easily drilled, or a pilot pin can be inserted (in the case of uncured concrete). The relatively large diameter and typically longer heating time of the TR-1 sensor minimize errors from contact resistance in granular samples or solid samples with pilot holes. Additionally, the dimensions of the TR-1 sensor conform to the specifications for the Lab Probe called out by the *IEEE 442-03 Guide for Soil Thermal Resistivity Measurements*. [10]

RK-1: The thick (60 mm long, 3.9 mm diameter) single needle RK-1 sensor measures thermal conductivity and thermal resistivity. It is designed specifically for use in hard materials like rock or cured concrete where a rotary hammer must be used to drill a hole to accommodate the sensor. The TR-1 sensor is generally more accurate than the RK-1 sensor and is the preferred choice in granular and solid materials as long as a hole can be made to accommodate the longer and thinner sensor. In instances where the material is too hard to drill a hole for the long, thin TR-1 sensor, a 5/32" or 4 mm rotary hammer. It is also necessary to use the included thermal grease to ensure good thermal contact between the RK-1 sensor and the test material.[35]

Based on the aforementioned and depending on the selection of the sensors, for A1-a soils, the RK-1 sensor was used, where due to the characteristics of it, the use of a rotary hammer should be used to create a pilot hole where the needle is inserted for each sample of compacted soil with various moisture contents. It is also necessary to use the included thermal Grease or Gel to ensure good thermal contact between the RK-1 sensor and the test material. In solid materials where a pilot hole has been drilled and the contact resistance can be significant, this thermal grease should be used, where the reading time should be extended to the maximum allowed of ten minutes to produce the most accurate results. In the *Figure 38* can be seen the measurements for different water content.



Fig. 38 Thermal Conductivity Measurement of Soil A1-a

For A7-6 soils, the TR-1 sensor was used. In this case it was not necessary to use a drill because being a fine soil facilitated the tasks to make the pilot hole. This is executed through a tool specially designed for this situation. Then, it is continued in the same way as for granular soils, with the placement of the GEL. See *Figure 39*

For both cases, the methodology for taking measurements is the same and easy to perform. Once the needle is inserted in the pilot hole, it is left to rest for 15 minutes before each measurement, in order that the needle balances its temperature with the soil. Then, the device is turned on and the measurements are started. Once finished with the measurement, depending on the sensor used (5 minutes for TR-1 and 10 minutes for RK-1) the needle is removed, and it is waited for another 15 minutes in order for the sensor to rebalance its temperature.



Fig. 39. Thermal Conductivity Measurement of soil A7-6

5.5.1 Calibration of the KD2 pro

Before starting with the measurements (every day), it is necessary to perform a process of calibration of the device to assure a correct accurate in the calculations of Thermal Conductivity provided by it.

Three standard materials it can be used to verify that the sensors are operating according to specifications. These three materials are a clear vial of glycerine (glycerol) for the KS-1 Sensor, a white plastic cylinder for the SH-1 needle sensor, and a TR-1 Verification Standard for the TR-1 and RK-1 single needle sensors. [35]

To perform the calibration, the needle must be inserted completely into the calibration cylinder containing the standard material. After this step, 15 minutes of equilibrium time is expected before taking the measurement. Once this time has elapsed, the measurement begins and then verifies if the given data of thermal conductivity is within the error intervals. In the *figure 38* below, this process can be seen.



Fig. 40. Verifying Sensor Performance

5.6. Aggregate Sludge CLSM and Stone Sawmilling Sludge Mixes

In this subsection, the analyses and tests carried out for both mixtures will be explained. It must be remembered that it has been called Aggregate Sludge CLSM, to the mix using recycled asphalt pavement aggregates (RAP) and aggregate sludge as the main components. The other Stone Sawmilling Sludge CLSM was prepared using recycled asphalt pavement aggregates (RAP) and two type of stone saw sludge as the main component; Diamond Wire Cut Sludge and Frame Wire Saw Sludge

After having characterized the material and determined the dosage to define each mixture, the next work was to perform the samples. For this, moulds were used *Figure 41* where the paste was placed for each combination of variables described in the previous chapter. Before casting the CLSM, oil must be placed inside the moulds to facilitate their detachment once the CLSM hardens.



Fig. 41 Moulds for Casting CLSM

Different mixtures were prepared using the laboratory mixer. The process of creation of the mixtures consists of determining the amounts of each one of the materials used in each sample, that is, the kg of; cement, aggregates (0-18,8-18, RAP, Sludge), additive and water determined in the calculation of dosages of each combination. Each proportion of material is placed in a mixing container without prior addition of water. Only the aggregates with the cement are mixed for one minute. This is done for a correct homogenization of the same. After this, the water is poured, which is introduced in two stages with two minutes lapses of mixing each one. Once this action is finished, the slump test is performed.

For this, a perfectly flat surface is prepared where the platform and the plastic cylinder are placed. The moulds are located nearby of them to create the CLSM's samples (*Figure 42*), these will be used for the measurement of thermal conductivity. Once the mixture is poured and levelled in the moulds, they are left to rest for two days, then they are extracted of the mould, and the matured process begins.

The Slump Test process is carried out by filling the plastic cylinder with the mixture. Once full and level, the cylinder is removed at a constant speed so that the mixture expands generating a circle. Then, with a tape measure the diameter is measured and thus we obtain the fluidity value of our mixture. Photos of the process can be seen in *Appendix 3*.



Fig. 42 Cast CLSM Samples in the Molds

It should be emphasized that for the mixture with 30% RAP content in AS_CLSM and for DWCS_CLSM and FWSS_CLSM mixtures (in its two combinations w/p 0.70% and 0.80%) the phenomenon of segregation has been observed in *Figure 43*. The segregation of the concrete is the separation of its components once it has been kneaded, causing the fresh concrete mixture to have a non-uniform distribution of its particles. If a concrete has good segregation resistance, this means that the aggregates are uniformly distributed in the mixture, both in vertical direction as in horizontal. Clearly this is not a good thing. Therefore, for the mixture with 30% RAP, it was decided to remove the analysis, while for the four Stones Sawmilling Sludge CLSM mixtures it was decided to continue the analysis to see what the results were.



Fig. 43 Segregation phenomena in Stone Saw Milling Sludge Mixes

5.7 Thermal Conductivity Measurement in CLSM's

Thermal conductivity of the Aggregate Sludge CLSM and Stone Sawmilling Sludge CLSM samples was measured at different mixes. The measurement was performed at; different ages (2,7,14,28 days), in wet condition and dry condition for AS_CLSM, in dry condition after drying in oven for two days at 60°C. For the SSS_CLSM, the measurements were taken only at 2,7 and 14 days.

The measurement process was executed in the same way for all samples, this consisted in making three holes in the upper face of the cylindrical sample in its fresh state with a minimum distance to the border of 1cm. The holes were made with the same tool used for soils (metal needle in the form of L) one day after casting the mixes.

The device used is the same one mentioned for soils and the selected sensor was the single needle TR-1 (100 mm long, 2.4 mm diameter). As seen in Figure 42, the measurement taking mode consisted of three measurements per sample, that is, one measurement per hole and thus obtain the average of the Thermal Conductivity. Likewise, numbers are placed in each hole to vary the sequence of measurements and reduce possible errors in measurements. This sequence also consists in varying the measurements between samples, for example; if the measurement for hole 1 of sample X has been taken, the next measurement will be for hole 1 of sample Y. That is, to reduce overheating errors in areas of influence of each hole that may influence the thermal conductivity calculation.

It is recalled that between the beginning of each daily measurement process the device must be calibrated. As well as, comply with the time lapses between measurements and sensor insertion (15 minutes for each). This is done so that the needle can balance the temperature of the sensor with that of the material, as well as with the environment between measurements.



Fig. 44 Thermal Conductivity Measurement on CLSM's Specimens

All the measurements were taken without the previous placement of GEL, with possible errors in the measurements since as explained above, the GEL contributes to the reduction of measurement error by covering the free space that can be generated between the sensor and the walls of the hole.

In the process of taking measurements in dry conditions (after oven drying), the decision to use GEL has been made. It will be seen in the next chapter if this has influenced the individual results of each sample.

CHAPTER 6

RESULTS AND DISCUSSIONS

This chapter describes the results of experimental investigation the results are further discussed based on different factors investigated and the trends observed during the measurements. Tests on the soils are explained first and then the tests on the CLSM samples.

The final analyses were based both on the numerical results of the tests carried out and on the qualitative judgments expressed by the experience acquired during the research, the results were also compared with models found in the literature.

6.1 Proctor Compaction Test

Once the modified Proctor Compaction studies were carried out, where for A_{1-a} soil six tests with moisture content were carried out: 0.0, 3.5, 5.0, 6.0, 7.5, 10%, and seven for soil A₇₋₆, with variations of: 10.8, 13.2, 15.7, 18.0, 20.4, 22.9, 26.1 %. For this soil it has not been possible to carry out the compaction with 0% water content. It has been tried twice and the results were negative with 90% loss of the material when comparing. Thereby, the results are presented in the following *Figures 43 and 44*. The table of calculations can be seen in the *Appendix 4*

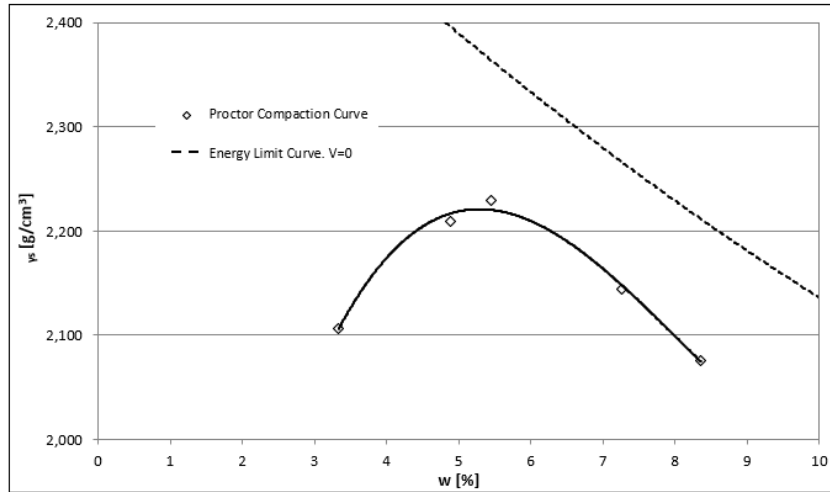


Fig. 45 Proctor Compaction Curve for soil A_{1-a}

It is observed that the compaction curve is far from the values of the maximum energy curve ($v=0$). This curve is determined from the specific density of the grain, varying moisture content from 0% to ρ_s . (Equation 24)

$$\gamma_s \frac{\rho_s}{[1 + (\frac{w}{100 \cdot \rho_s})]} \quad [eq. 24]$$

Where:

- γ_s = Density of the soil in dry conditions [g/cm³]
- w = moisture content in %
- ρ_s = specific density [g/cm³]

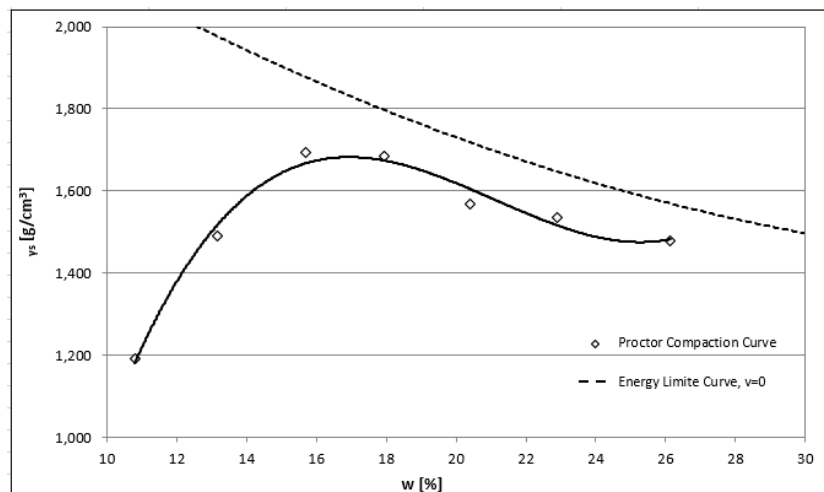


Fig. 46 Proctor Compaction Curve for soil A₇₋₆

In the soil A₇₋₆ the behaviour of the curve is different, and the results are close to values of the maximum energy curve.

For these types of soils and after making a third-degree polynomial extrapolation according to the results of the tests carried out, the optimum moisture values to obtain maximum density are expressed in *Table 19*.

Tab. 19 Optimal moisture for maximum densities

Soil	w_{optimum} [%]	$\gamma_{s,\text{max}}$ [g/cm ³]
A _{1-a}	5,28	2,220
A ₇₋₆	16,75	1,701

For both the soils, the density increased with moisture content in the initial stage and further reduced with the moisture addition. The optimum moisture content was identified at which the soils showed maximum density. A₇₋₆ soil had a much higher optimum moisture content than the A_{1-a}.

6.2 Thermal Conductivity in Soil

In this section, the results of geotechnical properties, as well as the values of thermal conductivity measured by KD2pro in both soils will be shown in *Table 20* for A_{1-a} soil and in *Table 21* for A₇₋₆. in function of different moisture content.

In the measurement of the thermal conductivity in the sample of soil A with humidity equal to 10.8%, an unusual value is observed if it is compared with the other results. Therefore, it was decided to exclude from the study since these were probably due to an error in the measurement and this could alter the results of subsequent analyses

Tab. 20 Geotechnical and Thermal Properties of A_{1-a}

Sample	MVA	w	M _{soil}	M _{water}	V _{sample}	V _{soil}	V _{water}	V _{air}	n	S _r	γ _s	k
[-]	[g/cm ³]	[%]	[g]	[g]	[cm ³]	[cm ³]	[cm ³]	[cm ³]		[%]	[g/cm ³]	[W/m ² ·K]
1	2,714	0,0	4635,9	0,0	2120,6	1708,1	0,0	412,4	0,19	0,0	2,186	0,589
2	2,714	3,34	4467,6	149,0	2120,6	1646,1	149,4	325,1	0,22	31,5	2,107	1,310
3	2,714	4,88	4683,9	228,5	2120,6	1725,8	229,1	165,7	0,19	58,0	2,209	1,934
4	2,714	5,44	4727,3	257,3	2120,6	1741,8	258,0	120,8	0,18	68,1	2,229	1,884
5	2,714	7,27	4548,0	330,4	2120,6	1675,7	331,3	113,6	0,21	74,5	2,145	1,878
6	2,714	8,36	4401,2	367,8	2120,6	1621,7	368,7	130,2	0,24	73,9	2,075	1,732

Tab. 21 Geotechnical and Thermal Properties of A₇₋₆

Sample	MVA	w	M _{soil}	M _{water}	V _{sample}	V _{soil}	V _{water}	V _{air}	n	S _r	γ _s	k
[-]	[g/cm ³]	[%]	[g]	[g]	[cm ³]	[cm ³]	[cm ³]	[cm ³]		[%]	[g/cm ³]	[W/m ² ·K]
1	2,667	13,17	3160,0	416,3	2120,6	1184,9	417,6	518,1	0,44	44,6	1,490	0,749
2	2,667	15,70	3594,6	564,5	2120,6	1347,8	566,2	206,6	0,36	73,3	1,695	1,061
3	2,667	17,96	3572,8	641,6	2120,6	1339,6	643,1	137,8	0,37	82,4	1,685	0,916
4	2,667	20,42	3325,3	679,0	2120,6	1246,8	680,4	193,3	0,40	82,6	1,568	0,946
5	2,667	22,89	3258,5	745,9	2120,6	1221,8	748,2	150,6	0,42	83,5	1,537	0,997
6	2,667	26,13	3137,4	819,9	2120,6	1176,4	821,6	122,6	0,45	87,0	1,480	0,957

After obtaining these results, it is analyzed how the thermal conductivity is influenced according to several variables such as: bulk density, moisture, degree of saturation of soil and volume of the solid.

6.2.1 Relation between Bulk Density and Thermal Conductivity.

The relation between bulk density and thermal conductivity in A_{1-a} soil is shown in *Figure 47*. It can be observed that as the density of the soil increases, the thermal conductivity also accompanies the same trend. This result is similar to what is established in the literature review. As the density of the soil increases, the porosity and the air content decrease in the interior, which increases the contact between the soil particles and results in a higher conductivity.

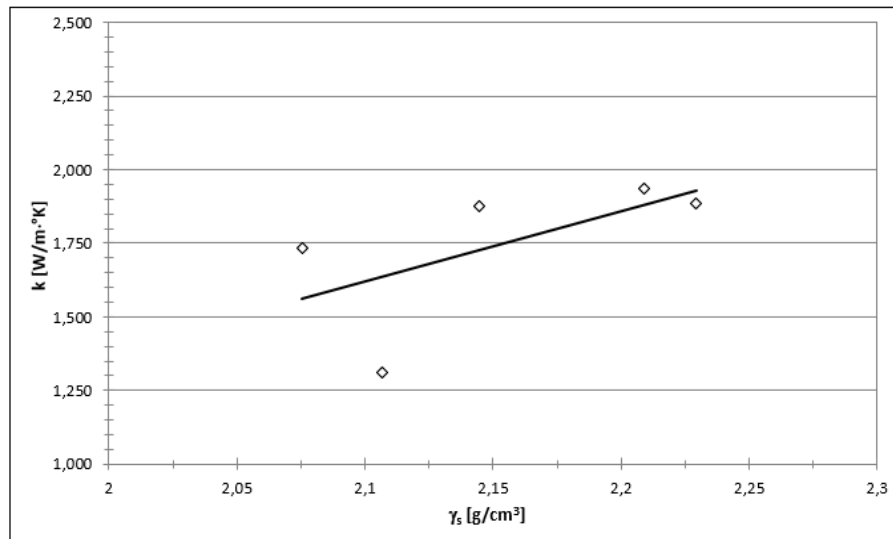


Fig. 47 Relationship Between Density and Thermal Conductivity – A_{1-a}

For A_{7-6} , given that this soil is very compressible and very plastic and resembles clay. This fine soil has the ability to retain more water in their pores, direct contact between soil grains is more difficult in this case than in soils where water is free to move from their pores, eventually this generates bridges between grains and reduces the heat transfer by conduction. It can be observed in *Figure 48* that the values of thermal conductivity are not affected in great magnitude when increasing its dry density, since they remain relatively constant. Consequently, the values of this are in turn lower than those obtained for A_{1-a}

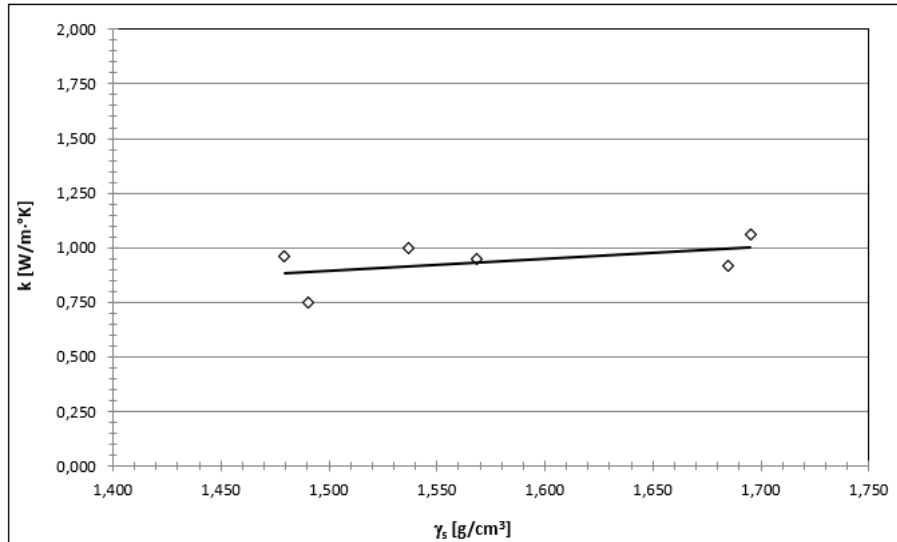


Fig. 48 relationship between density and thermal conductivity – A7-6

6.2.2 Relation between Water Content and Thermal Conductivity

To determine how the thermal conductivity is affected by the moisture content within the analysed soils, the measurements were conducted on the two types of soils by varying the moisture content. The fluid volume fraction is a dominant factor to the thermal conductivity of partially saturated soil. For A_{1-a} soil the trend showed in the follows *Figure 49* the same pattern as the Proctor Compaction Test curve since the highest values of thermal conductivity close to 2 [W/m²K] are between 6% and 7% water content. Likewise, we can observe how there is a critical moisture limit where, at values lower than this, the thermal conductivity decreases sharply. This agrees with what was seen and explained in *Chapter 2 Figure 9*. In this analysis this limit value we can take it for moisture content 4.5%.

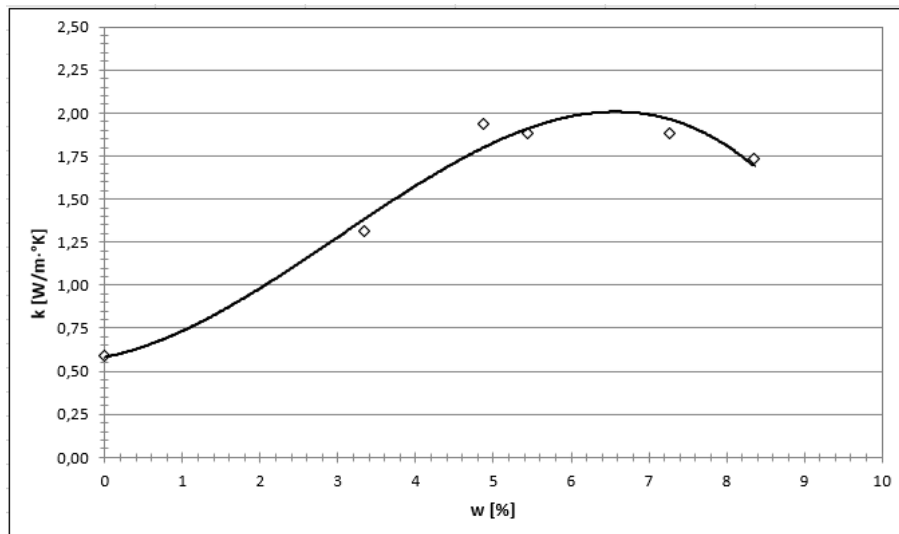


Fig. 49 relationship between water content and thermal conductivity – A-1-a

The presence of low water content within the structure of the soil makes the dry density lower, thus the soil would have a high voids ratio with substantial amounts of air. It is known that the thermal conductivity of air is too low ($\lambda_a = 0.024 \text{ W / (m} \cdot \text{K)}$) compared to those of water ($\lambda_w = 0.57 \text{ (W / (m} \cdot \text{K))}$), for this reason, low levels of thermal conductivity are obtained at low moisture content. As the water content increases, the grains of soil to move away from each other without having contact, thus generating thermal conductivity to decreases.

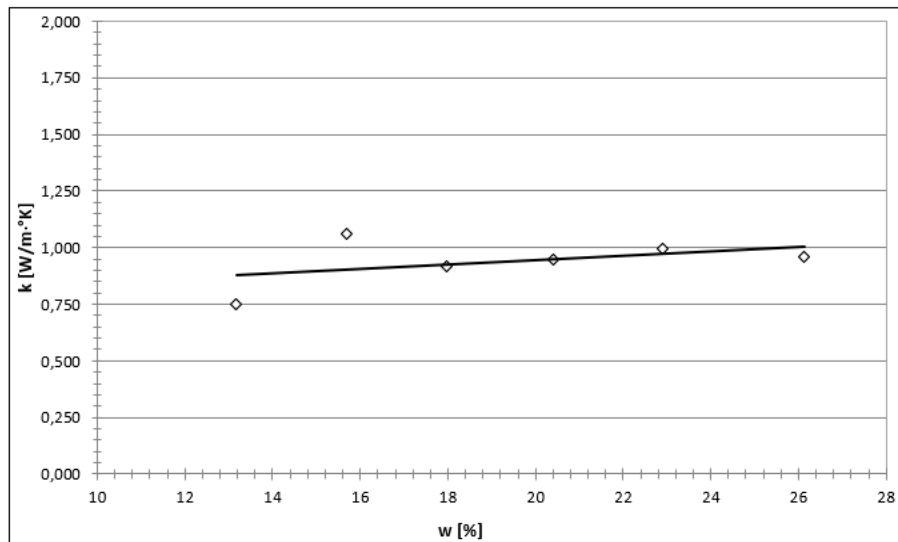


Fig. 50 Relationship Water Content and Thermal Conductivity – A_{7.6}

In case of clay like fine soil of A_{7.6}, the behaviour is like that obtained for bulk density. The trend is constant when varying the water content portions with values of thermal conductivity close to 1 [W / m²K]. In *Figure 50*. It can be seen that the ranges of values are substantially lower than those obtained for Coarse soils. This is could be due to the saturation phenomena of clays. This is further explained in the next section.

6.2.3 Degree of Saturation and Thermal Conductivity

Degree of saturation is referred to volume of voids filled with water inside the soil microstructure. This could affect the ability of a soil to conduct heat. The different degree of saturation obtained during the Compaction Proctor Test for the two types of soils is compared with their thermal conductivity. The *Figures 51 and 52* shows how thermal conductivity is improved by approaching values close to saturation greater than 50% for both fine and coarse soils. As expected, this is due to the removal of air content from the pores and hence causes the conductivity to rise.

The thermal conductivity on A_{1-a} soil is better than A₇₋₆. However, the maximum values are generated when the percentage of degree of saturation is greater than 60%, then remaining in a constant range between 1.75 - 2 [W / m ° K] for the first and around 1.0 [W / m ° K] for the seconds. This is important at the time of determining the water content that the pores must have in order to obtain acceptable thermal conductivity values.

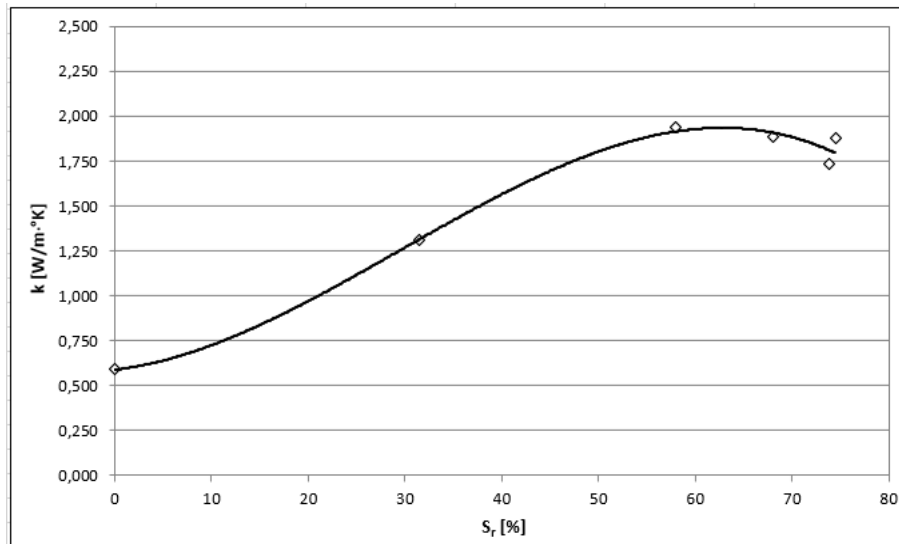


Fig. 51 Relationship between Degree of Saturation and Thermal Conductivity – A_{1-a}

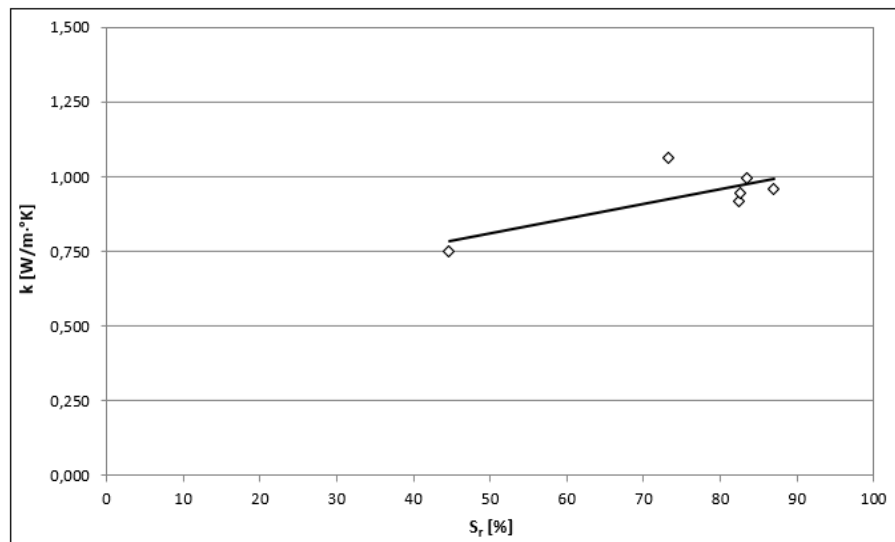


Fig. 52 Relationship between Degree of Saturation and Thermal Conductivity – A₇₋₆

6.2.4 Volume of Soil Grains and Thermal Conductivity

The highest thermal conductivity is obtained when the contact between the grains of the soil is as large as possible or when the greater amount of air and water is eliminated within the structure. This

also depends on the soil mineralogy, since as explained in *Chapter 2*, minerals such as quartz have the greatest ability as a heat conductor.

After carrying out the respective tests both for A_{1-a} and A₇₋₆ soil, it is verified that, for the first has a slight increase when increasing the solid content within the structure (*Figure 53*). While, the thermal conductivity values for the fine soil are within a nearly constant interval between 1200 and 1350 cm³, (*Figures 54*) this means that by varying the contents of soil volumes within the structure, this does not is affected.

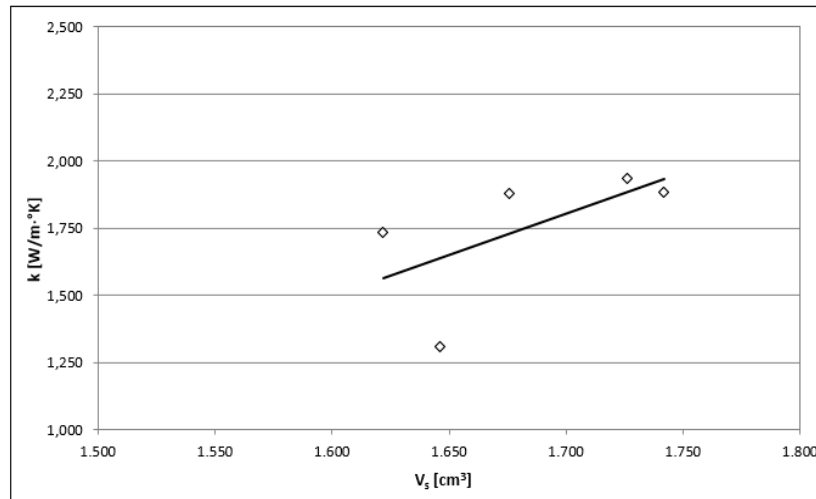


Fig. 53 Relationship between Volume of Soil Grains and Thermal Conductivity – A-1-a

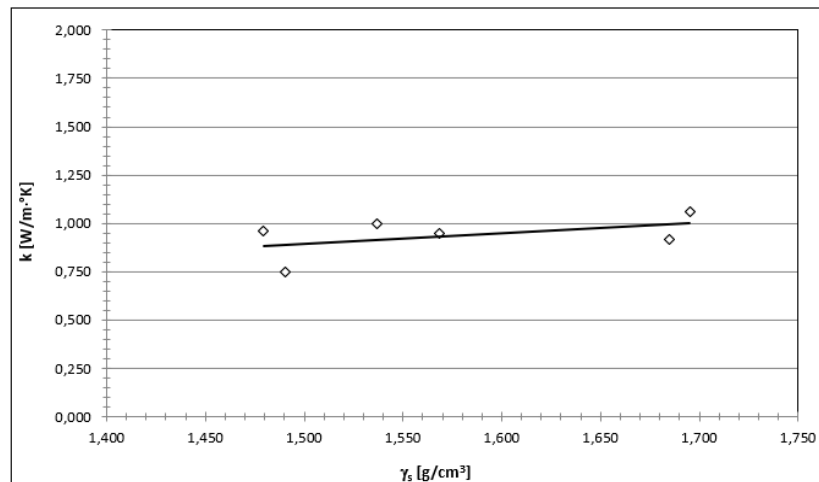


Fig. 54 Relationship between Volume of Soil Grains and Thermal Conductivity – A-7-6

As in previous analyses, coarse soils such as A_{1-a} provide values of thermal conductivity that reach almost double that for fine soils as well as in volume contents of soil. This could be due to the content of soil mineral and the difference in physical properties between the two.

6.3 Interpretation of Results.

The thermal conductivity results obtained during the experimental investigation on soils are compared with the information available on the literature to check the reliability of the data. *Figure 55* shows some characteristic ranges of thermal conductivity versus moisture content for soils that include sands, clays and silt, verifying that the results of thermal resistivity collected for each of our soil type, agrees with the ranges found in the graph (*Figure 9 -chapter 2-section 2.2*) taken from literature.

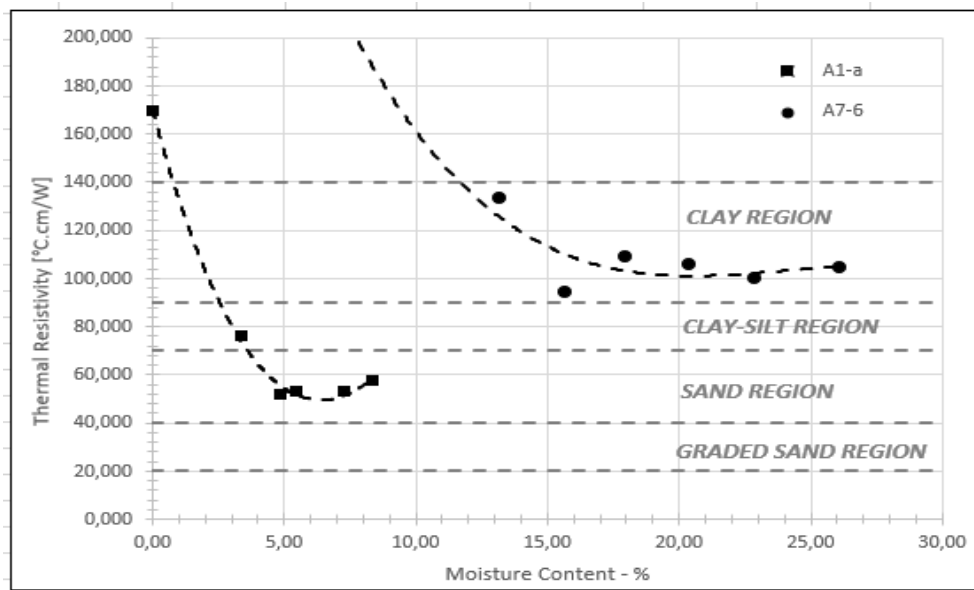


Fig. 55 Comparison of Thermal Conductivity Characteristics of Soil

Based on the results obtained after the corresponding measurements, it is observed that the values of resistivity ($1/k$) are coherent, since these are within the ranges established by previous studies found in literature [10], therefore, establish a correct analysis of the studied soils

6.4 Thermal Conductivity Models of Soil.

This section aims to develop a series of empirical models of thermal conductivity for wet soils that is based on the concept of normalized thermal conductivity with respect to dry and saturated states. These models integrate well the effects of porosity, the degree of saturation and moisture, for the analytical determination of k . The thermal conductivity (k) for saturated soils is calculated with the use of a geometric model to develop a generalized empirical relationship to evaluate the thermal conductivity of dry soils. A general relationship between the normalized thermal conductivity of the soils and the degree of saturation was used using a factor dependent on the type of soil to correlate the normalized thermal conductivity such as gravel, sand and silt.

The following sub-sections will show the comparison between the measured thermal conductivity and that calculated using the different models. In all cases, it is observed how the models overestimate k

[W/m^oK] with respect to the measurement in the laboratory. This may be because all the models were developed empirically for certain types of soils under certain conditions.

6.4.1 Kersten Model (1949)

As mentioned above, the values are overestimated, with fine soils having a better performance than coarse ones. This was one of the unfavorable points in Kersten's model since in the results proposed by him for different types of soils and minerals the same thing happened in its majority.

In this study it can be observed in *Figure 56* how for Fine soils (A₇₋₆) the adjustment has a slight correlation between measured and calculated values, while for Coarse soils the overstatement is greater. The *Tables 22,23* show the summary of results, while in Appendix 4 can be seen all of calculations done.

Tab. 22 Summary of $k_{calculated}$ and $k_{measured}$ for A_{1-a} (Kersten)

Kersten (1949) model - A_{1-a}			
w_{eff} [%]	V_d [kg/m ³]	$k_{meas.}$ [W/m ^o K]	$k_{calc.}$ [W/m ^o K]
0,00	2186,152	0,589	/
3,34	2106,774	1,310	2,281
4,88	2208,795	1,934	3,040
5,44	2229,237	1,884	3,249
7,27	2144,686	1,878	3,153
8,36	2075,498	1,732	2,976

Tab. 23 Summary of $k_{calculated}$ and $k_{measured}$ for A₇₋₆ (Kersten)

Kersten (1949) model - A₇₋₆			
w_{eff} [%]	V_d [kg/m ³]	$k_{meas.}$ [W/m ^o K]	$k_{calc.}$ [W/m ^o K]
13,17	1490,177	0,749	0,993
15,70	1695,110	1,061	1,447
17,96	1684,843	0,916	1,511
20,42	1568,132	0,946	1,347
22,89	1536,600	0,997	1,346
26,13	1479,517	0,957	1,302

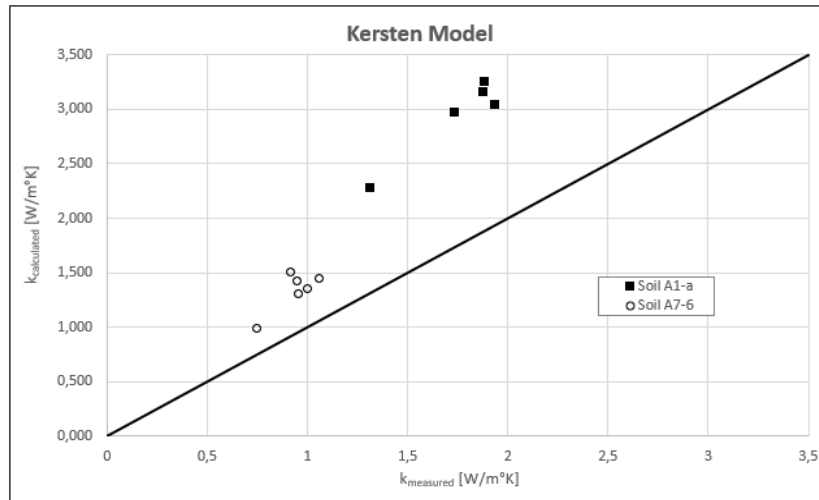


Fig. 56. Comparison between Predicted Thermal Conductivities a Measured Values - Kersten

6.4.2 Johansen Model (1975)

Figure 55 shows how Johansen's model behaves similarly to Kersten's, with an overestimation of the results. Likewise, for a better fit and to obtain more acceptable results, for A_{1-a} soil, an adjustment of the Equation 8 has been made, obtaining a coefficient of -0.10. for A₇₋₆ soil the same equations proposed by this model have been used. The adjustment can be made since these formulas are empirical and depend for each material and condition.

For values of k_s , those proposed by Kersten were taken based on the type of soil. These were 5.5 for coarse soils and 2.8 for fine soils, this can be seen in Table 24,25

Tab. 24 Summary of $k_{calculated}$ and $k_{measured}$ for A_{1-a} -Johansen

S_r [%]	k_r [W/m·°K]	n	k_{dry} [W/m·°K]	k_s [W/m·°K]	k_{sat} [W/m·°K]	$k_{calc.}$ [W/m·°K]	$k_{meas.}$ [W/m·°K]
0,00	/	0,19	0,046	5,5	3,575	0,000	0,589
31,49	0,649	0,22	0,045	5,5	3,350	2,189	1,310
58,03	0,835	0,19	0,046	5,5	3,641	3,046	1,934
68,11	0,883	0,18	0,046	5,5	3,703	3,276	1,884
74,47	0,910	0,21	0,046	5,5	3,456	3,150	1,878
73,91	0,908	0,24	0,045	5,5	3,266	2,970	1,732

Tab. 25 Summary of $k_{calculated}$ and $k_{measured}$ for A₇₋₆ -Johansen

S_r [%]	k_r [W/m·°K]	n	k_{dry} [W/m·°K]	k_s [W/m·°K]	k_{sat} [W/m·°K]	$k_{calc.}$ [W/m·°K]	$k_{meas.}$ [W/m·°K]
44,63	0,755	0,44	0,236	2,8	1,419	1,129	0,749
73,27	0,905	0,36	0,359	2,8	1,597	1,480	1,061
82,36	0,941	0,37	0,351	2,8	1,588	1,515	0,916
77,87	0,924	0,40	0,296	2,8	1,517	1,424	0,946
83,24	0,944	0,42	0,259	2,8	1,459	1,392	0,997
87,02	0,958	0,45	0,231	2,8	1,410	1,360	0,957

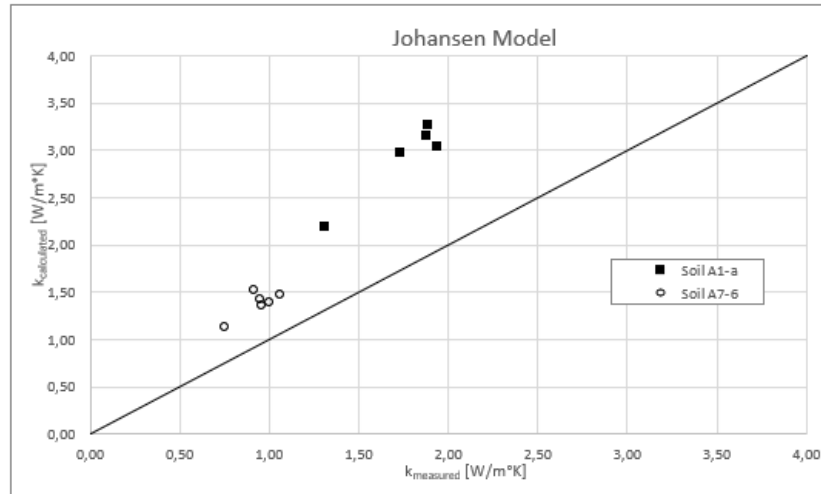


Fig. 57. Comparison between Predicted Thermal Conductivities a Measured Values - Johansen

6.4.3 Farouki Model (1981,1982)

The model and modifications proposed by Farouki in 1982 are the ones that have been best adjusted to this study, always talked about in terrain A₇₋₆ since, for coarse terrain, correlations have always had values of overestimates in all cases. This can be seen in *Figure 58*

As explained in *Chapter 2*, Farouki made modifications in the calculation of normalized thermal conductivity (k_r), since in this case it depends on the degree of saturation and constants based on tests (*Equation 13*). To obtain a more acceptable result, an adjustment has been made using Solver (Excel application) to find constants that are more correlated to the types of soils used in this thesis.

Tab. 26 Summary of $k_{calculated}$ and $k_{measured}$ for A_{1-a}-Farouki

S_r [%]	k_r [W/m ² ·K]	n	k_{dry} [W/m ² ·K]	k_e [W/m ² ·K]	k_{sat} [W/m ² ·K]	$k_{calc.}$ [W/m ² ·K]	$k_{meas.}$ [W/m ² ·K]
0,00	0,000	0,19	1,450	5,5	3,575	1,450	0,589
31,49	0,368	0,22	1,243	5,5	3,350	2,020	1,310
58,03	0,452	0,19	1,517	5,5	3,641	2,477	1,934
68,11	0,471	0,18	1,580	5,5	3,703	2,579	1,884
74,47	0,481	0,21	1,338	5,5	3,456	2,356	1,878
73,91	0,480	0,24	1,172	5,5	3,266	2,176	1,732

Tab. 27 Summary of $k_{calculated}$ and $k_{measured}$ for A₇₋₆ Farouki

S_r [%]	k_r [W/m ² ·K]	n	k_{dry} [W/m ² ·K]	k_e [W/m ² ·K]	k_{sat} [W/m ² ·K]	$k_{calc.}$ [W/m ² ·K]	$k_{meas.}$ [W/m ² ·K]
44,63	0,419	0,44	0,267	2,8	1,419	0,749	0,749
73,27	0,479	0,36	0,369	2,8	1,597	0,958	1,061
82,36	0,492	0,37	0,363	2,8	1,588	0,965	0,916
77,87	0,486	0,40	0,320	2,8	1,517	0,902	0,946
83,24	0,493	0,42	0,287	2,8	1,459	0,865	0,997
87,02	0,497	0,45	0,262	2,8	1,410	0,833	0,957

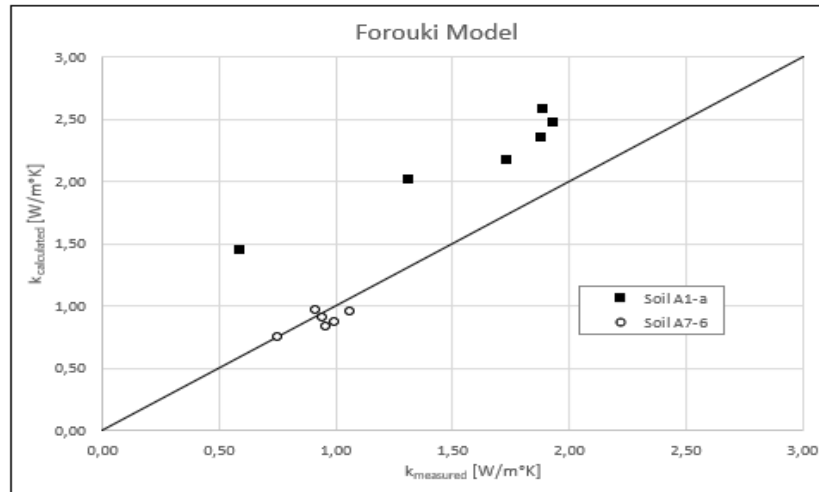


Fig. 58 Comparison between Predicted Thermal Conductivities a Measured Values - Farouki

6.4.4 Cote and Konrad Model (2005)

The last model analyzed was this, which can be seen in Figure 59 which has a little dispersion in both A_{1-a} and A₇₋₆ soils. This model uses a κ parameter for k_r calculations, this parameter is a function of the type of soil (Table 28 and 29). In this analysis, this parameter has been adjusted based on the soils that has been used. Therefore, the results of Coté and Konrad they are acceptable to what we expect, however, they are overestimated.

Tab. 28 Summary of $k_{calculated}$ and $k_{measured}$ for A_{1-a} -Cote and Konrad

S_r [%]	κ coarse sand	k_r	natural mineral soil		n	k_{dry} [W/m ² K]	k_e [W/m ² K]	k_{sat} [W/m ² K]	k_{calc} [W/m ² K]	$k_{meas.}$ [W/m ² K]
			χ	η						
0,00	0,50	0,000	1,70	1,80	0,19	0,759	5,5	3,575	0,759	0,589
31,49	0,50	0,187	1,70	1,80	0,22	0,673	5,5	3,350	1,173	1,310
58,03	0,50	0,409	1,70	1,80	0,19	0,786	5,5	3,641	1,953	1,934
68,11	0,50	0,516	1,70	1,80	0,18	0,811	5,5	3,703	2,304	1,884
74,47	0,50	0,593	1,70	1,80	0,21	0,713	5,5	3,456	2,340	1,878
73,91	0,50	0,586	1,70	1,80	0,24	0,641	5,5	3,266	2,180	1,732

Tab. 29 Summary of $k_{calculated}$ and $k_{measured}$ for A₇₋₆ - Cote and Konrad

S_r [%]	κ silt and clay	k_r [W/m ² K]	natural mineral soil		n	k_{dry} [W/m ² K]	k_e [W/m ² K]	k_{sat} [W/m ² K]	$k_{calc.}$ [W/m ² K]	$k_{meas.}$ [W/m ² K]
			χ	η						
44,63	0,98	0,440	0,75	1,20	0,44	0,222	2,8	1,419	0,749	0,749
73,27	0,98	0,728	0,75	1,20	0,36	0,274	2,8	1,597	1,237	1,061
82,36	0,98	0,820	0,75	1,20	0,37	0,271	2,8	1,588	1,351	0,916
82,61	0,98	0,823	0,75	1,20	0,40	0,250	2,8	1,517	1,293	0,946
83,46	0,98	0,831	0,75	1,20	0,42	0,233	2,8	1,459	1,252	0,997
87,02	0,98	0,867	0,75	1,20	0,45	0,219	2,8	1,410	1,252	0,957

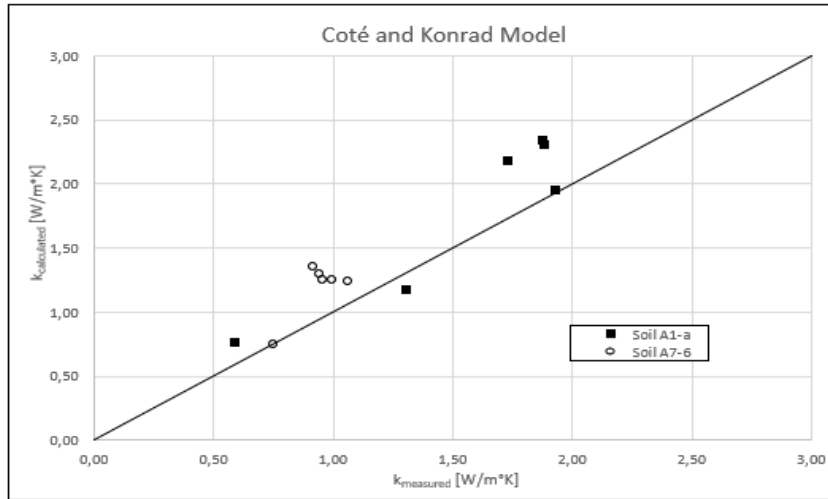


Fig. 59 Comparison between Predicted Thermal Conductivities a Measured Values – Coté and Konrad

6.4.5 Evaluation of de Models. [28]

After developing each model and perform their respective analyses. The purpose of this evaluation is to determine which of all the models is the most correlated with the measurements made in the laboratory for each type of terrain. In Figure 60 and 61, it can be observed, as the terrain A₇₋₆ has a better fit, than the soil A_{1-a}, although it is not the optimum and the results are not acceptable because in both soil there are a overestimate and high dispersion in the results.

On the other hand, it can be said that the Farouki model for fine soils is where the best results have been found, while the Cote a konrad models are the most acceptable for coarse soils. The models of Kersten and Johansen are those that have had low performance with more overestimate results.

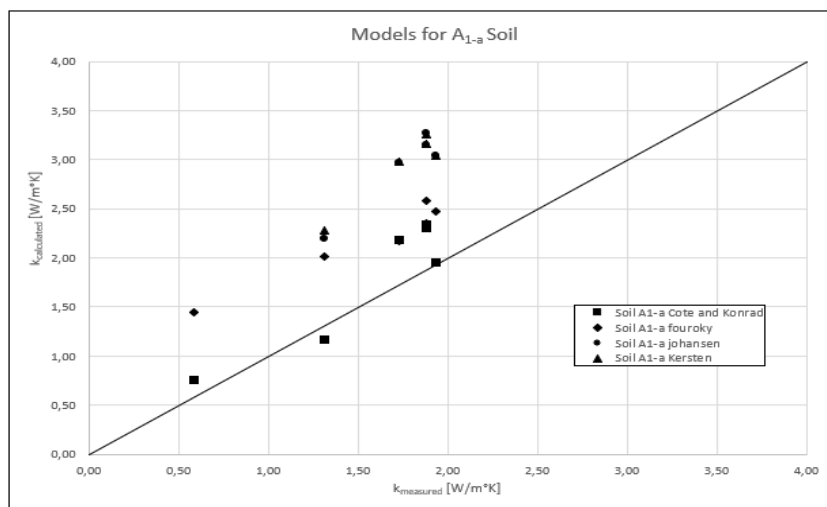


Fig. 60 Evaluation of Models between Predicted Thermal Conductivities a Measured Values for A_{1-a} soil

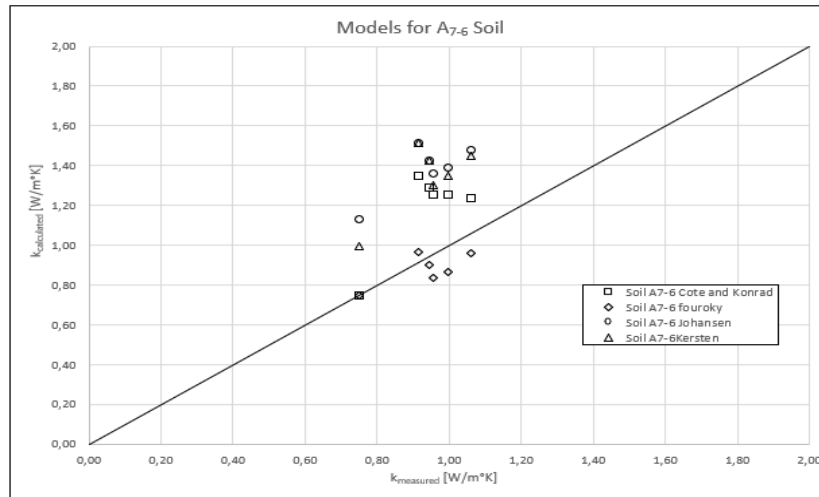


Fig. 61 Evaluation of Models between Predicted Thermal Conductivities a Measured Values for A₇₋₆ soil

6.5 Thermal Conductivity of CLSM's

The thermal conductivity of the CLSM was measured at different age and analysed know the influence of different parameters on the thermal conductivity

6.5.1. Influence of Cement Content on Thermal Conductivity

The cement content in the mixes were varied from 60, 80 and 100 kg/m³. The values of measurements are in Table 30. The Figure 62 shows how the trend of thermal conductivity when cement content varied.

Tab. 30 Thermal Conductivity Measurements as a function of Cement Content.

items	Cement Content [Kg/m ³]	Thermal conductivity [W/m.K]		
		7 days	14 days	28 days
C60_20_0,80	60	1,512	1,627	1,475
C80_20_0,80	80	1,661	1,662	1,697
C100_20_0,80	100	1,809	1,865	1,745

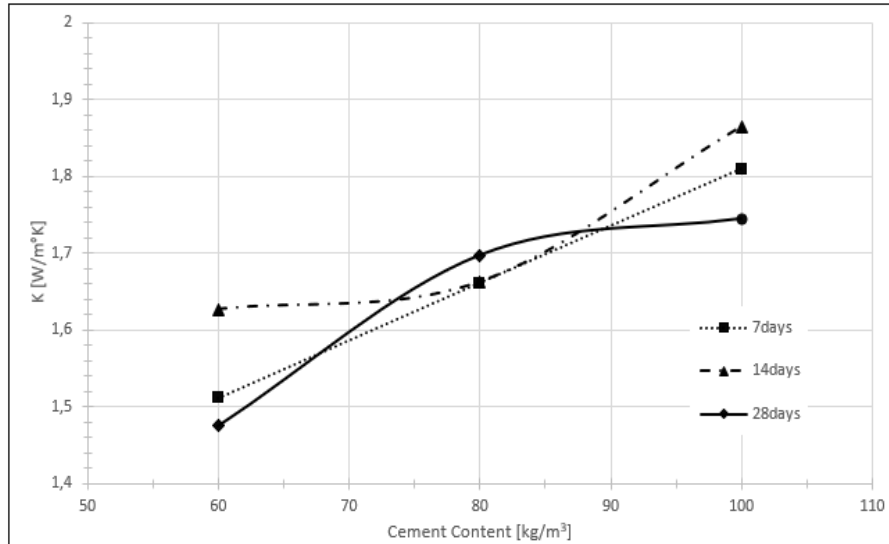


Fig. 62 Thermal Conductivity Variation with Different Cement Contents

It was observed that the cement content has a significant influence on the thermal conductivity of the mixes. As the cement content increases, the thermal conductivity of the mixes increases. This is could be due to the chemical composition of the hydration products. The mix with a cement content of 100 kg/m³ exhibited the highest conductivity whereas mix with 60 kg/m³ had the lowest conductivity.

6.5.2 Influence of Rap Content on Thermal Conductivity

For this type of samples and in accordance with what has been said in previous chapters, the results obtained in the measurements made in the laboratory for different RAP contents will be presented in Table 31. Four types of mix were made with: 0, 15, 20 and 30% of RAP, always for 1m³. The mix with 30% RAP content has been excluded, since it has presented the phenomenon of segregation and this has affected considerably the results of the measurements.

Tab. 31 Thermal Conductivity Measurements as a Function of Rap Content

items	Rap content	Thermal conductivity [W/m.K]		
	%	7 days	14 days	28 days
C100_0_0,80	0	1,670	1,549	1,429
C100_15_0,80	15	1,869	1,775	1,465
C100_20_0,80	20	1,809	1,865	1,745

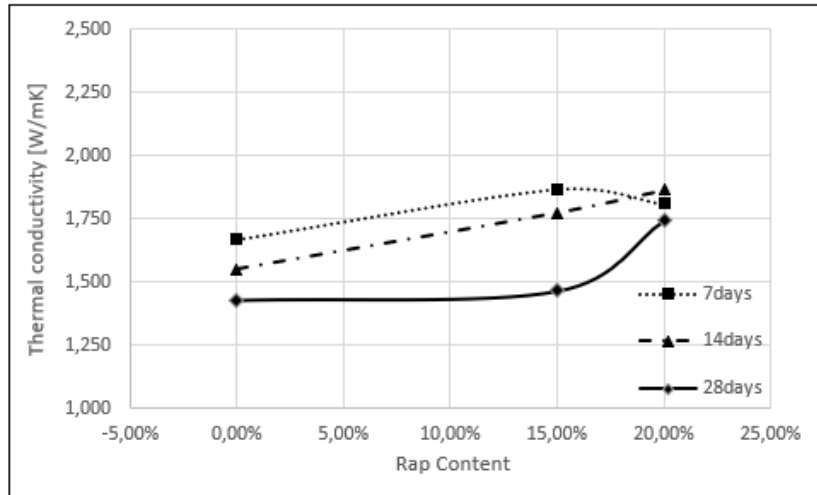


Fig. 63 Thermal Conductivity Variation with Different RAP Content for C100_0.80

Unlike how the cement content improves the properties of conducting heat, it can be observed that the content of RAP within the mix does not have a considerable influence. However, it can be said that by increasing the amount of RAP, the values of thermal conductivity slightly increase.

6.5.3 Influence of Water Content on Thermal Conductivity

The water content in the CLSM mix was controlled using the parameter water to powder ratio (W/P). As the W/P increases, the water content in the mix increases. The influence of the water content on the thermal conductivity is shown first in the table with the measured values and then in the fig with the variation of these.

Tab. 32 Thermal Conductivity Measurements as a Function of w/p ratio

items	W/P %	Thermal conductivity [W/m.K]		
		7 days	14 days	28 days
C100_20_0,70	0,70	1,632	1,635	1,333
C100_20_075	0,75	1,609	1,514	1,371
C100_20_0,80	0,80	1,809	1,865	1,745

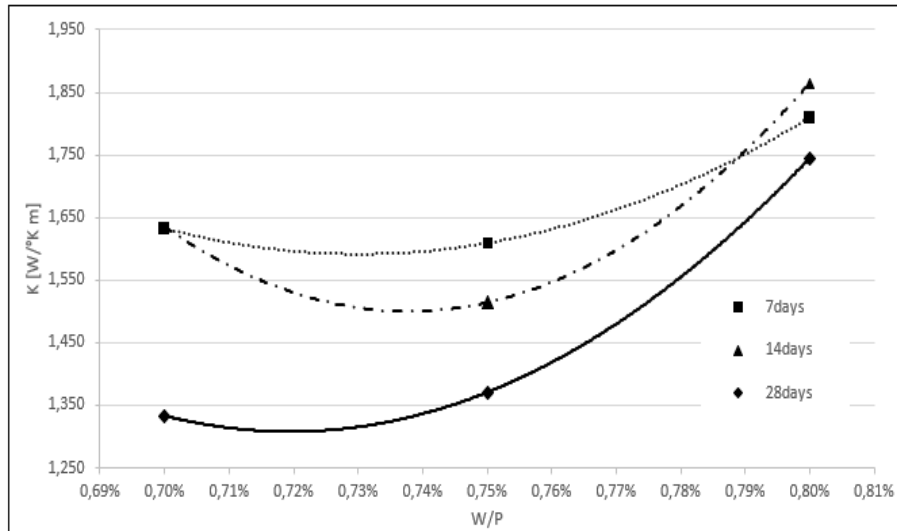


Fig. 64 Thermal Conductivity Variation with Different Water to Powder Ratio Content for C100_0.80

It was found that the thermal conductivity of the mixture increases with the increase in water content. This could be due to: the water lubricates the particles and generates greater contact between grains, as well as the water has greater aptitude to conduct the heat than the air and a greater quantity of water generates that the values of thermal conductivity increase.

6.5.4 Influence of Age on Thermal Conductivity

In this subsection we will analyze how the age (in days) can improve or not the thermal properties of the samples. To do this, the following graphs show how age affects the different variables analyzed above.

- Influence of age at different Cement Contents

From the *Figures 65*, it is evident that the influence of age on the thermal conductivity of the cement based composites are not significant. There is not much change in the thermal conductivity from the early days to the twenty eighth day. This is due to the following reasons. The aggregate skeleton of the CLSMs is densely packed and there is not much air voids inside. These mixes are highly impermeable and there is not much evaporation of water with time hence the thermal conductivity tends to be independent of the age of the specimens.

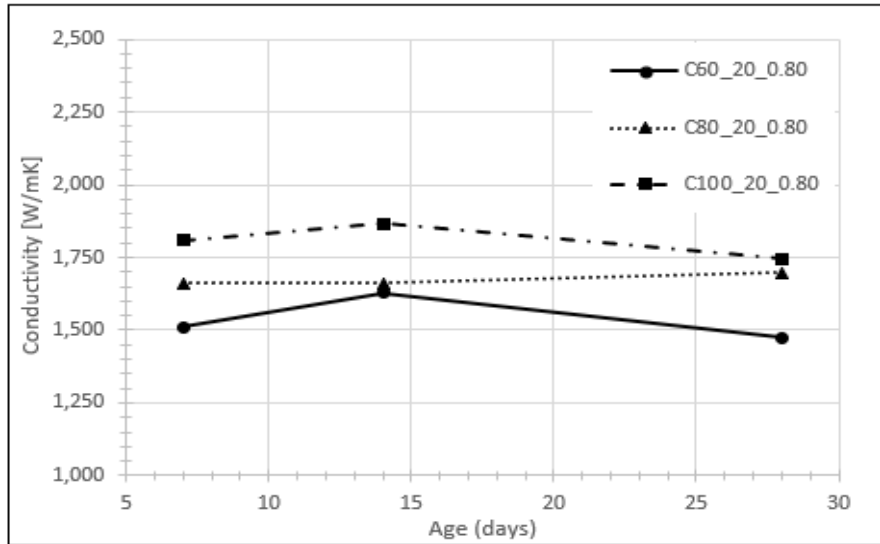


Fig. 65 Influence of Age on Thermal Conductivity with Diverse Cement Contents

- **Influence of age at different RAP content.**

Just as the RAP content does not increase the thermal conductivity of the mix, it can be said that as the age of the samples increases, their trend decreases, therefore the RAP content does not have a marked influence in improving the thermal conductivity of a mixture because in the analyzes carried out, their results have been unsatisfactory. This decrease in the values of k over time may be due to the fact that the RAP, being an aggregate with asphaltic base and with different granulometric properties, generates a greater porosity in addition to a change in the mineralogic composition of the samples.

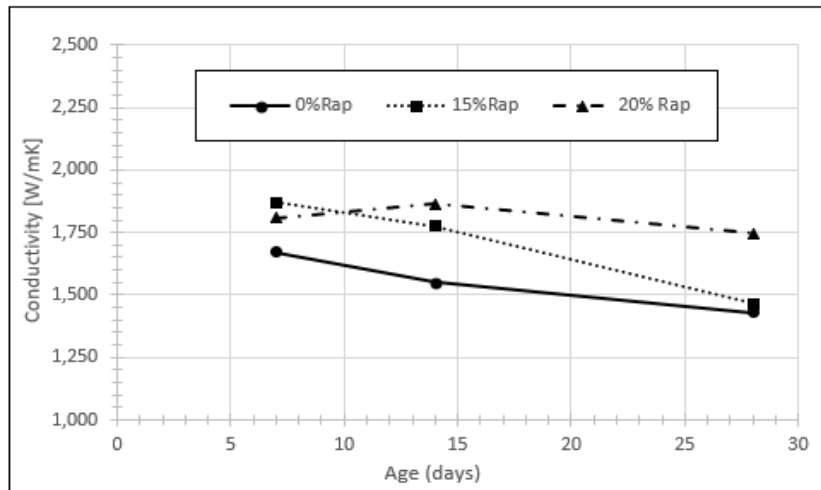


Fig. 66 Influence of Age on Thermal Conductivity with diverse %RAP content

- *Influence of age at different w/p ratio*

Surprisingly, the results in this variable have not been as expected, since it had been seen that increasing the water content within the mixture increased the capacity to remove heat, but it is observed in this case that the thermal conductivity decreases with the passage of time for the mixtures with 0.70 and 0.75% w / p ratio, however for 0.80% it has a more stable tendency, this may be due to having less water content within the mixture, it evaporates more quickly increasing the air content in the pores, thus decreasing the conductivity values.

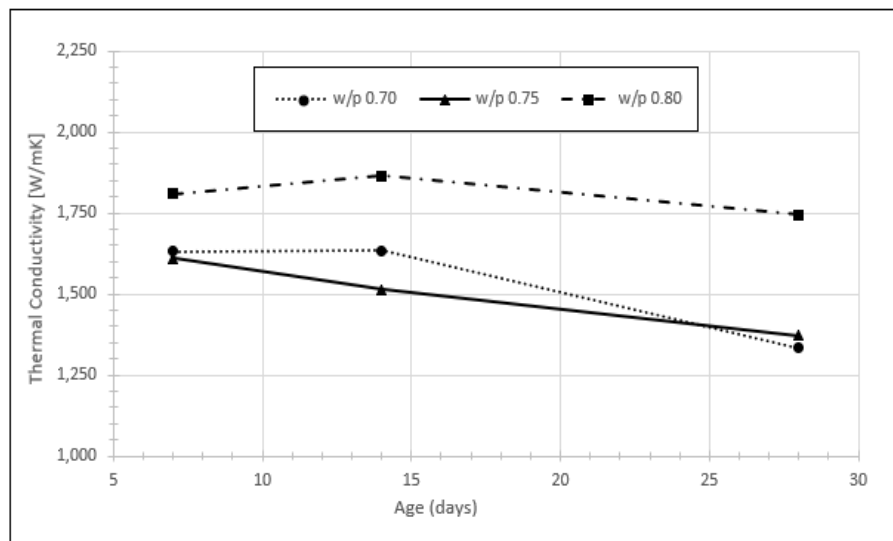


Fig. 67 Influence of Age on Thermal Conductivity with diverse w/p ratio for C100_20

6.6 Thermal conductivity model for CLSM.

A predictive model for the thermal conductivity of CLSM was developed in this section by selecting the measured thermal conductivity of the sample C100_20_0.80 as the reference. The relative values of all the samples will be shown in the following subsections as a function of cement contents, RAP content and water to powder ratio. And will be analyze the dependence of each test parameter on the thermal conductivity in relation to a reference parameter. The linear relationships observed during this analysis was then combined to form a predictive equation for the thermal conductivity of CLSMs as a function of each variable used in the mix.

The mixture with the following composition is selected as the reference:

- Cement Content = 100 kg / m³
- RAP Content in 1m³= 20%
- Water/Powder ratio in 1m³ 0.80%
- Age = 28 days

. This value will be called as follows in all the next analysis

$$k_{ref} = C100_20_0.80 = 1.745 \text{ [W/m}^\circ\text{K]}$$

6.6.1 Relationship as a function of Cement Content.

The first relationship to determine how far are the individual values of measurements at different ages with respect to that of as a function of different cement contents. The results obtained are shown in the following *Table 33*.

Tab. 33 Conductivity Ratio with different Cement Contents

items	cement content	Thermal conductivity Ratio [W/m.K]		
	[Kg/m ³]	7 days	14 days	28 days
C60_20_0,80	60	0,866	0,933	0,845
C80_20_0,80	80	0,952	0,953	0,973
C100_20_0,80	100	1,037	1,069	1,000

In the *Figure 68* can be seen the linear equation for relationship as Cement Content

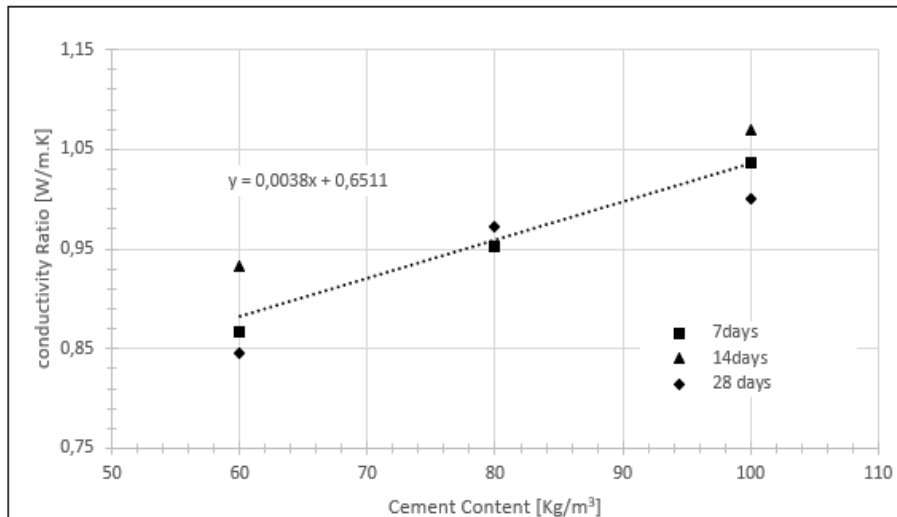


Fig. 68. Normalization curve of Cement Content

6.6.2 Relationship as a Function of RAP Content.

For RAP content the linear equation can be found in the *Figure 69* where all of ratios are exposes in *Table 34*.

Tab. 34 Conductivity Ratio with different RAP Content

items	RAP	Thermal conductivity Ratio		
	Content	[W/m.K]		
	%	7 days	14 days	28 days
C100_0_0,80	0%	0,957	0,888	0,819
C100_15_0,80	15%	1,071	1,017	0,840
C100_20_0,80	20%	1,037	1,069	1,000

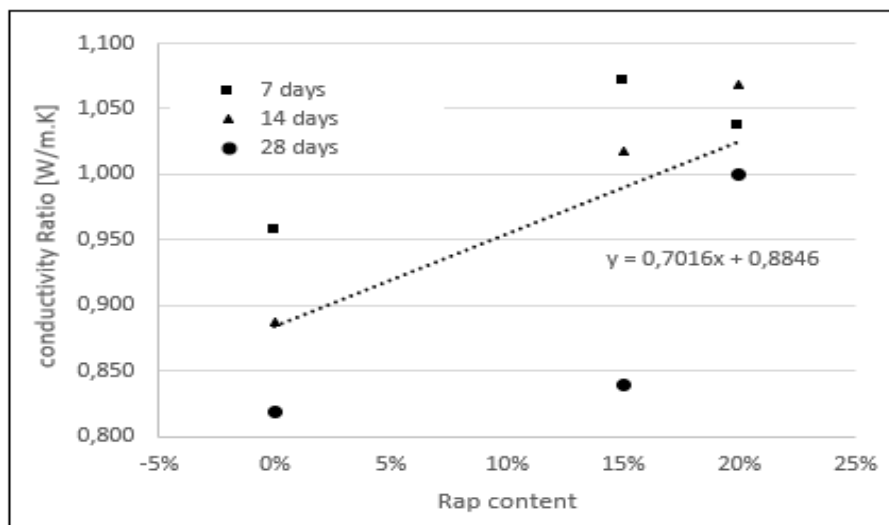


Fig. 69 Normalization curve of RAP Content

6.6.3 Relationship as a function of W/P ratio.

Finally, the last relation has been made in order to determine the adjustment equation that allows us to calculate the thermal conductivity values according to the different variables that have been used. *Table 35* and *Figure 70* exposes the results

Tab. 35 Conductivity Ratio with different w/p ratio

items	W/P	Thermal conductivity Ratio		
		[W/m.K]		
		7 days	14 days	28 days
C100_20_0,70	0,70	0,936	0,937	0,764
C100_20_0,75	0,75	0,922	0,868	0,786
C100_20_0,80	0,80	1,037	1,069	1,000

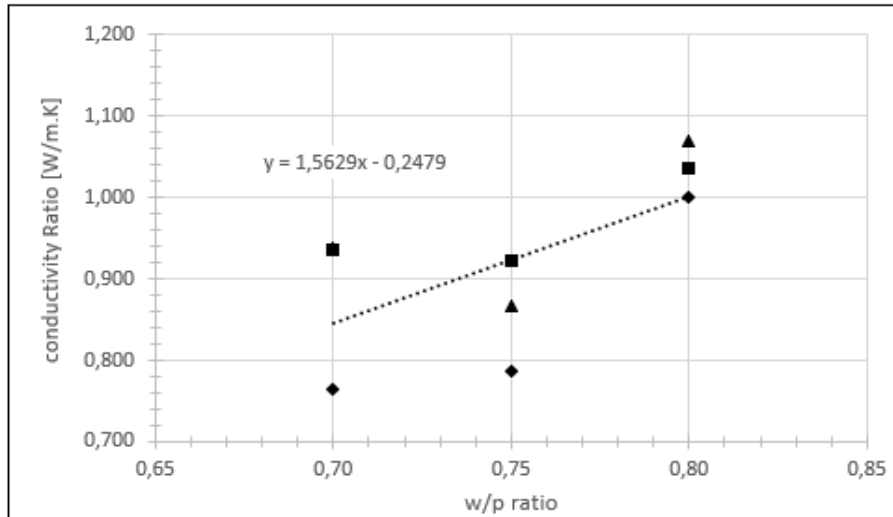


Fig. 70 Normalization curve of w/p ratio

6.6.4 Model Equation of Thermal Conductivity

Among the factors that influence thermal conductivity, observation of test results reveals that age does not provide a significant effect. Therefore, the thermal conductivity of the CLSM samples can be predicted by the relationship as functions of cement content, the RAP content and w/p ratio, as follows:

$$k = k_{ref} [(0.0038CC + 0.6511) \cdot (0.7016\%RAP + 0.8846) \cdot (1.5629\% \frac{w}{p} - 0.2479)]$$

Where:

- CC is a Cement Content [kg/m³] for each sample: 60,80 and 100 [kg/m³]
- %RAP is a Content RAP for each sample: 0,15,20 % in 1m³
- %w/p is a water to powder ratio inside the mix: 0.70,0.75,0.80 % in 1m³

The results and comparison between the thermal conductivity measured and calculated will be show, firstly for each set of Age in *Table 36* and the follow *Figures*

Tab. 36 Comparison Measurement and Calculation Values with Model

items	Comparison of the measuted and calculated values					
	7 days		14 days		28 days	
	$k_{measured}$	$K_{calculated}$	$k_{measured}$	$K_{calculated}$	$k_{measured}$	$K_{calculated}$
C60_20_0,8	1,51	1,58	1,63	1,58	1,48	1,58
C80_20_0,8	1,66	1,71	1,66	1,71	1,70	1,71
C100_20_0,8	1,81	1,85	1,86	1,85	1,74	1,85
C100_0_0,8	1,67	1,60	1,55	1,60	1,43	1,60
C100_15_0,8	1,87	1,78	1,77	1,78	1,47	1,78
C100_20_0,8	1,81	1,85	1,86	1,85	1,74	1,85
C100_20_0,7	1,63	1,56	1,64	1,56	1,33	1,56
C100_20_0,75	1,61	1,56	1,51	1,56	1,37	1,56
C100_20_0,80	1,81	1,85	1,86	1,85	1,74	1,85

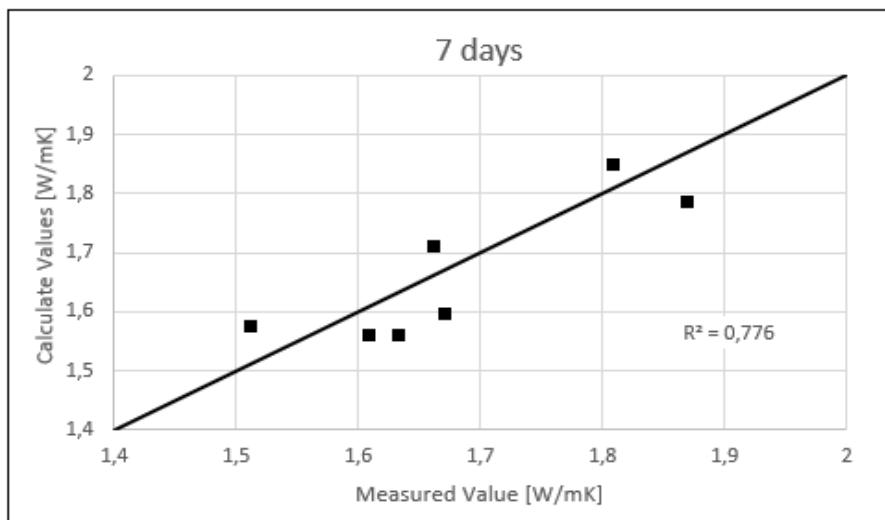


Fig. 71. Comparison of the Measured and Calculated values for 7 days

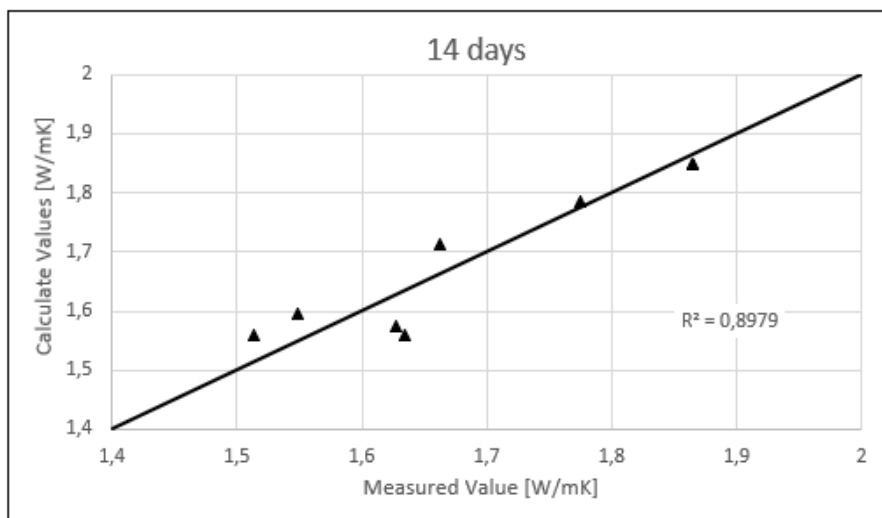


Fig. 72 Comparison of the Measured and Calculated values for 14 days

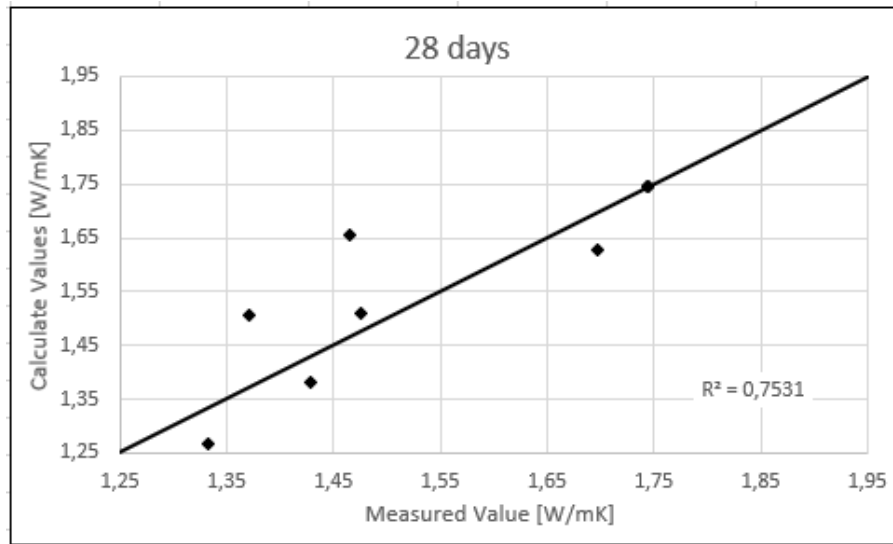


Fig. 73 Comparison of the Measured and Calculated values for 28 days

The model was able to predict the thermal conductivity reasonably well. The thermal conductivity values both measured and predicted for the for all the samples at all the ages are shown in *Figure 74*

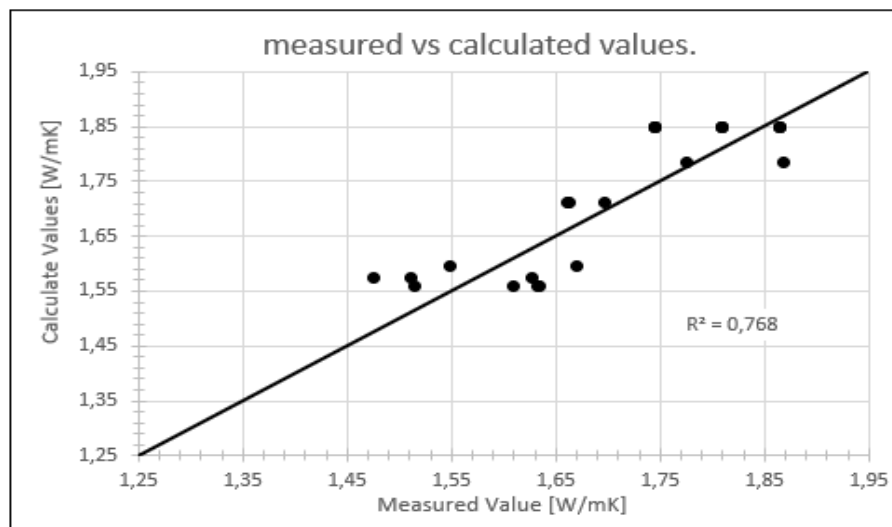


Fig. 74 Comparison of the Measured and Calculated value for model adopted

6.7 Thermal Stability

Thermal analysis of examined materials shows dry thermal resistivity's ranging from 50-400 C ° cm / watt, (*Figure75*.) The thermal conductivity of the soil is an important factor in the ampacity calculations. The thermal stability has a remarkable influence at high currents. If the soil tends to dry in the presence of the heat flow of the cable system, the thermal conductivities may decrease, giving increases in the temperature of the cable with the consequent damage of these and possible reduction in

the ampacity. A soil is defined as stable when the drying time is longer at practical levels of heat flow than the probable time at which the material re-moistens before it reaches its critical humidity.

The soil materials were:

- A_{1-a} soil for Massa Carrara (coarse soil)
- A₇₋₆ soil for Naples Airports (fine Soil)

The mix of CLSM selected included:

- C60_20_0.80 = 60 [kg/m³] Cement Content, 20% RAP content and 0.80% water to powder ratio.
- C80_20_08 = 80 [kg/m³] Cement Content, 20% RAP content and 0.80% water to powder ratio.
- C100_20_0.8 = 100 [kg/m³] Cement Content, 20% RAP content and 0.80% water to powder ratio.

For the CLSM mixtures, the values measured at 28 days have been taken as the conductivity value under wet conditions, these will be called cured conductivity. For dry conditions the conductivity measurements have been taken after two days of drying in the oven at 60 ° C.

- $k_{cured} = k$ measured after 28 days
- $k_{dry} = k$ measured after drying in oven

In the table shown below can be seen the values of the measurements for wet and dry conditions. Where ρ [°C cm / watt] is a Thermal Resistivity

Tab. 37 Thermal Conductivity and Resistivity Measured for Soils Samples

A1-a Soil			A7-6 Soil		
$w_{effective}$ [%]	k [W/m·°K]	ρ [°C cm/ W]	$w_{effective}$ [%]	k [W/m·°K]	ρ [°C cm/ W]
0,0	0,59	169,78	0,00	0,225	444,444
3,3	1,31	76,34	13,17	0,749	133,511
4,9	1,93	51,71	15,70	1,061	94,251
5,4	1,88	53,08	17,96	0,916	109,170
7,3	1,88	53,25	20,42	0,946	105,708
8,4	1,73	57,74	22,89	0,997	100,301
			26,13	0,957	104,493

Tab. 38 Results of Thermal Conductivity and Resistivity in Wet and Dry Conditions for AS CLSM Samples

items	w_{cured} [g]	w_{dry} [g]	w %	k_{cured} [W/m.K]	ρ_{cured} [°C cm/ W]	w %	k_{dry} [W/m.K]	ρ_{dry} [°C cm/ W]
C60_20_0,80	2847,5	2635,5	8,04	1,475	67,797	0,00	0,820	121,902
C80_20_0,80	2849,4	2613,2	9,04	1,697	58,928	0,00	1,092	91,617
C100_20_0,80	2839,2	2588,2	9,70	1,745	57,318	0,00	1,163	86,022

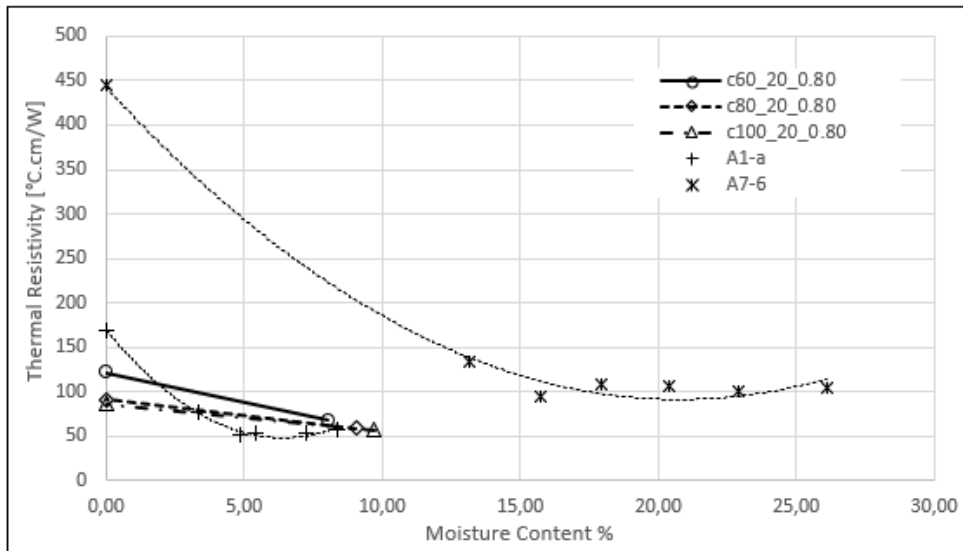


Fig. 75. Thermal Stability Curve for Backfill Materials

Figure 75 shows the behaviour of both materials by varying the water content within the samples. As mentioned either in literature or in the section “5.3.2 Water content and thermal conductivity”, soils have the particularity that by passing a lower values of water content, also called critical moisture, the resistivity increases sharply. This is because at low water contents in the structure, the density is also low, having high contents of pores, mostly full of air, which causes heat conduction to be affected. Therefore, both soils do not have a thermal stability below this critical value.

For the Aggregate Sludge CLSM mix, a totally different behaviour is observed since the thermal resistivity remains practically constant at water content variations, This kind of thermal stability is a desired property for the thermal backfill materials.

6.8 Stone Sawmilling Sludge CLSM

The analysis of this particular type of mixtures was carried out in the final phase of this thesis, in order to study and analyse how sludge with different metals content could influence the conduction of heat, since as it has been expressed throughout the work, mineralogical content is one of the variables that have most influence at the time to eliminate heat when the cables are buried. taking the two types of this aggregate, and using the same methodology used for Aggregate Sludge CLSM in the creation as for taking measurements, with the particularity that due to the lack of time, these were taken only in 2, 7 and 14 days. In the Table 39 shown below you can see the summary of the results obtained for the two types of limes used; Diamond Wire Cut Sludge (DWCS) And Frame Wire Saw Sludge (FWSS). The mixtures were made for both types of Sludge with these characteristics:

- C100_20_0.7 = 100 [kg/m³] Cement Content, 20% RAP content and 0.70% water to powder ratio.
- C100_20_0.8 = 100 [kg/m³] Cement Content, 20% RAP content and 0.80% water to powder ratio

Detailed mineralogical assessment of the sludge were not conducted but as per the information received from the plant frame wire saw sludge(FWSS) has the maximum metallic content.

Tab. 39 Thermal Conductivity Measurements on Stones Sawmilling Sludges CLSM's

NAME	items	W/P %	Thermal conductivity [W/m.K]		
			2 days	7 days	14 days
DWCS	C100_20_0,70	0,70%	1,514	1,652	1,519
	C100_20_0,80	0,80%	1,774	1,605	1,468
FWSS	C100_20_0,70	0,70%	1,947	1,908	1,675
	C100_20_0,80	0,80%	1,789	1,695	1,506

For a better understanding of the behaviour of this type of aggregate and to make a comparison with AS_CLSM, the *Table 40* will show the values of both types of sludge along with the *Figures 76* to analyse and better understand what is the trend and influence of these sludges over time for each w/p ratio.

Tab. 40 Summary of Thermal Conductivity Measurements on DWCS and FWSS CLSM's and AS_ CLSM

NAME	items	W/P %	Thermal conductivity [W/m.K]		
			2 days	7 days	14 days
DWCS	C100_20_0,70	0,70%	1,514	1,652	1,519
	C100_20_0,80	0,80%	1,774	1,605	1,468
FWSS	C100_20_0,70	0,70%	1,947	1,908	1,675
	C100_20_0,80	0,80%	1,789	1,695	1,506
Aggregate Sludge	C100_20_0,70	0,70%	1,729	1,632	1,635
	C100_20_0,80	0,80%	1,913	1,809	1,865

Figure 76 shows how, after 7 days, both mix DWCS and FWSS CLSMs for 0.70% w / p ratio, tend to suffer a slight decrease in thermal conductor aptitudes, both with a similar slope. Although FWSS_0.70 has a drop a bit sharper from the value taken two days, this, however, is higher than the DWSC_0.70 at the end of the 14.

The analysis for w / p 0.80 has been excluded because of its not acceptable results, this can be due to the phenomenon of segregation q have undergone these mixes.

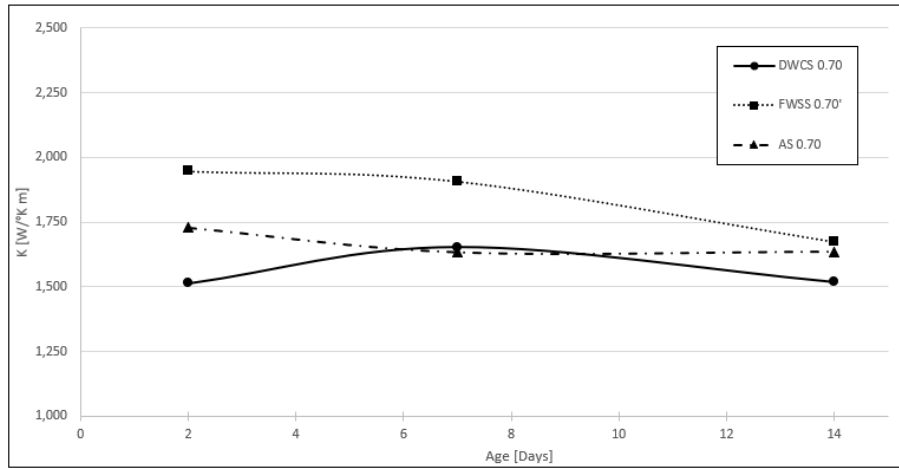


Fig. 76 Influence of Age on Thermal Conductivity with 0.7% w/p ratio for Sludges CLSM

The mix with FWSS showed a higher thermal conductivity compared to the other two sludge.

After the individual analysis of both mixes with metallic contents, it is observed that for the mixtures made with *Aggregate Sludge CLSM* the behaviour is much more stable and constant as the curing process advances with the days. Therefore, it can be concluded that this type of mixtures have more acceptable and consistent results when selecting a material that has high thermal conductivity.

The analysis for w / p 0.80 has been excluded because of its not acceptable results, this can be due to the phenomenon of segregation q have undergone this mix.

CHAPTER 7

CONCLUSIONS

Thermal conductivity of backfilling materials and the factors affecting their thermal performance was examined in this study. Literature review was performed on different backfilling materials including soils and cement based materials, scope and objectives of the current study was chosen based on this literature search. The experimental evaluation consisted of the analysis of thermal conductivity of two different soils with different properties and two different Controlled Low Strength Materials (CLSMs). The following conclusions were drawn from the study.

1. Two soils considered in this study (A_{1-a} and A_{7-6} according to AASHTO classification) exhibits difference in their thermal properties. Thermal conductivity of A_{1-a} is almost double that of A_{7-6} in optimum moisture content. The main factors that affect the thermal performance of soils are their density, water content, degree of saturation, volume of solid and mineralogical composition.

Thermal conductivity of soil of type A_{1-a} exhibited more dependence on its density, water content, and the degree of saturation. It was found that the thermal conductivity increases when these factors increase. Comparatively thermal behaviour of soil A_{7-6} was independent of these factors. Difference in mineralogical composition of the soils could be one reason for this but it was not considered in this study.

2. It was observed that, there exists a critical water content in case of soils below which their thermal resistivity increases exponentially. Moisture content is the most influencing factor for the thermal conductivity of soils. For the A_{1-a} soil an exponential increase in the thermal resistivity was observed below the water content between 4,5 and 5 %, while for A₇₋₆ the critical water content was obtained at 15%.
3. Both the Soils exhibited a very low thermal stability and the thermal resistivity increases sharply with the drying our phenomenon. This is a crucial point to consider when designing thermal back-fills for high- voltage cables.
4. The thermal conductivity results obtained during this study were analyzed according to the different models available in the literature. Kersten (1949), Johansen (1975), Farouki (1981,1982) and Cote and Konrad (2005) models were more reliable for the modeling of A_{1-a} and A₇₋₆ Soil. It can be said that the Farouki model for fine soils is where the best results have been found, while the Cote a Konrad models are the most acceptable for coarse soils. The models of Kersten and Johansen overestimated the results.
5. In case of cement based CLSMs, the thermal conductivity is influenced mainly by the cement content, while the variation of the RAP content, the water to powder ratio and the age of the samples show a very low influence on the thermal conductivity. The different CLSMs considered during the study had different compositions. *Aggregate Sludge CLSMs (AS_CLSM)* exhibited highest thermal conductivity. Thermal conductivity of *Stones Sawmilling Sludges CLSM's*, were lower than that of AS_CLSM and over time these decreased even more.
6. CLSM possess high thermal stability and the variation in thermal conductivity with the reduction in water content is very low. It was also observed that the variation in thermal conductivity with the age of the specimens is not significant. This is due to the early hardening takes place in the cement based specimen and further water evaporation is not significantly altering their thermal performance.
7. Segregation of the cement based mix badly affects the thermal conductivity. Non-homogeneity of the mix results in high thermal resistivity with variations in results. This has been clearly seen in the sample of C100_30_0.80 of AS_CLSM as well as in the four samples of *Stones Sawmilling Sludges CLSM's*.
8. In a segregated mix, the water evaporates faster, and the pores fill are with air (bad thermal conductor) The water retained inside the mixtures does not allow the particles to have an effective contact between them due to bridges formed by the air
9. The thermal conductivity of CLSMs was modeled considering the different factors influencing it such as; Cement Content, RAP content and water to powder ratio. Age was not considered

due to its low influence on thermal conductivity. The regression coefficient was 77%. The model predicts the thermal conductivity values reasonably well.

10. Needle type thermal conductivity tester (KD2 pro) can be used for the determination of thermal conductivity in construction materials. This device is a great tool for taking measurements, for its speed, ease of operation and reliability. One possible source of measurement error in this device is due to the contact resistance between the needle and sample. This could be taken care of for better reliability.

FUTURE RESEARCH

The potential of CLSMs to be used as thermal backfills is recognized from this study. Different Recycled materials and construction and demolition wastes could be attempted for the formulation of such cement based thermal backfills. Future studies can be conducted to enhance the thermal conductivity of cement based CLSMs with different compositions.

Soils could be used as a thermal backfill only when their thermal stability is ensured at low moisture contents, Future studies could be performed to improve the thermal stability of soils

APPENDIX

APPENDIX 1: HVDC INTERCONNECTION INPUTS AND PARAMETERS

INPUTS AND PARAMETERS

A. Electrical System Data:

$U_0 := 320$ (DC voltage, kV)

$I_N = 950.0$ (Nominal Current, A)

B. Cable Construction Data:

$A_c := 2500$ (geometric cross-section area of conductor, mm²)

$d_c := 62.8$ (diameter of conductor, mm)

$d_{ic} = 66.8$ (diameter over conductor screen, mm)

$d_{in} = 106.8$ (diameter over insulation, mm)

$d_{oc} = 110.1$ (diameter over insulation screen, mm)

$d_{bls} = 112.4$ (diameter above swelling tape/bedding, mm)

$d_{als} = 115.0$ (diameter over aluminium sheath, mm)

$d_o = 127.1$ (external diameter of the cable, mm)

C. Electrical Characteristics:

- $Rd_{c0} := 1.27 \cdot 10^{-5}$ (D.C.resistance of the conductor at 20degC as per IEC 228, Ohm/m)
- $\rho_{alu} := 2.8264 \cdot 10^{-8}$ (electrical resistivity of conductor aluminium, Ohm.m)
- $\alpha A_{20} := 4.03 \cdot 10^{-3}$ (constant aluminium temperature coefficient, 1/K)

D. Thermal Properties:

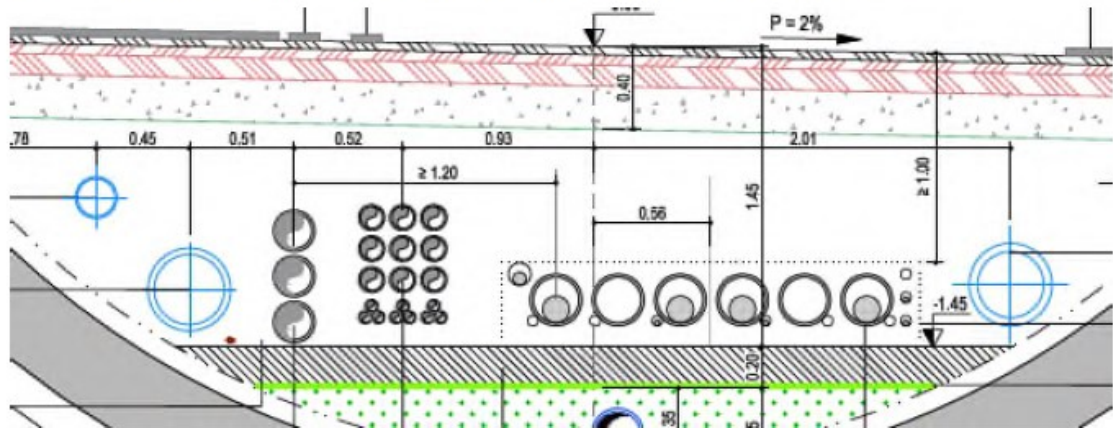
- $\rho_{xlpe} := 3.5$ (thermal resistivity of XLPE, K.m/W)
- $\rho_{sc} := 2.5$ (thermal resistivity of S/C screens, K.m/W)
- $\rho_{pe} := 3.5$ (thermal resistivity of PE/HDPE, K.m/W)
- $\rho_b := 6$ (thermal resistivity of swelling tape/bedding, K.m/W)
- $\rho_{soil} := 1.2$ (thermal soil resistivity, K.m/W)
- $\rho_{backfill} := 0.8$ (thermal resistivity of special backfill, K.m/W)
- $\sigma_{Cu} := 401$ (thermal conductivity of copper, W/K.m)
- $\sigma_{Al} := 204$ (thermal conductivity of aluminium, W/K.m)

E. Temperatures:

- $\theta_{max} := 70$ (max. working temperature of the conductor, degC)
- $\theta_{ground} := 35 + 5$ (max. ground temperature, degC) $\theta_{ground} = 40.0$

F. Laying Characteristics:

Cables are laid in flat formation, in ducts buried in a concrete block

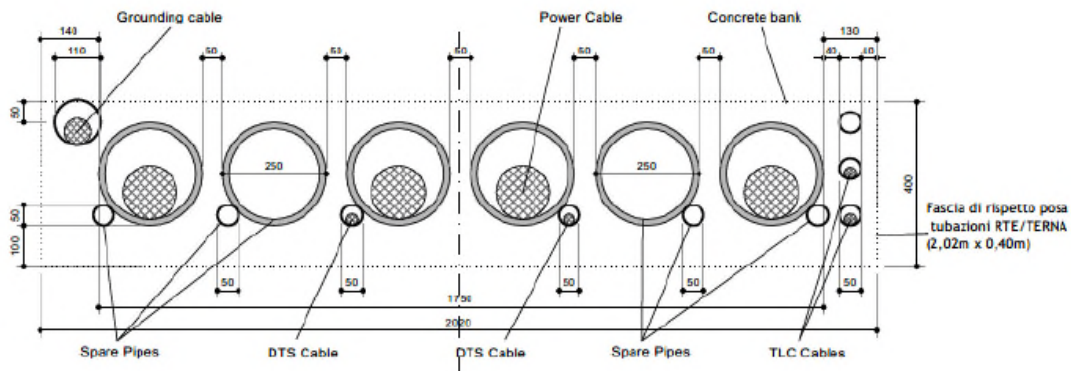


Ducts characteristics:

- $d_{duct} := 220.6$ (Inner diameter of duct, mm)
- $do_{duct} := 250$ (Inner diameter of duct, mm)
- $U := 1.87$ $V := 0.312$ $W := 0.0037$ (Thermal exchange coefficients of plastic ducts, K.m/W)

Ducts spacing:

Rete RTE/TERNA
Scala 1:10



$$s_{axc} := 110 + d_{duct} \quad (\text{axial spacing of the duct centres inside a circuit, mm}) \quad s_{axc} = 360.0$$

Thermally controlled backfill characteristics:

$$W_{DB} := 5 \cdot s_{axc} + d_{duct} + 100 \quad (\text{Width of concrete block, mm}) \quad W_{DB} = 2150.0$$

$$H_{DB} := 620 \quad (\text{Height of concrete block, mm})$$

$$B_{DB} := 1450.0 \quad (\text{Depth to bottom of concrete block, mm})$$

$$x := H_{DB} \quad (\text{Minimum dimension of concrete, mm}) \quad x = 620.0$$

$$y := W_{DB} \quad (\text{Maximum dimension of concrete, mm}) \quad y = 2150.0$$

$$T_{DB} := B_{DB} - H_{DB} \quad (\text{Depth to top of concrete block, mm}) \quad T_{DB} = 830.0$$

$$h_{DB} := B_{DB} - \frac{H_{DB}}{2} \quad (\text{Depth of concrete block centre, mm}) \quad h_{DB} = 1140$$

Ducts position:

$$hg := B_{DB} - 200 \quad (\text{distance from ground surface to duct axis, mm}) \quad hg = 1250.0$$

CALCULATION OF TEMPERATURES AT NOMINAL LOAD

All previous parameters are still valid with the exception of the following:

Loading current $I_{load_p} := I_N$ $I_{load} = \begin{pmatrix} 950 \\ 950 \\ 950 \\ 950 \end{pmatrix} A$ $p := 1..4$

1. Temperature of Conductor

DC Resistance of Conductor at operating temperature

$$\theta_{cond} := \begin{pmatrix} 68.4 \\ 70.0 \\ 69.8 \\ 67.9 \end{pmatrix} \quad Rdc_{1_p} := Rdc_0 \cdot [1 + \alpha A_{20} \cdot (\theta_{cond_p} - 20)] \quad Rdc_1 = \begin{pmatrix} 1.52 \times 10^{-5} \\ 1.53 \times 10^{-5} \\ 1.52 \times 10^{-5} \\ 1.52 \times 10^{-5} \end{pmatrix} \text{ ohm/m}$$

Duct air gap temperature

$$\theta_{m_{duct}} := \begin{pmatrix} 61.2 \\ 63.2 \\ 63.0 \\ 60.6 \end{pmatrix} \quad T_{pa_p} := \frac{U}{1 + 0.1 \cdot (V + W \cdot \theta_{m_{duct}_p}) \cdot d_o}$$

Conductor operating temperature

APPENDIX 2: CHARACTERIZATION OF SOILS

- **Atterberg Limit**

Tab. A2. 1 Atterberg limit for survey 1

Limite liquido					
ID	Penetrazione	Tara	Umido lordo	Secco lordo	W
[-]	[mm]	[g]	[g]	[g]	[%]
1	8,55	2,126	31,281	26,090	21,7
2	8,85	2,116	22,828	19,188	21,3
3	11,10	2,137	27,788	23,071	22,5
4	12,10	2,133	23,243	19,117	24,3
5	12,75	2,132	31,475	25,863	23,6
6	13,30	2,125	26,862	21,898	25,1

Limite plastico				
ID	Tara	Umido lordo	Secco lordo	W
[-]	[g]	[g]	[g]	[%]
1	-	-	-	-
2	-	-	-	-

Passante 63 μ m	Limite liquido	Limite plastico	Indice di plasticità	Indice di gruppo	Classificazione
8,9	22,4	-	0,0	0,0	A1-a

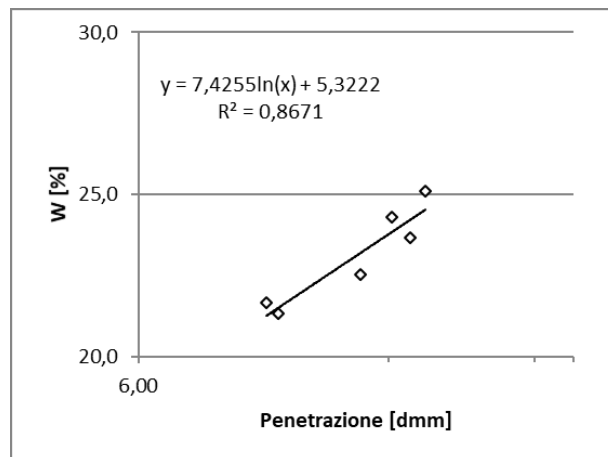


Fig. A2. 1 Atterberg limit for survey 1

Tab. A2. 2 Atterberg limit for survey 2

Limite liquido					
ID	Penetrazione	Tara	Umido lordo	Secco lordo	W
[-]	[mm]	[g]	[g]	[g]	[%]
1	7,60	2,072	28,126	24,084	18,4
2	9,35	2,068	30,539	25,882	19,6
3	12,00	2,065	27,552	23,171	20,8
4	14,60	2,070	28,410	23,976	20,2
5	15,00	2,084	27,719	23,139	21,8

Limite plastico				
ID	Tara	Umido lordo	Secco lordo	W
[-]	[g]	[g]	[g]	[%]
1	-	-	-	-
2	-	-	-	-

Passante 63 μ m	Limite liquido	Limite plastico	Indice di plasticità	Indice di gruppo	Classificazione
8,2	19,6	-	0,0	0,0	A1-a

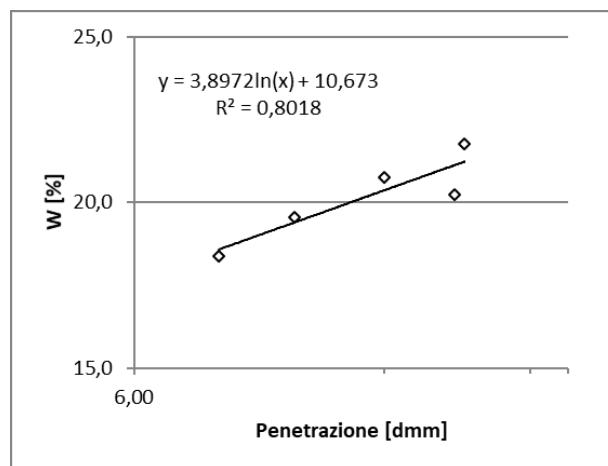


Fig. A2. 2 Atterberg limit for survey 2

Tab. A2. 3 Atterberg limit for survey 10

Limite liquido					
ID	Penetrazione	Tara	Umido lordo	Secco lordo	W
[-]	[mm]	[g]	[g]	[g]	[%]
1	6,90	2,108	28,854	24,392	20,0
2	7,85	2,110	25,786	21,551	21,8
3	9,80	2,108	27,644	22,639	24,4
4	13,30	2,114	24,720	20,432	23,4
5	14,10	2,107	25,512	20,842	24,9
Limite plastico					
ID	Tara	Umido lordo	Secco lordo	W	
[-]	[g]	[g]	[g]	[%]	
1	-	-	-	-	
2	-	-	-	-	
Passante 63 μ m	Limite liquido	Limite plastico	Indice di plasticità	Indice di gruppo	Classificazione
9,8	22,9	-	0,0	0,0	A1-a

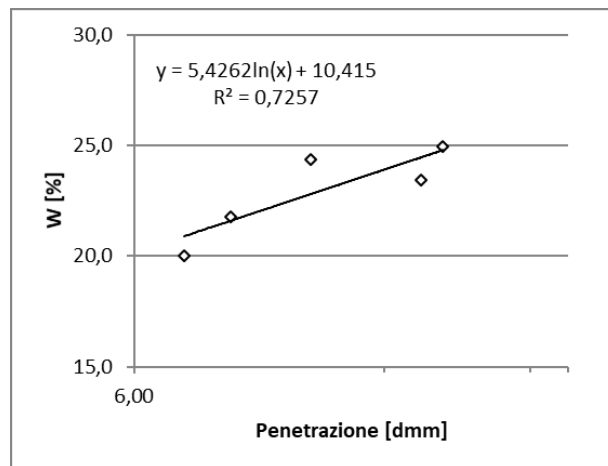


Fig. A2. 3 Atterberg limit for survey 10

- **Specific Density**

Tab. A2. 4 Specific Gravity of Soils

Soil	Pycnometer	M _P	M _{P+M}	M _{P+M+H₂O}	T °C	V _p	ρ _w	ρ _s	ρ _s	ρ _{saverage}
		[g]	[g]	[g]	[°C]	[m ³]	[kg/m ³]	[kg/m ³]	[g/cm ³]	[g/cm ³]
A1-a	6-F	1041,6	1644,7	2703,5	20,40	0,001283	998,19	2712	2,712	2,714
	T-A	885,2	1501,7	2658,2	20,10	0,001385	998,26	2716	2,716	
A7-6	W-I	900,1	1511	2667,5	20,20	0,001388	998,23	2664	2,664	2,667
	Y-B	900,1	1514,8	2656,7	20,30	0,001374	998,21	2670	2,670	

-Optimitation Curves

Tab. A2. 5 Curve of optimization for 0% RAP

D [mm]	Passing [%]					Reference	Δ
	Coarse sand 0-8	Gravel 8-18	RAP	Sludge	CP		
16	100,0	100,0	100,0	100,0	100,0	100,0	1,0E-08
12,5	100,0	84,6	100,0	100,0	96,6	93,8	8,0E+00
8	100,0	15,0	88,7	99,7	81,5	83,4	3,8E+00
6,3	99,3	2,6	80,2	99,3	78,3	78,2	1,3E-03
4	86,3	0,2	58,4	98,8	70,3	69,1	1,5E+00
2	64,4	0,2	32,8	98,2	57,7	56,7	1,2E+00
1	43,1	0,2	14,8	97,3	45,5	45,9	2,0E-01
0,5	26,2	0,2	6,2	96,2	35,6	36,7	1,0E+00
0,25	12,6	0,2	3,0	93,2	27,3	28,7	1,8E+00
0,125	6,0	0,2	1,8	85,8	22,0	21,7	6,3E-02
0,063	3,0	0,2	0,9	73,7	17,7	15,8	3,5E+00
Σ							
0,57	0,22	0,00	0,22	1,00	Σ	2,1E+01	
56,7	21,7	0,0	21,6				

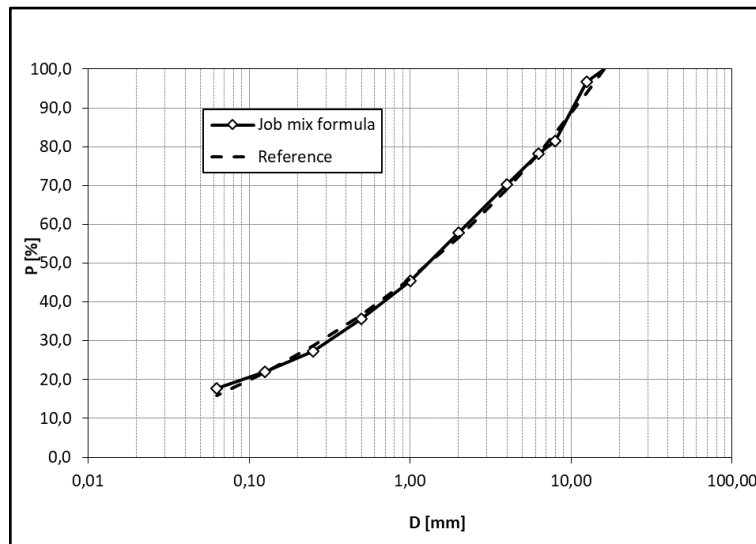


Fig. A2. 4 Curve of Job mix Formula and Reference for 0% RAP

Tab. A2. 6 Curve of optimization for 15% RAP

D [mm]	Passing [%]					Reference	Δ
	Coarse sand 0-8	Gravel 8-18	RAP	Sludge	CP		
16	100,0	100,0	100,0	100,0	100,0	100,0	1,0E-08
12,5	100,0	84,6	100,0	100,0	97,2	93,8	1,2E+01
8	100,0	15,0	88,7	99,7	83,1	83,4	1,2E-01
6,3	99,3	2,6	80,2	99,3	79,1	78,2	8,4E-01
4	86,3	0,2	58,4	98,8	69,6	69,1	3,4E-01
2	64,4	0,2	32,8	98,2	56,1	56,7	3,0E-01
1	43,1	0,2	14,8	97,3	43,9	45,9	4,2E+00
0,5	26,2	0,2	6,2	96,2	34,9	36,7	3,0E+00
0,25	12,6	0,2	3,0	93,2	27,8	28,7	7,2E-01
0,125	6,0	0,2	1,8	85,8	23,0	21,7	1,7E+00
0,063	3,0	0,2	0,9	73,7	18,8	15,8	8,8E+00
Σ							
0,44	0,18	0,15	0,23			3,2E+01	
43,7	17,9	15,0	23,4				

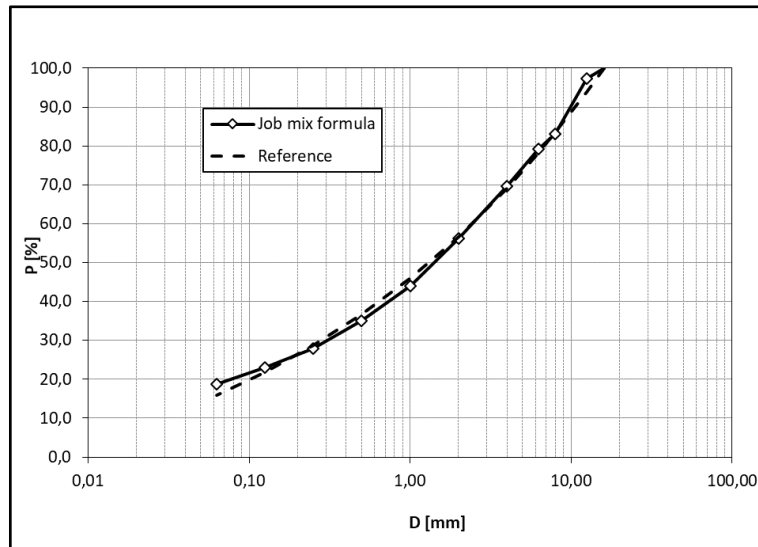


Fig. A2. 5 Curve of Job mix Formula and Reference for 15% RAP

Tab. A2. 7 Curve of optimization for 20% RAP

D [mm]	Passing [%]					Reference	Δ
	Coarse sand 0-8	Gravel 8-18	RAP	Sludge	CP		
16	100,0	100,0	100,0	100,0	100,0	100,0	0,0E+00
12,5	100,0	84,6	100,0	100,0	97,4	93,8	1,3E+01
8	100,0	15,0	88,7	99,7	83,6	83,4	3,7E-02
6,3	99,3	2,6	80,2	99,3	79,4	78,2	1,5E+00
4	86,3	0,2	58,4	98,8	69,4	69,1	1,4E-01
2	64,4	0,2	32,8	98,2	55,6	56,7	1,2E+00
1	43,1	0,2	14,8	97,3	43,4	45,9	6,7E+00
0,5	26,2	0,2	6,2	96,2	34,7	36,7	3,9E+00
0,25	12,6	0,2	3,0	93,2	28,0	28,7	4,6E-01
0,125	6,0	0,2	1,8	85,8	23,4	21,7	2,7E+00
0,063	3,0	0,2	0,9	73,7	19,1	15,8	1,1E+01

0,39	0,17	0,20	0,24
39,4	16,6	20,0	24,0

4,1E+01

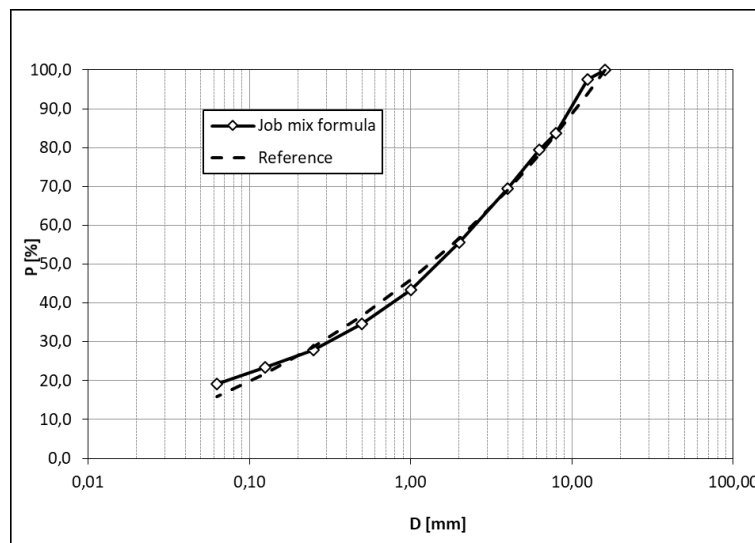


Fig. A2. 6 Curve of Job mix Formula and Reference for 20% RAP

Tab. A2. 8 Curve of optimization for 30% RAP

D [mm]	Passing [%]					Reference	Δ
	Coarse sand 0-8	Gravel 8-18	RAP	Sludge	CP		
16	100,0	100,0	100,0	100,0	100,0	100,0	0,0E+00
12,5	100,0	84,6	100,0	100,0	97,8	93,8	1,6E+01
8	100,0	15,0	88,7	99,7	84,7	83,4	1,6E+00
6,3	99,3	2,6	80,2	99,3	80,0	78,2	3,2E+00
4	86,3	0,2	58,4	98,8	69,0	69,1	1,5E-03
2	64,4	0,2	32,8	98,2	54,5	56,7	4,8E+00
1	43,1	0,2	14,8	97,3	42,3	45,9	1,3E+01
0,5	26,2	0,2	6,2	96,2	34,2	36,7	6,0E+00
0,25	12,6	0,2	3,0	93,2	28,3	28,7	1,2E-01
0,125	6,0	0,2	1,8	85,8	24,1	21,7	5,5E+00
0,063	3,0	0,2	0,9	73,7	19,8	15,8	1,6E+01

0,31	0,14	0,30	0,25
30,8	14,0	30,0	25,2

6,7E+01

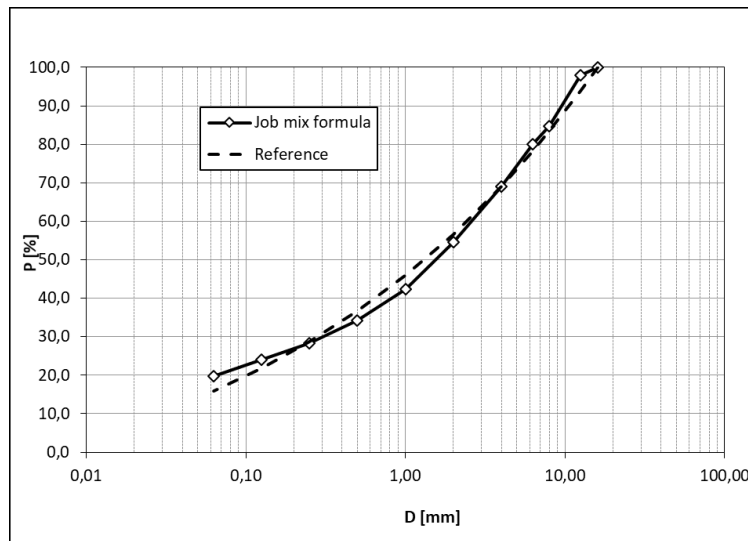


Fig. A2. 7 Curve of Job mix Formula and Reference for 30% RAP

APPENDIX 3: MOULD VOLUME



REFERENCES

- [1] H. Interconnection, “Inputs and parameter s,” vol. 0, pp. 1–9.
- [2] J. Sundberg, “Evaluation of thermal transfer processes and back-fill material around buried high voltage power cables,” 2016.
- [3] G. Roercls, “Engineering Classification of Soil,” vol. 0, no. 10, 1945.
- [4] C. Strade, “Corpo stradale,” 2015.
- [5] N. . Abu-Hamdeh and R. C. Reeder, “Soil Thermal Conductivity: Effects of Density, Moisture, Salt Concentration, and Organic Matter,” *Soil Sci. Soc. Am. J.*, vol. 64, no. 64, pp. 1285–1290, 2000.
- [6] N. H. Abu-Hamdeh, “SW—Soil and Water: Measurement of the Thermal Conductivity of Sandy Loam and Clay Loam Soils using Single and Dual Probes,” *J. Agric. Eng. Res.*, vol. 80, no. 2, pp. 209–216, 2001.
- [7] N. Zhang and Z. Wang, “Review of soil thermal conductivity and predictive models,” *International Journal of Thermal Sciences*, vol. 117. pp. 172–183, 2017.
- [8] Y. Dong, J. S. McCartney, and N. Lu, “Critical Review of Thermal Conductivity Models for Unsaturated Soils,” *Geotech. Geol. Eng.*, vol. 33, no. 2, pp. 207–221, 2015.
- [9] Z. Tian, Y. Lu, R. Horton, and T. Ren, “A simplified de Vries-based model to estimate thermal conductivity of unfrozen and frozen soil,” *Eur. J. Soil Sci.*, vol. 67, no. 5, pp. 564–572, 2016.
- [10] “IEEE Guide for Soil Thermal Resistivity Measurements,” 2003.
- [11] Lawrence A. Salomone and William D. Kovacs, “Thermal resistivity of soils,” *J. Geotech. Engrg*, vol. 110, no. 3, pp. 375–389, 1984.
- [12] E. C. R. Bascom, N. Patel, and D. Parmar, “Thermal Environment Design Considerations for

- Ampacity of Buried Power Cables,” *Ieee*, 2014.
- [13] M. Gangadhara Rao, P. Kolay, and D. Singh, “Thermal characteristics of a class F fly ash,” *Cem. Concr. Res.*, vol. 28, no. 6, pp. 841–846, 1998.
- [14] P. K. Kolay and D. N. Singh, “Application of coal ash in fluidized thermal beds,” *J. Mater. Civ. Eng.*, vol. 14, no. 5, pp. 441–444, 2002.
- [15] J. A. Williams, D. Parmar, and M. W. Conroy, “Controlled backfill optimization to achieve high ampacities on transmission cables,” *IEEE Trans. Power Deliv.*, vol. 9, no. 1, pp. 544–552, 1994.
- [16] “Method of manufacture and installation flowable thermal backfills,” 2006.
- [17] A. C. I. American Concrete Institute, “Guide to thermal properties of concrete and Masonry Systems,” no. ACI 122R-02, p. 21, 2002.
- [18] K. Reinschmidt, S. Anderson, and D. Cline, “PHYSIOCHEMICAL CHARACTERISTICS OF CONTROLLED LOW STRENGTH MATERIALS INFLUENCING THE ELECTROCHEMICAL PERFORMANCE AND SERVICE LIFE OF METALLIC MATERIALS,” 2005.
- [19] K.-H. Kim, S.-E. Jeon, J.-K. Kim, and S. Yang, “An experimental study on thermal conductivity of concrete,” *Cem. Concr. Res.*, vol. 33, no. 3, pp. 363–371, 2003.
- [20] M. . Khan, “Factors affecting the thermal properties of concrete and applicability of its prediction models,” *Build. Environ.*, vol. 37, no. 6, pp. 607–614, 2002.
- [21] M. Rerak and P. Ocloń, “The effect of soil and cable backfill thermal conductivity on the temperature distribution in underground cable system.”
- [22] P. Ocloń, P. Cisek, M. Pilarczyk, and D. Taler, “Numerical simulation of heat dissipation processes in underground power cable system situated in thermal backfill and buried in a multilayered soil,” *Energy Convers. Manag.*, vol. 95, no. March, pp. 352–370, 2015.
- [23] H. Brakelmann, J. Stammen, J. Dietrich, R. Böing, and H.-P. May, “A new backfill material with an extremely high thermal conductivity,” in *8th International Conference on Insulated Power Cables*, 2011.
- [24] ASTM D4832-16, “Standard Test Method for Preparation and Testing of Controlled Low Strength Material (CLSM) Test Cylinders,” *ASTM Int. West Conshohocken*, vol. 4, no. C, pp. 1–6, 2016.
- [25] D. A. de Vries and A. J. Peck, “On the cylindrical probe method of measuring thermal conductivity with special reference to soils,” *Aust. J. Phys.*, vol. 11, pp. 255–271, 1958.
- [26] J. Côté and J.-M. Konrad, “A generalized thermal conductivity model for soils and construction materials,” *Can. Geotech. J.*, vol. 42, no. 2, pp. 443–458, 2005.
- [27] J. Côté and J.-M. Konrad, “Thermal conductivity of base-course materials,” *Can. Geotech. J.*,

- vol. 42, no. 1, pp. 61–78, 2005.
- [28] Eliana Victoria Torres Segovia, “Master of Science of Civil Engineering ‘Mix design and mechanical properties of flowable cement mortar containing RAP for road construction,’” Politecnico di Torino, 2017.
- [29] “De Un Hormigón Tiene Una Importancia Trascendental En Las Características Del,” *Cemento*.
- [30] G. Hermedia, “Aditivos Para Concreto,” *Sika*, pp. 1–28, 2010.
- [31] G. C. Products, “Grace Concrete Products ADVA CAST 575 High-range water-reducing admixture,” pp. 6–7.
- [32] J. J. H. and R. Brouwers H.J., “Self-compacting concrete: the role of the particle size distribution,” *First Int. Symp. Des. Perform. Use Self-Consolidating Concr.*, vol. 0, no. May, pp. 109–118, 2005.
- [33] A. compaction machine- Matest, “<http://www.matest.com/>.”
- [34] M. of C. P. Test, “<http://www.impact-test.co.uk/>” .
- [35] D. Devices, “KD2 Pro Thermal Properties Analyzer, Operator’s Manual,” p. 68, 2012.
- [36] T. Della Norma, “UNI EN 1097-10:2004 - 01-02-2004 - Prove per determinare le proprietà meccaniche e fisiche degli aggregati - Determinazione dell’altezza di suzione dell’acqua,” 2004.
- [37] A. C. T. A. for S. U. Rammer, “https://www.marui-group.co.jp/en/products/items2_2/item2_2_3/.”
- [38] A. G. Mengistu, L. D. van Rensburg, and S. S. W. Mavimbela, “The effect of soil water and temperature on thermal properties of two soils developed from aeolian sands in South Africa,” *Catena*, vol. 158, pp. 184–193, Nov. 2017.